THE DESIGN AND CONSTRUCTION OF A FAR-INFRARED SPECTROMETER FOR THE SPECTRAL REGION OF 30 TO 1600 MICRONS

T. F. Tao
A. J. Capell

THE DESIGN AND CONSTRUCTION OF A FAR-INFRARED SPECTROMETER FOR THE SPECTRAL REGION OF 30 TO 1600 MICRONS

T. F. Tao and A. J. Capell

Department of Engineering
University of California
Los Angeles, California

FOREWORD

This report, "The Design and Construction of a Far-infrared Spectrometer for the Spectral Region of 30 to 1600 Microns," by T. F. Tao and A. J. Capell, No. 67-9, was carried out in the Department of Engineering, University of California, Los Angeles.

The report is based on a Master of Science thesis submitted by A. J. Capell.

TABLE OF CONTENTS

TABLE OF CONTENTS (Continued)

TABLE OF CONTENTS (Continued)

LIST OF TABLES

LIST OF FIGURES

LIST OF FIGURES (Continued)

CHAPTER I

Introduction

Section 1. Definition of the Far-Infrared Region

The region of the electromagnetic spectrum with which this thesis is concerned lies between the near infrared and microwave regions. For this reason, the region is referred to as the far-infrared or submillimeter region. In terms of wave length, the region is usually defined as being from 20 microns to 2000 microns (0.020mm to 2mm). Since the energy associated with an electromagnetic wave is proportional to the spatial frequency of the wave, it is often convenient to define the region being concerned in units of inverse centimeters. Spectroscopists have traditionally defined the spacial frequency or wave number as $k = 1/\lambda$ in cm^{-1} units, in contrast to the definition used by physicists, e.g., $k = 2\pi/\lambda$. In spectroscopic notation, the region concerned lies between $5 \ cm^{-1}$ and $500 \ cm^{-1}$ as shown in Figure 1. A discussion of the use of wave number in radiation formulas can be found in Reference 1.

Section 2. Generation of Far-Infrared Energy

In terms of energy sources, there are currently three types being used in the far-infrared. Traditionally, the region has been approached from the near infrared side by developing new thermal sources, and from the microwave or millimeter region by spark oscillators and harmonic generation. Recently, submillimeter gas lasers have been developed and are being applied to far-infrared spectroscopy.

A. Thermal Sources

Of the many thermal sources investigated during this century, only four have enjoyed popular use in the far-infrared.

1
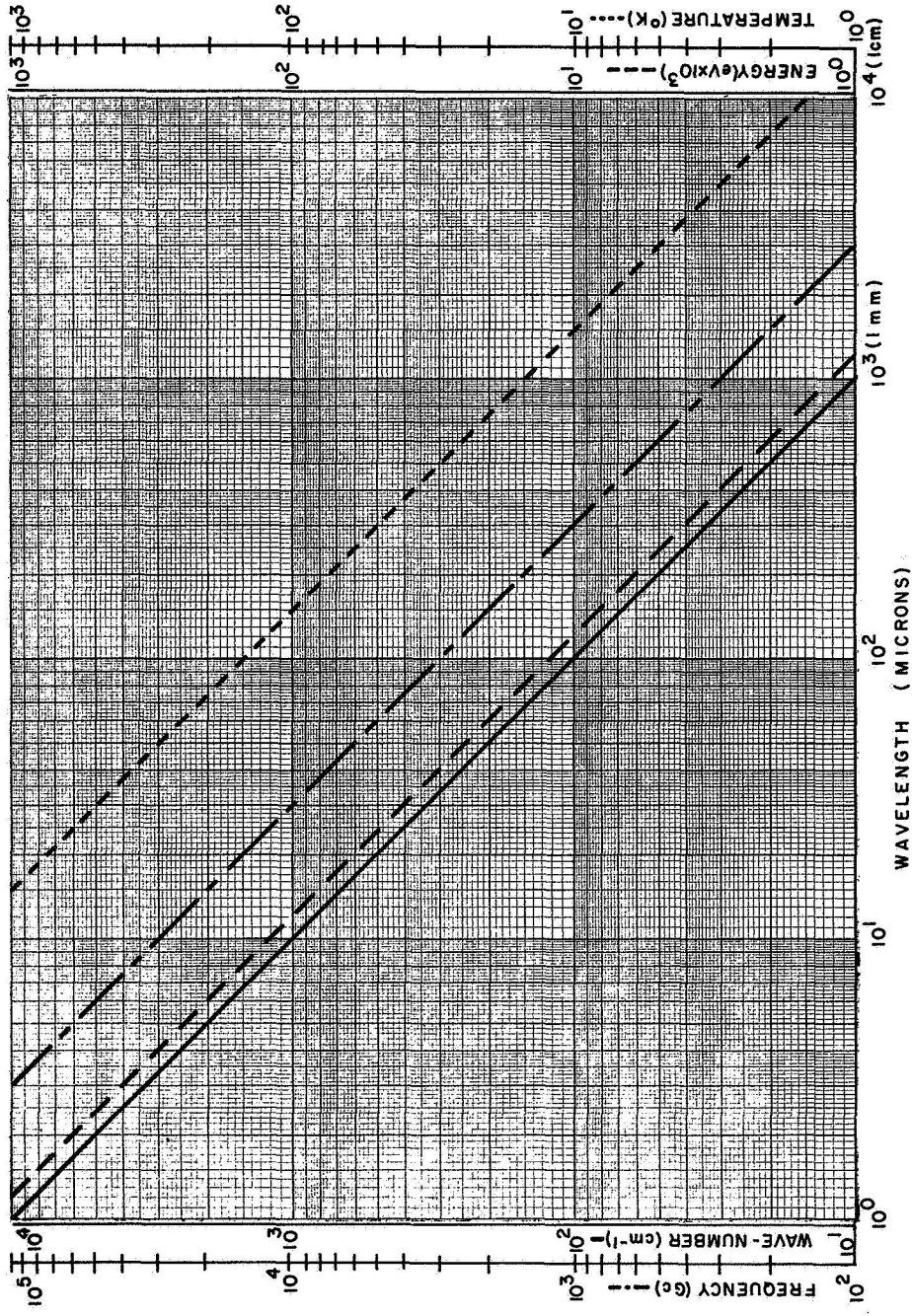
WAVELENGTH VS. WAVE NUMBER, FREQUENCY,
ENERGY AND TEMPERATURE

FIGURE 1

The Welsbach mantle, globar, and Nernst glower sources are usually used for wavelengths less than 100 microns, and the high pressure mercury arc lamp in quartz envelope for longer wavelengths.

The Welsbach mantle consists of a cloth net impregnated with thorium and cesium oxides heated from within by a gas flame. It produces much less radiation below 6 microns than above, and therefore, is a valuable source for the far-infrared. Rubens and Wood[2] used this source to 130 microns. Lord and McCubbin[3] have made excellent use of this source out to 100 microns with only slight modification.

The globar is a rod of bonded silicon carbide in the form of a cylinder about 2 inches long and 3/16 inches in diameter. Its temperature is developed and maintained by joule heating. It generates a radiation field with an almost continuous spectrum to about 15 microns. The Nernst glower is a mixture of zirconium, yttrium, and thorium oxides in the form of a hollow rod approximately 25 mm long by 2 mm in diameter. It must be initially heated by using an external resistance coil, its temperature being maintained by internal resistance heating. Its spectrum is similar to that of the globar. Its low mechanical strength makes the globar difficult to use. The globar and Nernst glower are discussed in Reference 4.

The high pressure quartz mercury discharge tube is the only source with appreciable energy in the region of wavelengths greater than 100 microns. The quartz envelope is fairly opaque from 10 to 50 microns. This source, which has been used as early as 1911,[4] is discussed by McCubbin and Sinton,[5] and Lord and McCubbin.[2] It has been compared to the globar by Plyer, Yates and Gebbie.[6]

Since these sources follow the black body radiation curve, their intensities are very low at long wavelengths, and hence, great difficulty is realized in isolating the far-infrared energy from the much more intense shorter-wave energies.

B. Electrical Sources

The first electrical sources were investigated by Lebedew[10] in the form of a spark oscillator consisting of two electrodes spaced very closely together and immersed in oil for cooling. The resulting radiation had a fundamental wavelength of 6 mm. Later investigators found that the radiation from these spark oscillators was rich in harmonics.[11, 12] By 1925 Nichols and Tear[13] had constructed a similar device which generated energy at .22 mm or 220 microns, which was well into the far-infrared. The main disadvantage of this type of source is the characteristic discrete rather than continuous spectra, which is more desirable spectroscopically speaking. Since the electrodes were very small, it was very difficult to increase the energy output without destroying them. The next type of electrical source investigated was the "mass radiator".[14, 15] These consisted of metal particles suspended in oil, through which was sent an electrical spark. These sources were found to radiate energy with wavelengths from 129 microns to 5 cm.

The electrical type source most recently being investigated is the harmonic generation of microwave energy using the currently available high energy klystron and magnetron sources, in conjunction with solid, liquid, or gaseous non-linear media.

Section 3.   Isolation of the Far-Infrared Region

A.   Pre World War II

The long wavelength infrared region was first isolated by Rubens and Wood[2,16] in 1911.   They used the focal isolation method, which consisted of utilizing the variation of index of refraction of a quartz lens with wavelength.   The lens focused only the longer wavelengths near the center of the image on a screen where a hole was placed allowing only the desired energy to pass through.

The diffraction grating came into popular usage during the 1920's.   First, Rubens[17] constructed a spectrometer using wire gratings.   These gratings consisted of closely spaced long thin parallel wires supported on a metal frame, and were used as trans- mission gratings.   This instrument was used from 80 to 400 mi- crons.   Soon afterwards, Czerny,[18,19] Barnes[20] and Cartwright and Czerny[21] used the same type of appartus to study molecular structure in the far-infrared.

The next improvement of the far-infrared instruments came in the form of lamellar gratings.[22]   These being used in reflection had spectra at least four times the intensity of that of the wire grid. Instruments using this type of grating were built and used by Kuhne,[23] Cartwright and Czerny,[24,25] Koch,[26] Maar,[27] Dahlke[28] and Hopf.[29].   Some of these instruments were used out to 500 mi- crons.   Both the wire and lamellar gratings exhibit only odd order spectra.

The first high resolution far-infrared spectrometer was developed by Randall.[30,31]   This was a very large instrument, using echelette gratings ruled on the University of Michigan ruling engine.   The large mirrors and gratings used were able to produce

resolution of .5 cm^{-1} between 18 and 200 microns. This instrument was used to obtain high resolution spectra of water vapor.[32]

All of the above spectrometers used various types of filter-ing systems to eliminate the overwhelming visible and near infrared energies. For transmission filters, crystalline and fused quartz, paraffin, turpentine or camphor soot, and selective interrupting with KBr and KI crystals were used. Since ac detection methods were not developed yet, these interrupters were hand operated. Restrahlen crystals such as KBr, KI, NaCl, KRS-5, TlCl, CaF$_2$, TlBr, etc., were used extensively to isolate various wavelength bands by selective reflection. Reflection curves for these and other crystals may be found in References 33 and 34.

B. Post World War II

In 1947 White[35] introduced the concept of using echelette gratings as broad band reflection filters for the infrared. These merely reflected the longer wavelengths into the zeroth order spectrum as would a plane mirror, and "scattered" the shorter wavelengths out of the main beam of the instrument into higher order spectra. The first spectrometer in the literature to use these filters was built by Oetgen, et al,[36] (1952). This instrument also used only echelette gratings for dispersive elements. All short wave energy was eliminated by carefully selected filter com-binations for use in conjunction with each grating.

McCubbin and Sinton[7] (1952) designed a very compact spec-trometer which covered the range from 100 to 700 microns. This instrument used a combination of focal isolation and echelette gratings.

In 1957 Lord and McCubbin[3] described a small grating spectrometer for the range of 5 to 200 microns. This instrument used echelette gratings in a double pass arrangement, selective chopping, and various transmission and reststrahlen filters to achieve a resolution of .5 to 1 cm^{-1} throughout its range.

In the same year, Yoshinaga, et al.,[37] described a large spectrometer which covered the very wide range from 18 to 1000 microns. This instrument used six echelette gratings, grating filters, reststrahlen filters, sooted polyethylene, crystal quartz and selective chopping to obtain the excellent resolution of better than .5 cm^{-1} throughout the entire range. This was the first auto-matic instrument to use the Czerny-Turner[38] monochromator arrangement.

Since 1961, many new types of filters have been developed. Using carefully selected reststrahlen crystal powders suspended in transparent sheets of polyethylene, Yamada, et al.,[39] developed excellent transmission filters with cut-off wavelengths that could be shifted with choice of crystal powders.

Metallic mesh filters were proposed by Renk and Genzel,[40] Mitsuishi, et al.,[41] and Vogel and Genzel.[42] These filters are used in reflection and are similar to the reflection-grating filters.

In 1963 Moller[43-46] devised the most convenient type of filter for the far-infrared. These filters are transmission-grating filters made by grooving polyethylene sheets. The cutoff wave-length is determined by the grating constant as in the reflection-grating filter. Being transmission type filters, they require no special position in the spectrometer, and hence, are very convenient

to use. These filters can be used uniquely to isolate the far-infrared region. Spectrometers using these filters have been described in the literature.[45,47]

During the last ten years, many papers on far-infrared technique have appeared in the literature. For a comprehensive bibliography on the far-infrared, see Palik.[48,49]

Section 4. Detection in the Far-Infrared Region

There are basically only two different types of detectors used in the infrared, thermal and photodetectors; the most prominent difference being their response times. All these detectors are discussed in detail in References 4 and 50. For completeness, the general properties of the most common detectors will be discussed below.

A. Thermal Detectors

The three most common thermal detectors are the radiation thermcouple, the bolometer, and the pneumatic cell. The radiation thermocouple, which operates by the thermoelectric effect, has a response time of approximately 36 msec. It has a resistance of about 5 ohms, and is usually operated at less than 5 cps. The detectivity is 1.4×10^9 cm cps$^{1/2}$/watt. Its simple construction and low cost make the thermocouple very popular in commercial instruments.

There are three main types of bolometers, the thermistor, semiconductor and superconductor. All bolometers measure radiation by the change in their resistance with temperature. The thermistor bolometers have response times of the order of 1.5 msec, and are frequency independent below 30 cps. Their resistance is about 2.4 megohms, and detectivity is about 1.95×10^8 cmcps$^{1/2}$/watt.

The carbon bolometer consists of a carbon composition resistor, which is operated at liquid helium temperatures. The detectivity is 4.25×10^{10} cmcps$^{1/2}$/watt with a response time of 10 msec. It usually operates at 13 cps, and has a resistance of .12 megohms.

The superconducting bolometer utilizes the extremely steep slope of the resistance-temperature curve near the superconducting transition temperature of the detector material. This mode of operation requires extremely constant temperature control, and hence is not the most easily used detector. The response time, which is the best for thermal detectors, is 0.5 msec. Its detectivity is 4.8×10^{9} cmcps$^{1/2}$/watt at 360 cps, with a resistance of 0.2 ohms.

The last thermal detector is the Golay pneumatic cell. This detector consists of a gas filled cell connected to a flexible membrane with a reflecting film on the side opposite the gas. Radiation passing through a window heats the gas and thus causes the membrane-mirror to flex. This flexure, or displacement, of the mirror is detected by a secondary light system consisting of a visible light source, line grid, and photocell. This detector has a spectral response which is almost uniform from the visible to the microwave regions. Its detectivity is 1.67×10^{9} cmcps$^{1/2}$/watt at 10 cps, with a response time of 20 msec. This detector is the most widely used in infrared spectroscopy. In work with other detectors, the Golay cell is often referred to as a standard for comparison.

B. Photodetectors

Of the many photon effects used in photodetectors, only three enjoy much popularity. These are the photoconductive, photovoltaic, and photoelectromagnetic modes. The detectors consist of thin poly-crystalline films, or single crystals.

The lead salt photoconductors were developed first. These are made of lead combined with sulfur, selenium, or tellurium. Their spectral range extends at most to about 3, 6, and 4 microns respectively. They operate both at liquid nitrogen and room temperatures.

Germanium doped with a multitude of dopants has been widely used as an infrared detector. The dopants and respective long wavelength limits in microns are as follows: Gold: 7, Gold-antimony: 6, Zinc: 39.5, Zinc-antimony: 15, Copper: 27, and Cadmium: 21.5. Germanium-Silicon alloys can also be doped to make suitable detectors. With Gold as the dopant, this combination has a cut-off wavelength of 10.1 microns, as compared to 13.3 microns with zinc-antimony. All the above detectors are single crystal and operate in the photoconductive mode.

Indium antimonide is another compound semiconductor used for photodetection. This compound has been used in the photoconductive, photovoltaic, and photoelectromagnetic modes. The three modes have cut-off wavelengths ranging from 5.4 to 7.3 microns, with operating temperatures of 77 degrees K and 295 degrees K.

Similar to In Sb, there is the compound In As, which has cut-off wavelengths ranging from 3.4 to 3.8 microns depending on the mode of operation.

Finally, tellurium can be used intrinsically to 3.8 microns; thallous sulfide to 1.1 micron, and mercury telluride-cadmium telluride to wavelengths greater than 40 microns.

All the above photodetectors have response times less than one microsecond, except Ge: Au, Sb with 0.11 msec, Te with 0.06 msec, and $T\ell_2 S$ with 0.53 msec. Their detectivities range from

5×10^6 to 1.7×10^{10} cm cps$^{1/2}$/watt with modulating frequencies from 90 to 900 cps.

CHAPTER II

Design of Far-Infrared Instrumentation

Section 1. Introduction

The basic problems of designing and building a far-infrared spectrometer have been outlined by Oetjen, et al.[36] They specify the problems as... " (1) finding a source having a sufficient amount of radiation in the wavelength region in which absorption measurements are to be made; (2) eliminating or rendering ineffective radiation of other spectral regions which might be present with sufficient intensity to be detected; (3) providing a detector which is sensitive to radiation of the spectral region of interest, and equipping this detector with a suitable amplifier and recorder; (4) obtaining materials which are transparent to the radiation, so that these materials may be used as windows; (5) designing a monochromator in which the radiation is dispersed sufficiently to provide a spectrum having the proper resolution... "

The outstanding features making the far-infrared region more difficult are that (1) most thermal sources emit exceedingly small amounts of far-infrared radiation relative to that of shorter wavelengths, and (2) the energy associated with far-infrared photons is very small. These two features make the filtering and detecting problems very difficult in the far-infrared.

The magnitude of the filtering problem has also been demonstrated by Oetjen, et al. They consider the relative intensities of radiation in each spectral order of a grating blazed at 100 microns. The 100 micron radiation is diffracted into the first order. Then, for the nth order spectrum, the wavelength 100/n microns is diffracted into the same direction as that of the 100 micron radiation.

12

Taking the dispersion of the grating for each order into account, the relative intensity of each order reaching the detector is proportional to J_λ/n, where

$$J_\lambda = \frac{C_1 \lambda^{-5}}{e^{c_2/\lambda T} - 1}$$

is the radiant power per unit wavelength at wavelength λ from a black body whose temperature is T degrees K. C_1 is chosen such that J_λ is unity at 100 microns. The source temperature is taken to be 1300 degrees K. The relative intensity of each order is listed in Table I.

TABLE I

Wavelength (microns)	Order	Relative Intensity
100	1	1
50	2	8
33 1/3	3	24
25	4	54
20	5	99
16 2/3	6	101
14 2/7	7	241
10-13	8-10	1371
7-10	11-14	3870
4-7	15-25	25100
1-4	26-100	145000
1-100	1-100	175000

Two results are evident from this table. First, the ratio of un-wanted radiation to that of the desired 100 micron radiation is about 1.75×10^5. For a reasonable signal to noise ratio of 100, it is necessary to filter out 1.75×10^7 or about 20 million times the energy

desired. Second, it can be seen that most of the unwanted energy that must be filtered out lies near the peak of the blackbody curve.

The above table has been calculated for the blaze condition, and hence, represents the worst condition. Also, the fact that the efficiency of the grating falls off with order number has been neglected. Lord and McCubbin[3] have also pointed out that the angular width of the grating blaze is inversely proportional to order number, so that off blaze operation decreases the intensity of the higher order spectra much more than that of the first order. This off blaze attenuation of higher order spectra can be used as a relative filtering device.

A second, but much less prominent, problem existing in far-infrared spectrometry is the fact that the atmospheric water vapor has a very complex absorption spectrum in this region. As a result of this, the water vapor must be removed from the instrument. The only positive manner in which this can be done is to enclose the instrument so that it can be evacuated. This action causes the far-infrared spectrometer to be very heavy and cumbersome.

Finally, as will be shown later, since the far-infrared energy emitted from available sources is very small, very large optics are necessary to capture as much of this energy as possible. Because of this necessity of using large optics the instrument again becomes large and cumbersome.

Section 2. Optical Arrangements

A. General Considerations

The optical arrangement of any spectrometer can be divided into three main parts; the foreoptics, the monochromator, and the detector optics. In general, the foreoptics contains one or more

light or energy sources, the chopper, various filters, and a number of mirrors or lenses to provide a reasonably compact geometric arrangement.

The light then enters the monochromator, which contains the dispersing elements, the entrance and exit slits, and also a number of mirrors or lenses. The entrance slit being illuminated with a narrow band of polychromatic light is dispersed and imaged at the exit slit plane as a spectrum, which consists of monochromatic images of the entrance slit. The exit slit then isolates a small portion of this spectrum.

The detector optics consist of any or all optical elements between the exit slit and detector element. These consist of either mirrors, lenses, or light pipes.

The above descriptions are concerned with any general spectral region. Specifically, in the far-infrared, no materials have been found which transmit energy in this spectral region, and are suitable for making lenses. With this restriction, only first surface mirrors can be used. Since it is desirable to have highly reflecting surfaces, these mirrors almost always have metallic surfaces. They are made by machining solid pieces of metal to the desired shape and then polishing, or by grinding pyrex blanks and then aluminizing. Mirrors of the latter type are available commercially to very high quality, since optimal requirements of shape to within $\lambda/4$ in angstroms in the visible region, are at least a hundred times better than what is needed in the far-infrared.

Since it is common for mirrors used in the visible region to be coated with silicon oxide to prevent oxidation of the reflecting surface, one must be very careful in specifying mirrors for use in

the far-infrared. This extra coating does not transmit in the far-infrared region.

B. The Monochromator

The most important part of the optical design is that of the monochromator. This section solely determines the resolution of the instrument.

Again, since no suitable materials that transmit in the far-infrared have been found for fabricating prisms, the plane diffraction grating is universally used for the dispersive element in far-infrared spectrometers.

There are a number of optical arrangements used for plane grating monochromators. These are the Ebert,[51] Ebert-Fastie,[52] Littrow,[53] Pfund[54] and Czerny-Turner[38] arrangements. These arrangements, which are shown in Figure 2, have been analyzed theoretically and numerically using electronic computers by various authors.[55-70] Other authors[3,71-75] have described multiple pass arrangements, which have the radiation suffering multiple reflections at the grating, and hence, produce very high dispersion. Still more sophisticated instruments have been designed using multiple monochromators.[75,77] These instruments use the primary monochromator as a pre-dispersing device for the following monochromator. This arrangement replaces the need for filters used in the conventional single monochromator system, and has been used often in the near infrared region with a prism in the primary monochromator. This type of system is used when extremely high resolution is necessary.

C. The Foreoptics

Depending on the types of filters used, many arrangements of the optical elements comprising the foreoptics section of the

PFUND

EBERT   EBERT−FASTIE

SYMMETRIC   ASYMMETRIC

LITTROW   CZERNY − TURNER
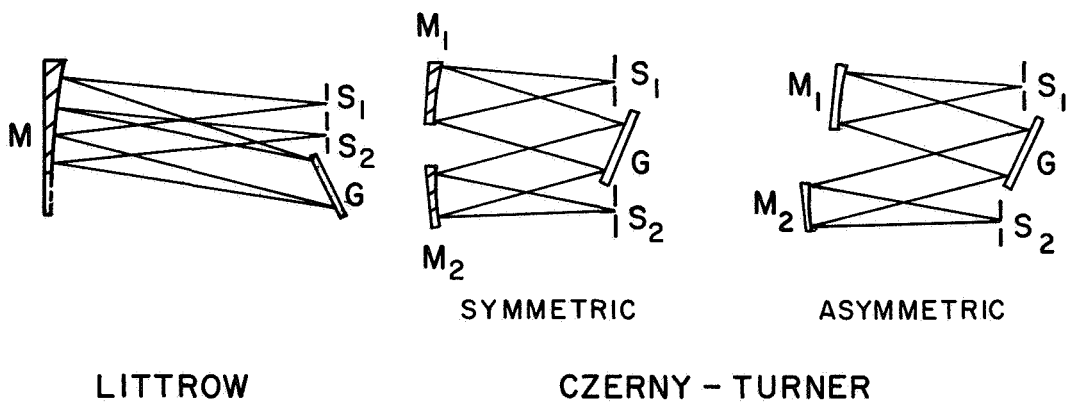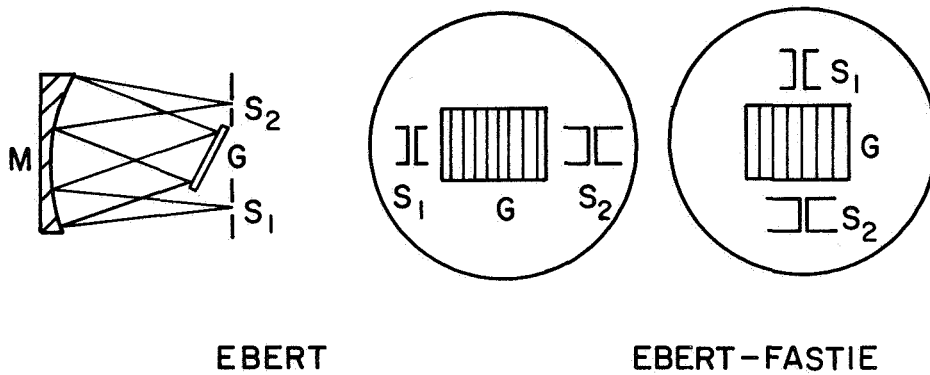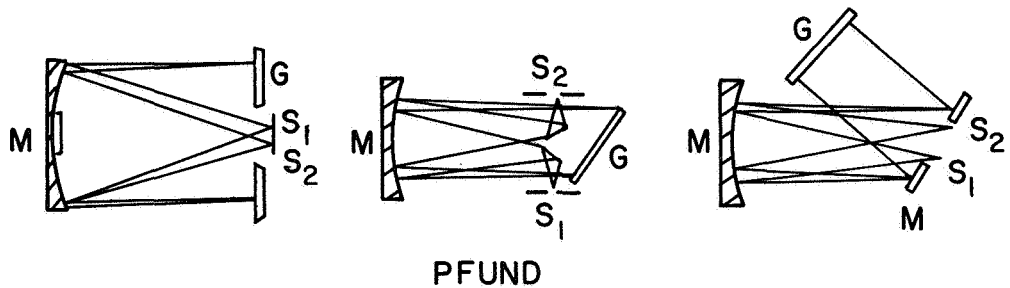
PLANE GRATING MONOCHROMATORS

FIGURE 2

spectrometer can be devised. Generally speaking, there are a number of design criteria which apply to this arrangement irrespective of the type of elements used. These are: (1) the chopper should lie between the source and entrance slit; (2) to avoid heating the chopper blade, the more intense shorter wave energy should be filtered out before the chopper; (3) to eliminate chopped stray radiation and emission of radiation by the chopper blades due to heating by the reference signal lamp, the radiation should be filtered after the chopper also; (4) to obtain good wave form for the detector electronics, and to be able to achieve high chopping frequencies, the beam aperature should be as small as possible at the chopper; and (5) large aperature and short focal length optics must be used to retain as much of energy emitted by the source as possible.

D. The Detector Optics

Since most detectors have very small sensitive areas, a very difficult problem exists in reducing the size of the image of the exit slit to that of the detector. This is desirable so that as much of the energy leaving the exit slit arrives and is absorbed by the detector. There are a number of optical condensing systems which are used for this purpose. They are the off-axis ellipsoidal mirror,[78] the Pfund[55] system, the light pipe and condensing cone,[79-84] the toroidal mirror, and the beam-spitter arrangement of Benesch and Strong.[85] These systems are illustrated in Figure 3.

The particular choice of detector optics depends upon the relative aperature sizes of the exit slit and detector sensitive area; and the type of detector used. For example, those detectors operating at cyrogenic temperatures are almost exclusively illuminated by the light-pipe condensing-cone optical system. On the other hand,
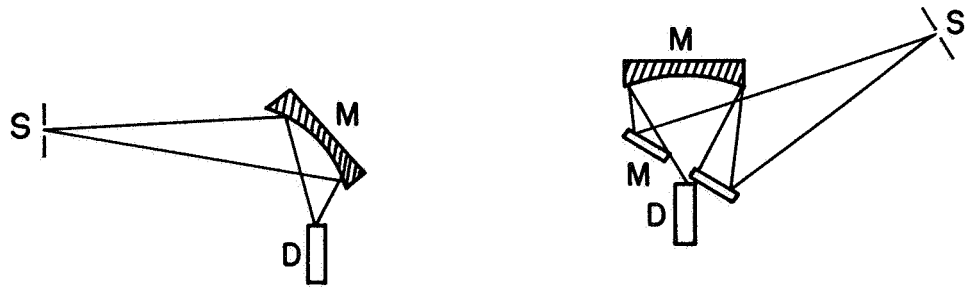
OFF-AXIS ELLIPSOID

PFUND
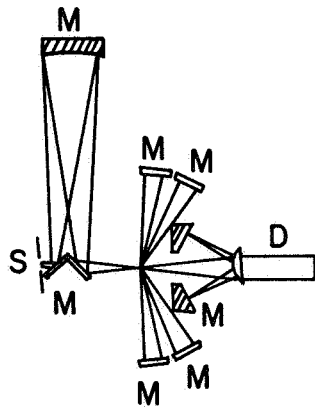
BEAM-SPLITTER
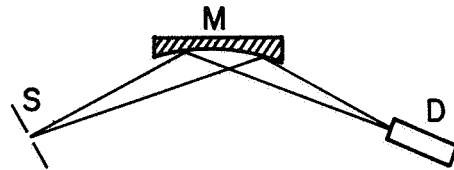
TOROID
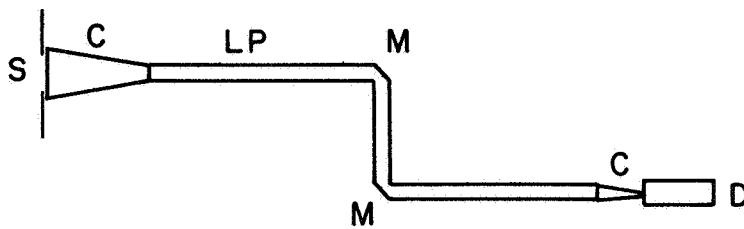
LIGHT-PIPE CONDENSING-CONE

DETECTOR OPTICS

FIGURE 3

room temperature operated detectors are usually more amenable to some type of mirror illumination.

Section 3. Dispersive Elements

There are several properties of dispersing elements which must be discussed. They are the angular dispersion, the resolving power, and the effective transmission. There are two types of dispersing elements used in infrared spectroscopy, the prism and the diffraction grating. As mentioned before, the lack of far-infrared transmitting materials for fabrication of prisms has resulted in the use of the diffraction grating. Since prisms are used in the near and middle infrared to about 60 microns, a short discussion of their properties will be included for completeness. The following discussion follows that of Strong.[86]

A. Prisms

Figure 4A illustrates a prism being illuminated for minimum deviation illuminated by a collimated beam of polychromatic light. The beam lies at an angle δ relative to the base of the prism. The apex angle, primary face, and base length of the prism are 2 ϵ, f, and b, respectively. If i, i', r, and r' are the angles of incidence and refraction at the primary and secondary faces, then

$$i' = r = \epsilon \qquad \text{and} \qquad i = r' = \epsilon + \delta .$$

Hence, Snell's law at the secondary face gives

$$N \sin \epsilon = \sin (\epsilon + \delta) ,$$

where N is the index of refraction of the prism material. For minimum deviation, the angle of total deviation is given by $\alpha = 2\delta$, and therefore,

$$\frac{d\alpha}{dN} = \frac{d(2\delta)}{dN} = \frac{2 \sin \epsilon}{\cos (\epsilon + \delta)}$$
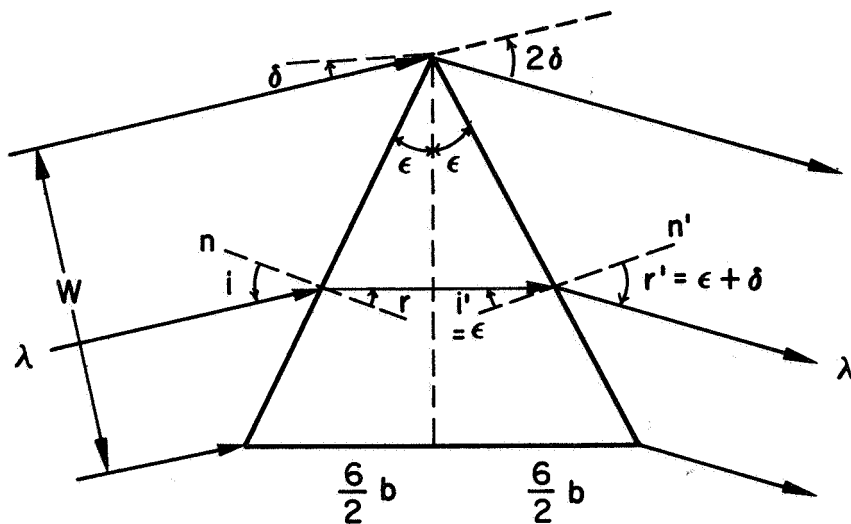
(A)

DISPERSION BY A PRISM

FIGURE 4A
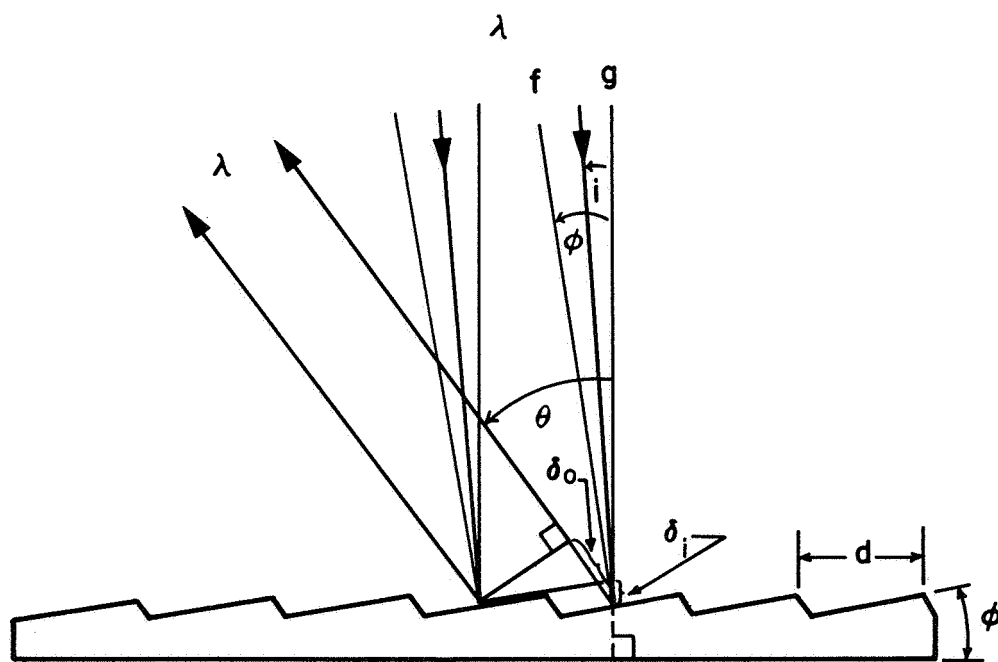
(B)

DISPERSION BY AN ECHELETTE GRATING

FIGURE 4B

From the geometry, $\sin \epsilon = b/2f$ and $\cos(\epsilon + \delta) = w/f$, where w is the projection of the primary face onto the beam. Hence,

$$\frac{d\alpha}{dN} = \frac{b}{w}$$

Defining the prism material property $N(\lambda)$ as the index of refraction as a function of wavelength, then the prism material can be described by $dN/d\lambda$. Finally, the angular dispersion of the prism, defined as $d\alpha/d\lambda$, is given by

$$\frac{d\alpha}{d\lambda} = \frac{d\alpha}{dN} \frac{dN}{d\lambda} = \frac{b}{w} \frac{dN}{d\lambda}$$

Using the Rayleigh resolution criterion the minimum angle between two rays of light just resolvable when viewed under diffraction-limited conditions is given by

$$\delta \alpha_R = \frac{\lambda}{w}$$

where ω is the width of the diffracting aperature. Hence, the spectral resolving power of a prism is given by

$$\frac{\lambda}{\delta\lambda_R} = \frac{\lambda \left(\frac{d\alpha}{d\lambda} \right)}{d\alpha_R} = b \left(\frac{dN}{d\lambda} \right)$$

The effective transmission of a prism consists of several factors. The spectral transmission properties determine the absolute transmission and the usable wavelength region within which the material can be used, and the surface conditions determine the amount of energy which is reflected at each surface. This reflection loss is due to the non-normal incidence of light passing through the prism, and any irregularity of the surface relative to the wavelength. Table II lists various properties of prism materials used in the infrared.

TABLE II

PROPERTIES OF PRISM MATERIALS

(After Smith, Jones, and Chasmar[50])

Material	Usable Long Wavelength Limit (microns)
*Quartz	3.5
LiF	6
CaF_2	9
Rock Salt	16
AgCl	20
KRS-6	25
KBr	28
KRS-5	40
CsBr	40
CsI	50

*Crystalline or fused

B. Diffraction Gratings

In general, there are two types of diffraction gratings, the amplitude and phase gratings. In each type, the corresponding parameter is varied periodically across the wave front incident on the grating surface. This periodic variation is caused by ruling equal parallel straight grooves of special shapes on the smooth grating surface. The characteristic amplitude pattern is the result of a complex interaction of diffraction and interference effects. Each of the above types may be either transmission or reflection gratings where the latter are almost always of the phase type. In practice, a number of special forms of these gratings have been developed. Figure 5 illustrates the wire,[17] lamellar,[22] echelle,[87-88] echelette[89-92] and echelon[93] type gratings.

The wire grating, the first to be widely used in infrared spectrometry, has been replaced in practice by the echelette reflection grating. The echelle and echelon gratings have found use in optical high-resolution spectrometry, and the lamellar grating has found wide use in far-infrared interferometry.[94-98] Since the echelette reflection grating is the only type used in far-infrared spectrometers, it will be the only type analyzed here. The analysis consists of finding the intensity distribution resulting from the periodic phase retardation of the incident wave front by the grating grooves. The following analysis is based on that by Jenkins and White.[99]

Referring to Figure 4B, consider an ideal echelette grating of grating constant d, and facet angle θ. For monochromatic illumination, the amplitude contribution of a single facet due to diffraction is the well known function

$$a = a_o \frac{\sin \beta}{\beta} \, ,$$
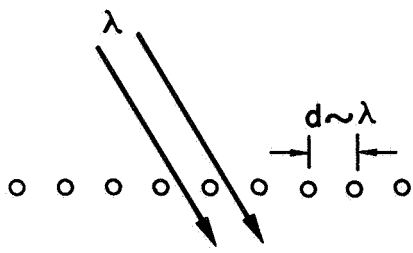
WIRE
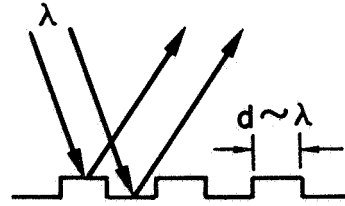
LAMELLAR
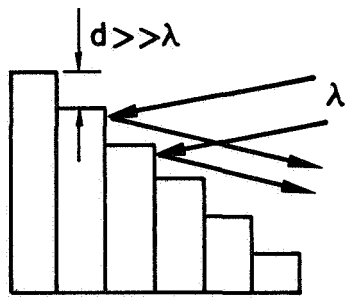
ECHELON
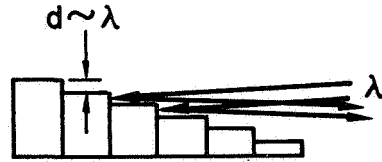
ECHELLE
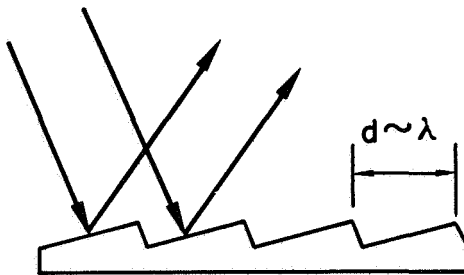
ECHELETTE

PLANE GRATINGS

FIGURE 5

where

$$a_o = \frac{bd}{x} \quad , \quad \beta = \pi d(\sin i + \sin \theta)/\lambda \quad ,$$

x is the distance between the grating and the screen on which the amplitude a is being determined, i is the incident angle, and θ is the angle through which the light is diffracted. Since the phase of the incident wave front will be retarded by equal amounts δ from one facet to the next, the resultant complex amplitude for N facets will be the sum of those for each facet, i.e.,

$$A = a(1 + e^{i\delta} + e^{i2\delta} + \cdots + e^{i(N-1)\delta})$$

$$= a \frac{1 - e^{iN\delta}}{1 - e^{i\delta}} \quad .$$

The intensity is proportional to

$$A^2 = AA^* = a^2 \frac{(1-e^{iN\delta})(1-e^{-N\delta})}{(1-e^{i\delta})(1-e^{-i\delta})} = a^2 \frac{1-\cos N\delta}{1-\cos \delta} \quad ,$$

or, with

$$1 - \cos N\delta = 2 \sin^2\left(\frac{N\delta}{2}\right) ,$$

$$A^2 = a^2 \frac{\sin^2\left(\frac{N\delta}{2}\right)}{\sin^2\left(\frac{\delta}{2}\right)} \quad .$$

Combining results, the resulting intensity distribution is given by

$$I \sim A^2 = A_o^2 \frac{\sin^2\beta}{\beta^2} \frac{\sin^2\left(\frac{N\alpha}{2}\right)}{\sin^2\left(\frac{\alpha}{2}\right)} \quad .$$

The factor containing N is due to interference of the N facets, while that containing β is the single-facet diffraction envelope. The interference factor has principal maxima of magnitude N^2 at $\delta/2 = m\pi$.

From Figure 4B, the geometry reveals that

$$\delta = 2\pi d (\sin i + \sin \theta)/\lambda \, ,$$

and hence, the principal maxima are located at

$$m \lambda = d (\sin i + \sin \theta) \, .$$

This is known as the grating equation, and m is called the order number. The interger m represents physically the number of wavelengths in the path difference from corresponding points on two adjacent facets and represents the order of interference. The relative intensities of different orders are governed by the diffraction envelope function. From the diffraction curve it is evident that there also exist secondary maxima. These maxima are not equally spaced, and their intensities fall off on either side of each principal maximum. Since there are $N-2$ of these secondary maxima, they increase in number with N, but at the same time, their intensity decreases.

In practical spectroscopy, N is very large and the secondary maxima are negligible. In this case, the principal maxima are the spectrum lines, which are just the images of the illuminated entrance slit of the spectrometer.

The above discussion considers only monochromatic light. For polychromatic light incident on the grating, similar intensity distributions will occur for each wavelength present in the incident light. Hence, each order will be a line spectrum. For white light sources, each order spectrum will be spread out into continuous spectra composed of an infinite number of adjacent images of the slit in light of the different wavelengths present. At any point in a given order spectrum, the light will be very nearly monochromatic because of the narrowness of the slit images formed by the grating

and monochromator mirrors. This is where mirror aberrations and slit width have a tremendous effect on the final resolving power of the spectrometer.

The angular dispersion of the diffraction grating is obtained easily from the grating equation. It is given by

$$\frac{d\theta}{d\lambda} = \frac{m}{d \cos \theta} \cdot$$

This shows that the dispersion increases for each order, is inversely proportional to the grating constant and the cosine of the diffraction angle, being larger for larger angles.

The linear dispersion in the exit slit focal plane of the telescope mirror is given by $d\ell/d\lambda$, where $d\ell$ is the distance along the exit slit plane between two spectrum lines. This is given approximately by $d\ell = fd\theta$, where f is the focal length of the telescope mirror. Hence, the linear dispersion is given by

$$\frac{d\ell}{d\lambda} = \frac{fm}{d \cos \theta} \cdot$$

From the grating equation, it is evident that various wavelengths will occur simultaneously at the exit slit since for a given angle θ,

$$d(\sin i + \sin \theta) = \lambda_1 = 2\lambda_2 = 3\lambda_3 = \ldots,$$

i.e., $\lambda_1, \frac{\lambda_1}{2}, \ldots, \frac{\lambda_1}{m}, \ldots$ will all "overlap" at the same diffraction angle θ. This phenomenon, which was discussed in Chapter II, Section 1, is a primary difficulty in far-infrared spectroscopy. These higher order spectra must be removed by various filtering mechanisms.

As in the case of the prism, the spectral resolving power of the diffraction grating is given by

$$\frac{\lambda}{\delta\lambda_R} = \frac{\lambda}{d\theta_R} \left(\frac{d\theta}{d\lambda} \right) ,$$

where $d\theta_R$ is the minimum angle between two spectral lines which are just resolvable using the Rayleigh criterion, and θ is the diffraction angle. Hence, from the Rayleigh criterion for a rectangular aperature,

$$d\theta_R = \frac{\lambda}{B} = \frac{\lambda}{N d \cos \theta} ,$$

where B is the width of the diffracted beam. Hence,

$$\frac{\lambda}{\delta\lambda_R} = N d \cos \theta \frac{m}{d \cos \theta} = Nm .$$

Thus, in a given order, the resolving power is determined solely by the number of grooves N.

The resolving power for given angles can be found by combining the above equation with the grating equation. This is given by

$$\frac{\lambda}{\delta\lambda_R} = \frac{Nd}{\lambda} (\sin i + \sin \theta) .$$

The theoretical maximum resolving power obtainable with any grating occurs when $i = \theta = 90^\circ$, and has the value of $\lambda/\delta\lambda_R = 2Nd/\lambda = 2W/\lambda$, where W is the total width of the grating. In practical situations, where it is necessary to have large beam widths, the resolving power is much less than this value. A comparison between experimental and theoretical resolving power is given by Sassa.[100]

The preceding analysis assumes an ideal grating, which corresponds to an infinitely thin surface containing multiple slits. The echelette reflection grating obviously does not meet these requirements, since the sides of each facet will also have an effect on the diffraction-interference pattern. The relative intensities of the

different orders for the echelette grating will not be governed by the simple function

$$\sin^2 \beta / \beta^2$$

as in the ideal case. This modification results in the reappearance of some orders which were missing in the ideal case. The latter occurred when $\sin^2 \beta / \beta^2$ vanished, and hence, any maxima corresponding to this angle would be missing. The modification of the intensity distribution caused by the echelette groove shape does not have any effect on the positions of the spectral lines. The most important effect of the groove shape is that the relative intensity of the different orders is determined by the angular distribution of the light diffracted by a single groove. This angular distribution is a complex factor and was first controlled by groove shape by Wood.[89] By properly controlling the groove shape, echelette gratings can concentrate up to ninety percent of light of a particular wavelength in a single order, while less than one percent is diffracted into each of the remaining orders.

From the grating equation and the relation for β in terms of i, θ, d and λ, it is evident that

$$\beta = \frac{\pi d}{\lambda} (\sin i + \sin \theta) = m \pi$$

Hence, the intensity distribution in terms of order number is given by

$$I \sim A^2 = A_o^2 \frac{\sin^2 m \pi}{(m \pi)^2} \frac{\sin^2 \left(\frac{N \delta}{2} \right)}{\sin^2 \left(\frac{d}{2} \right)} \quad ,$$

i.e., for a given order, I is inversely proportional to m^2. This result is why only the first order spectrum is used in far-infrared grating spectrometers; it is the order of highest energy.

There still remains several modifications of the above results due to non-ideal conditions imposed on the grating. First, the grating is not illuminated by perfectly collimated light since mirrors or lenses always possess some aberration. The effect of this condition and how to minimize it is discussed by Mielenz[101] and Murty.[102] Second, the ruling of echelette gratings is an extremely difficult task, and the result of poor quality gratings can be very deleterious to results obtained from them in interpreting spectra. Poor quality gratings usually have two effects on the resulting spectra; these are low intensity due to non-optically flat facet-surfaces, which cause diffuse scattering, and the appearance of ghosts due to aperiodic ruling of the grating. The latter phenomenon is very common and usually caused by errors in the ruling engine lead screw or non-uniform cutting of the groove depths. These ghosts are relatively bright spectrum lines or dark bands which appear in the spectrum, but are not predicted by the ideal grating theory.

Theories for the different types of ghosts and their interpretation are discussed by Palmer,[103] Stewart and Galloway,[104] Palmer, et al.,[105] and Hessel and Oliver.[106] A series of articles by Harrison,[107-111] Stroke,[112-114] and Babcock[115, 116] describe the art of producing extremely precise gratings.

Finally, much more sophisticated methods have been applied to the problem of determining the theoretical energy distribution of diffraction gratings. Selected articles on this subject are by Stamm and Whalen,[117] Meecham, et al.,[118-119] Madden and Strong,[120] and Sakayanagi.[121]

Section 4. Energy Limited Resolving Power

The Rayleigh criterion for the limit of resolution is only applicable to systems in which the resolution is diffraction limited.

In spectral regions, such as the far-infrared, which have energy sources of very limited intensity, or detectors of poor detectivity, the slits must be opened large enough to be able to detect a signal at the exit slit. This opening of the slits removes the condition of diffraction-limited resolution. The problem of energy-limited resolving power has been discussed by Strong.[86, 122] This article shows that the energy emergent through the exit slit is given by

$$W = B_\lambda \, \ell w \, S \, \Delta \, \lambda \, T / f^2 \quad \text{watts,}$$

where B_λ is the spectral brightness at the entrance slit in watts per steradian solid angle, per unit spectral band pass, ℓ and w are the length and width of the equal entrance and exit slits, S is the effective projected area of the grating, $\Delta\lambda$ is the wavelength band pass determined by the size of the slits and dispersion of the system, T is the transmission factor for the system, and f is the equal focal length of the collimator and telescope mirrors. The appropriate form of $\Delta\lambda$ as defined above is from the linear dispersion of the system, i.e.,

$$\frac{\Delta \ell}{\Delta \lambda} = f \frac{d\theta}{d\lambda} \quad ,$$

where $\Delta\ell$ is the distance between two adjacent spectrum lines separated by $\Delta\lambda$. Since $\Delta\ell = w$, then

$$\lambda = \frac{w}{f} \frac{d\lambda}{d\theta}$$

Combining this equation with that for w, the result is given by

$$\Delta\lambda = \left[\frac{Wf}{B_\lambda \, \ell S T \, d\theta/d\lambda} \right]^{1/2}$$

If the minimum detectable power by the detector is W^*, then the above relation must be modified, and is given by

$$\Delta\lambda = \left[\frac{W^*f}{B_\lambda \; \ell ST \; d\theta/d\lambda} \right]^{1/2} .$$

The specialized equation for an echelette grating being used in the first order is

$$\Delta\lambda = \left[\frac{W^*f \; d \cos \theta}{B_\lambda \; \ell ST} \right]^{1/2} ,$$

wherein the angular dispersion is

$$\frac{d\theta}{d\lambda} = \frac{1}{d \cos \theta} .$$

For black-body energy sources, B_λ is given by the Planck radiation law

$$B_\lambda = \frac{2hc^2}{\lambda^5} \frac{e^{-hc/\lambda k \Theta}}{1 - e^{-hc/\lambda k \Theta}} ,$$

where k is Boltzmann's constant, h is Planck's constant, c is the speed of light, and Θ is the absolute temperature. For long wavelengths, i.e., in the far-infrared, $\frac{hc}{\lambda k \Theta} \ll 1$, and B_λ reduces to the Rayleigh-Jeans law

$$B_\lambda = \frac{2ck\Theta}{\lambda^4} .$$

For this case,

$$\Delta\lambda = \left[\frac{W^*f \; d \cos \theta \; \lambda^4}{\ell ST \; 2 \, ck \Theta} \right]^{1/2} .$$

In terms of wave number, from $\lambda \nu = c$,

$$\Delta\nu = \frac{c}{\lambda^2} \Delta\lambda ,$$

and hence,

$$\Delta\nu = \left[\frac{W^* \, fd \, c \, \cos \theta}{\ell ST \; 2k\Theta} \right]^{1/2} .$$

This equation provides much insight to the design of far-infrared spectrometers. First, to reduce $\Delta\nu$ by one half, it is necessary to increase the detector sensitivity or the available energy, or the dispersion by a factor of four. Second, the wave number resolving power is independent of wavelength in the far-infrared except in that d must be increased with wavelength. In terms of spectrometer components, the minimum detectable power should be as low as possible; and the geometrical factor $(f/\ell S)^{1/2}$ should be as small as possible. The latter condition requires that the focal length should be short, the slit length long, and the projected area of the grating large. These requirements specify fast optics, which have their own inherent problems. The most significant of these problems is the poor imaging properties of spheroidal and paraboloidal mirrors for off-axis rays. With long slits and fast optics, the off-axis rays eminating from the entrance slit ends are poorly imaged at the exit slit plane, and hence, create much difficulty in shaping the exit slit to conform to the non-straight spectrum lines. This latter condition is required so that the exit slit can isolate adjacent spectrum lines over their whole length, and hence, provide good spectral purity and resolving power. The transmission factor T occurring in the above equation is discussed for various spectral orders by Barrekette and Christensen.[123] Much effort has been expended on the task of minimizing the aberration effects in spectrometers by improving the optical arrangements of monochromators. This problem has been discussed in Chapter II, Section 2. Some specific references on this subject are References 58 through 62.

A comparison of some of the above properties of grating, prism, and Fabry-Perot etalon type spectrometers is given by Jacquinot.[124]

Section 5. Filters

The types of filters used in the far-infrared can be classified as either transmission or reflection filters. Within each of these categories, there are several basically different filters. As was discussed in Chapter II, Section 1, when working in the first order of a given grating, all the higher-energy, higher-order wavelengths must be filtered out. The overall filtering task for any wavelength region in the far-infrared is accomplished in steps. First, all the energy radiated by the source with wavelengths shorter than about 12 microns can be eliminated using one or more 0.1 mm thick sheets of black polyethylene. This filter, which consists of carbon dispersed in high-density polyethylene, transmits with the transmission increasing with wavelength throughout the entire far-infrared region. The transmission reaches 50 percent at about 25 microns, and is better than 80 percent at 125 microns, as shown in Figure 6A. The number of sheets necessary to remove the desired amount of short-wavelength energy can be determined experimentally. Another long-wavelength pass filter for the far-infrared is crystalline quartz. As seen in Figure 6B, when natural Brazilian quartz is used along the y-crystalline axis, the cut-on curve is very sharp, beginning to transmit at about 40 microns, and reaching 50 percent transmission at about 55 microns.[126, 127] When the Golay pneumatic cell is used as the detector, its quartz window acts as a filter, and therefore, it is not necessary to use further quartz.

Another type of long wavelength pass filter consists of flat plates roughened by grinding with different grades of carborundum grit. These plates scatter the short wavelengths out of the beam, but do not effect the long wavelengths. The cut-on curve is very slow, as shown by Strong[128] and Figure 6C. The cut-on wavelength can be shifted by choice of grit size.
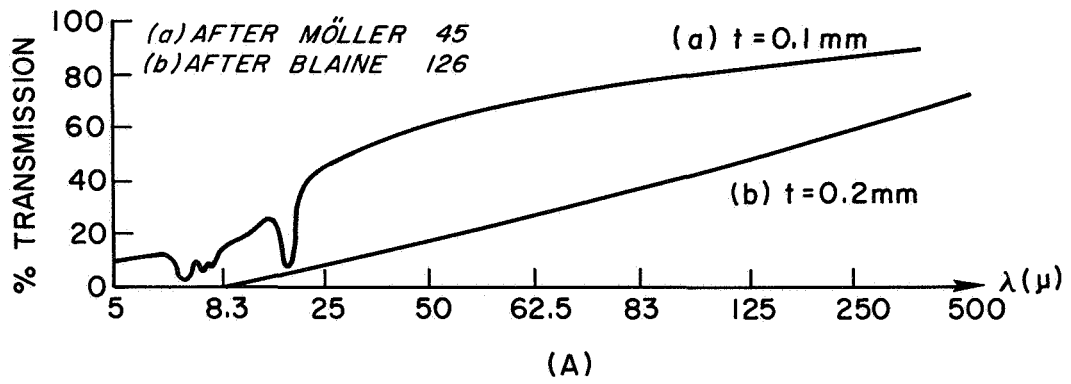
FILTERING CURVE FOR BLACK POLYETHYLENE

FIGURE 6A
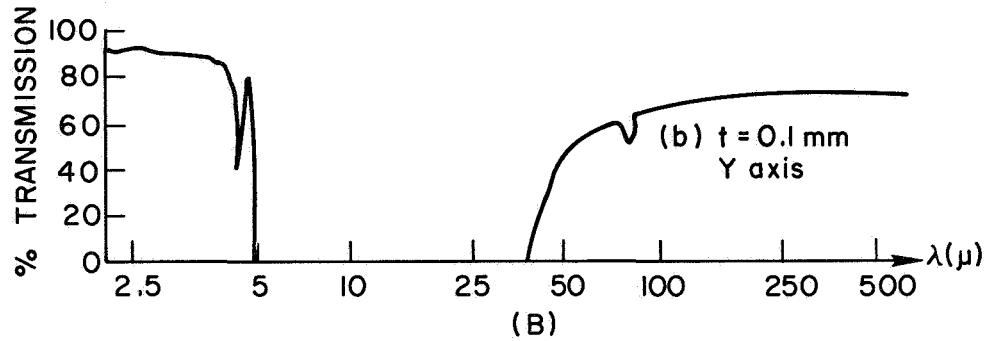
FILTERING CURVE FOR CRYSTALLINE QUARTZ

FIGURE 6B
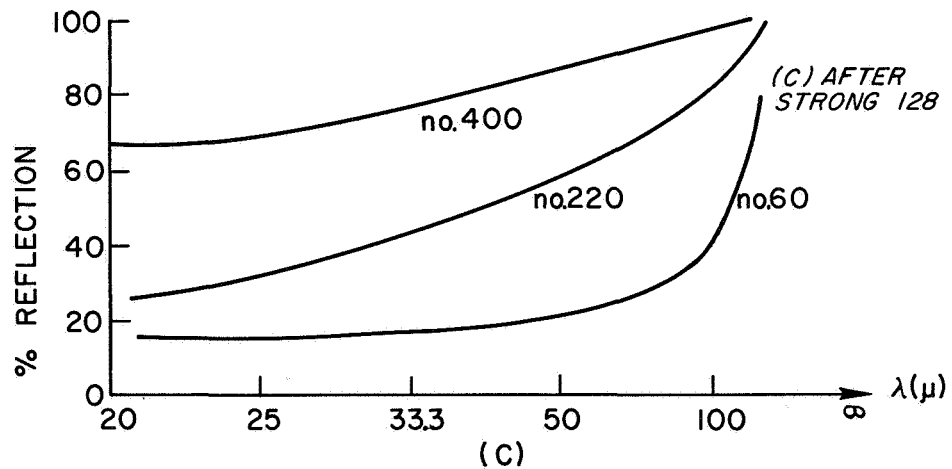
FILTERING CURVE FOR ROUGHENED BRASS

FIGURE 6C

The remainder of the filtering task consists of finding a set of filters with as sharp cut-on curves as possible, and with cut-on wavelengths which occur in succession in such a way that the set covers the entire region to be investigated. It is also required that each filter or combination of filters be opaque for wavelengths between the cut-on wavelength and the region where the black polyethylene or quartz filters begin to transmit. This task has been accomplished in a variety of ways in the far-infrared by spectroscopists. The filtering methods which have been developed are restricted to sub-regions of the far-infrared. The region between 25 and about 250 microns is covered by the use of reststrahlen or residual-ray reflection plates or by powder filters made by dispersing reststrahlen crystal powders in high-density polyethylene. The region of wavelengths greater than 250 microns is covered by either reflection grating filters, metal-mesh reflection filters, or transmission-grating filters. Each of these filter types will be discussed in detail.

A. Reststrahlen

Reststrahlen reflection has been used for filtering in the far-infrared longer than any other method. The technique consists of utilizing the strong reflection bands typical of most ionic crystals in the infrared. This strong reflection band is well explained by classical solid state theory.[129] By considering a linear or one-dimensional crystal lattice consisting of two kinds of atoms of masses m and M, the resulting dispersion relation is given by

$$\omega^2 = \beta \left(\frac{1}{m} + \frac{1}{M} \right) \pm \beta \left[\left(\frac{1}{m} + \frac{1}{M} \right)^2 - \frac{4 \sin^2 ka}{Mm} \right]^{1/2}$$

where β is the elastic force constant, a the lattice constant, and k the wave number of the lattice phonon given by $k = 2\pi/\lambda$.

This dispersion relation has two well known branches of frequency versus wave number. The acoustical and optical modes correspond respectively to the minus and plus signs. If the influence of an electromagnetic field, given by

$$E = E_o \, e^{iwt}$$

on this system is analyzed, the amplitudes of the oscillations of the two masses are found to be given by

$$\eta = \frac{(e/M)\, E_o}{\omega_o^2 - \omega^2} \, ,$$

and

$$\xi = - \frac{(e/M)\, E_o}{\omega_o^2 - \omega^2} \, ,$$

where

$$\omega_o^2 = 2\beta \left(\frac{1}{m} + \frac{1}{M} \right) .$$

Hence, it is evident that a resonance will occur for $\omega = \omega_o$. This absorption maximum is associated with the motion of charges of opposite sign toward each other. The maximum of the reflection at the surface of an ionic crystal has a frequency which is very close to that of the absorption resonance.

The reststrahlen reflection bands have been measured for a multitude of crystals by Sinton and Davis,[130] Yoshinaga,[131] Plyler and Acquista,[132] and Mitsuishi, et al.[133] These curves have been collected and organized by McCarthy.[134] As can be seen from the curves in Figure 7, these crystals have good cut-on curves, but they transmit about 4 percent below the cut-on wavelength. This property requires at least three reflections in order to reduce the unwanted energy to an acceptable level. Methods for improving the
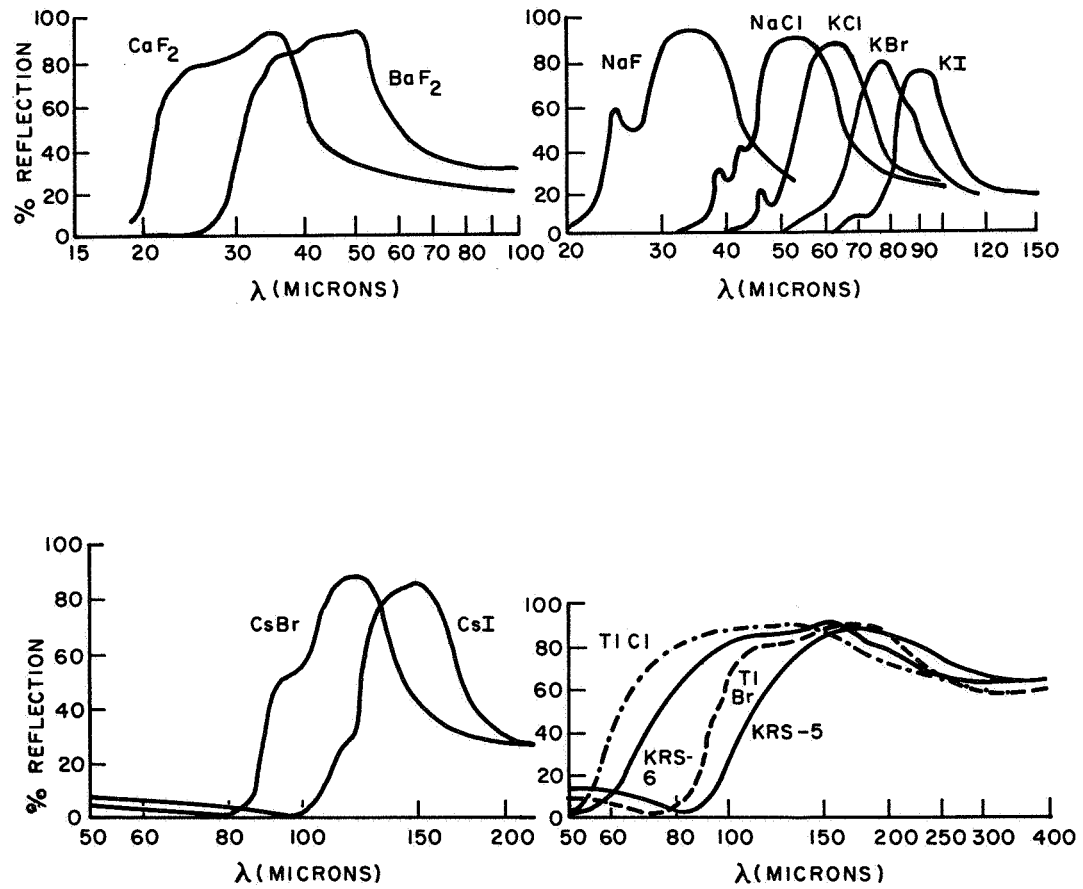
RESTSTRAHLEN REFLECTION CURVES

FIGURE 7

reflection of reststrahlen crystals has been discussed by Turner, et al.[33] In the region where these crystals can be used as filters, better filters have been devised. These are the crystal powder transmission filters developed by Yoshinaga.[39]

B. Powder Transmission Filters

In 1961, it was reported that polyethylene sheets containing finely ground powders of reststrahlen crystals made excellent filters for the far-infrared from 25 to 300 microns. High-density poly-ethylene has no absorption bands at wavelengths greater than 14 microns, and 1 mm thick sheets transmit 90 percent or more throughout the far-infrared.[127] Hence, this material is ideal for a medium in which to suspend powders of various substances in order to measure their far-infrared absorption spectra. As shown above, reststrahlen crystals have very strong absorption bands in the region from 20 to 120 microns. Single crystals of these materials cannot be made thin enough to transmit enough energy in the far-infrared, but by grinding these crystals into fine powders, and suspending them in polyethylene, their absorption bands can be used to isolate successive wavelength regions from 25 to 300 microns. The cut-on wavelength of these filters can be shifted by appropriate choice of crystals. The steepness of the cut-on curves can be increased by using finer powder size and/or thinner sheets of polyethylene.

Various techniques have been proposed for making these filters. The original authors[39] place a sheet of polyethylene on a heated set of rollers which have been plated with copper, nickel and chromium. When the sheet becomes soft, measured amounts of powders are added by pouring uniformly over the sheet. The poly-ethylene and powders are then mixed with a spatula for about thirty minutes with the rollers still rotating. After complete mixing, the

electricity is turned off and the sheet mixture cooled and hardened. After stopping the rollers, the sheets are removed. This procedure results in sheets about 0.3 mm thick, which are then cut to the desired sample size.

The particle size is very critical in these filters. The above reference shows that the commercially obtained powder is so course that the radiation can pass through the spaces between the particles, and hence, the transmission never reaches zero, even in the region of reststrahlen absorption. They also show that the steepness of the cut-on curve varies directly with the fineness of the powder, and that a particle size of about 10 microns is desirable. This can be achieved by using a mortar and pestal or by ball milling, and then checking with a 10 micron sieve.

The proper amount of powder is also very important. Too much powder will cause the cut-on curve to lose steepness, and too little will not make the filter opaque in the reststrahlen absorption region. The optimum amount of powder was given as 250 mg. The polyethylene sheet thickness of 0.3 mm was used since it was found to be too difficult to make thinner sheets containing several kinds of powders.

Figure 8A shows the transmission spectra of reststrahlen powders in polyethylene. It can be seen that for most of the crystals, there is an opaque region on the short wave side of the cut-on wavelength, and then the powders begin to transmit again. By properly combining several powders, transmission curves can be obtained that are opaque from the cut-on wavelength to about 20 microns. Selected combinations of powders as suggested by the above authors are also shown in Figure 8A. These filters transmit better than 80 percent in the long wave regions, and transmit less than 0.1 percent
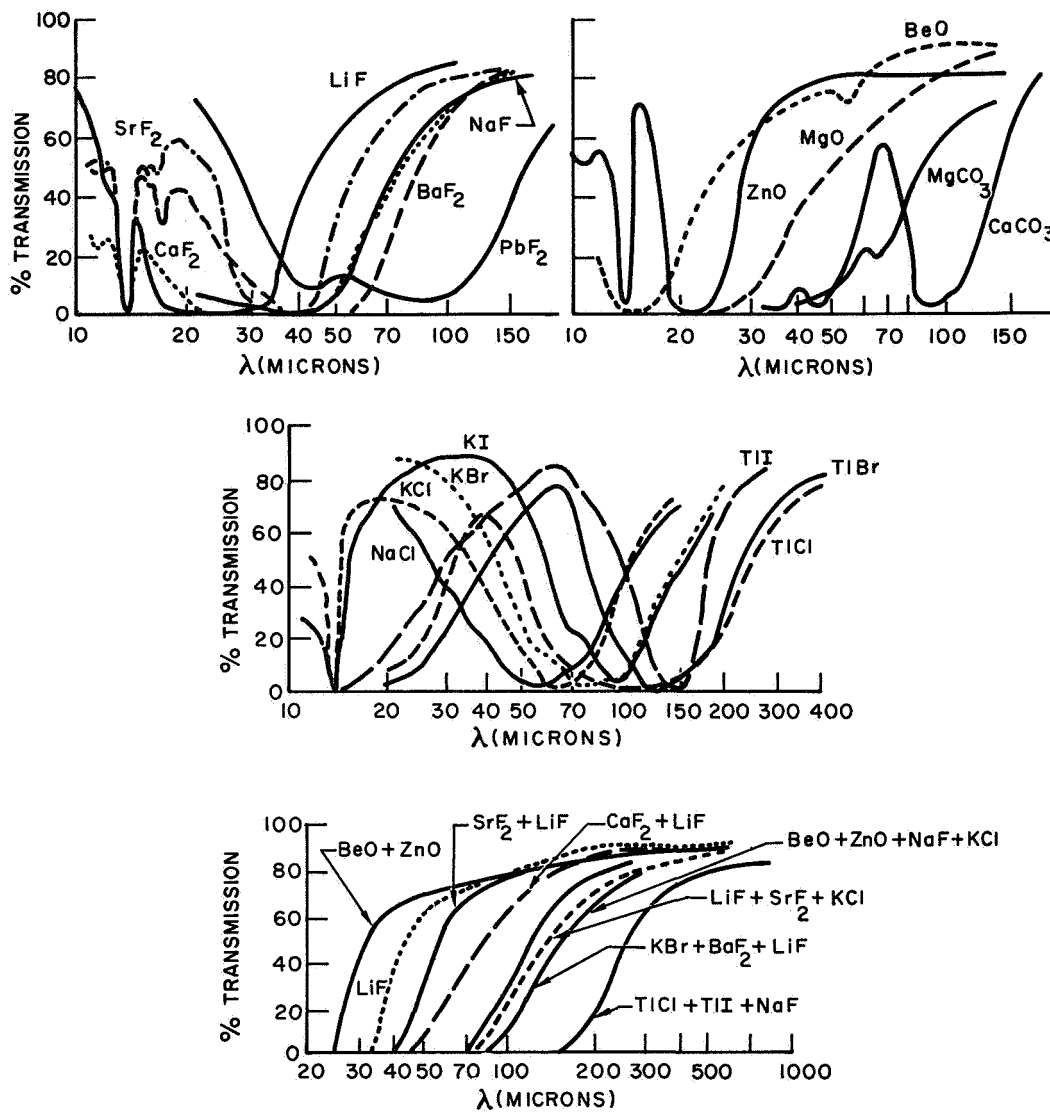
POWDER FILTER CURVES (YOSHINAGA)

FIGURE 8A

in the opaque regions. By comparison, these properties are much better than those of the reststrahlen reflection filters which transmit 4 percent of the undesirable wavelengths.

Further inorganic crystals have been investigated by Manley and Williams.[127] They have reported an error in the $T\ell C\ell$, $T\ell I$, NaF filter transmission curve, which appeared in Yoshinaga's article.[39] These authors used a much simpler manufacturing procedure. The dry materials were ball-milled to pass through a 300 mesh sieve and then mixed with polythene on steam-heated rollers. The crude sheets were removed from the rollers and then pressed between stainless steel laminating plates at 140°C and 1500 psi in a steam-heated hydraulic press. The sheet thickness was controlled by the length of time in the press. The compounds were dispersed at a total concentration of 35 percent in sheets of 250 microns thickness. The curves for these filters are shown in Figure 8B. These authors carried out a thorough investigation of the effects of particle size. Comparing results to those of Clewell[128] and Henry,[129] they found that the maximum particle size for a single inorganic compound filler in a transmission filter is about half that of the wavelength of the reststrahlen-absorption peak. For a filter consisting of several inorganic materials, a range of particle sizes should be used according to the reststrahlen absorption bands present. A small portion of material whose particle size is small compared to $\lambda/2$ should be present to scatter short wave radiation and prevent it from passing through the spaces between the larger particles.

A third procedure for manufacturing these filters is given by Möller, et al.[46] Selected amounts of polyethylene powder and crystal powder are carefully mixed. The desired quantity is placed between sheets of aluminum foil and placed between the heated plates of a hydraulic press, without the use of a die. Pressures of 135 to
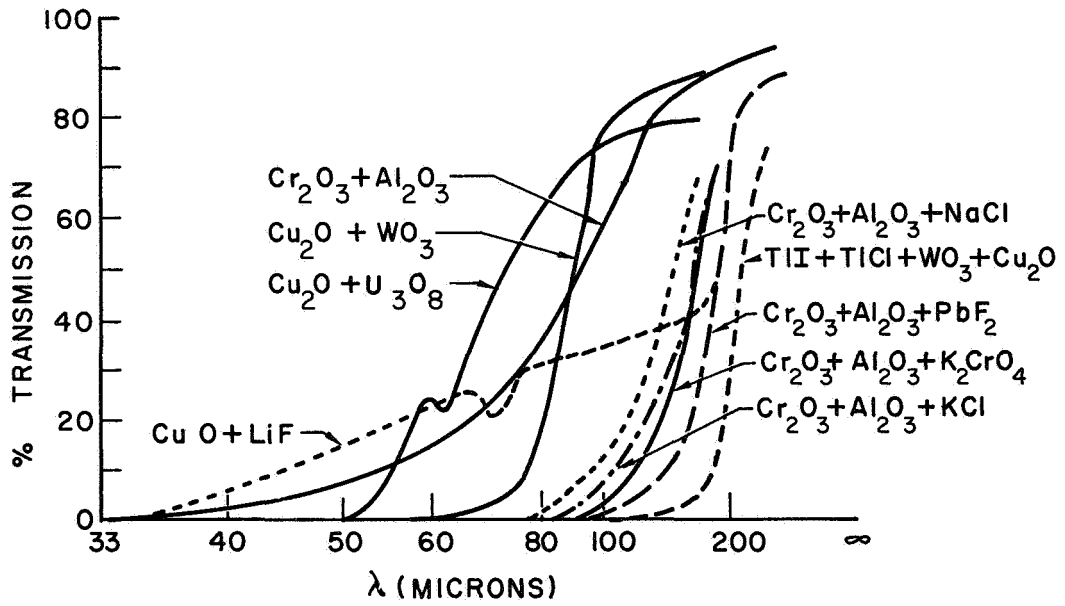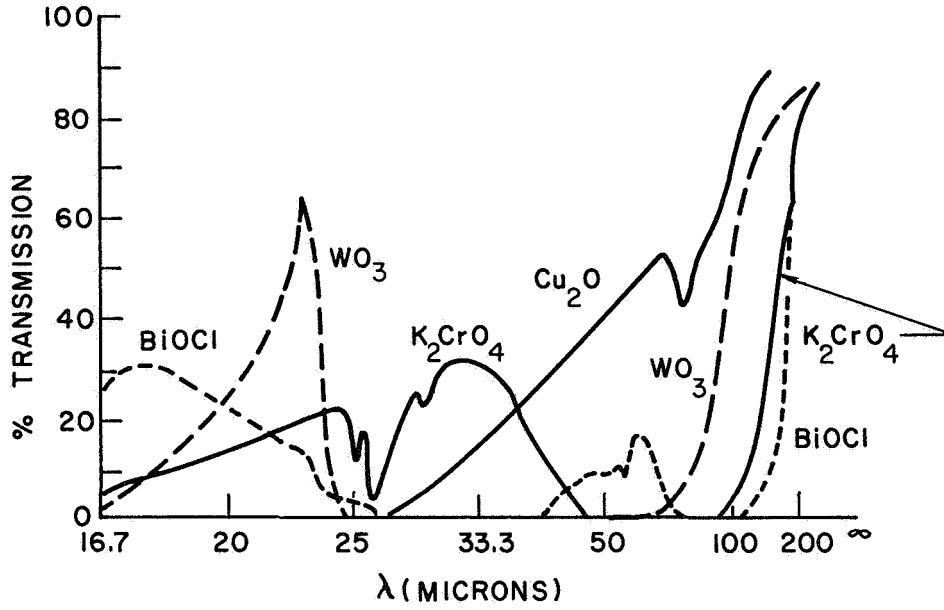
POWDER FILTER CURVES (MANLEY)

FIGURE 8B

270 atmospheres with a plate temperature of 150 degrees C are applied for 5 to 10 seconds. Upon removal, the composite is placed between two metal plates for cooling, after which the aluminum foil is easily removed. In order to achieve a homogeneous distribution of the powder in the polyethylene, the sheet is cut into several pieces and then repressed. This procedure is repeated five to ten times to assure uniform suspension. In order to avoid interference fringes, the filters should be wedge shaped. Alternately, in the long-wave-length regions, several very thin filters may be used.

C. Reflection-Grating Filters

The use of an echelette reflection grating as a simple mirror to remove short wavelength light from a beam containing infrared radiation of all wavelengths was first proposed by White.[35] Light of wavelengths short compared to the grating constant is diffracted out of the beam into dispersed spectra, whereas light of wavelengths long compared to the grating constant, can only go into the undis-persed zero order spectrum, which falls in the direction of normal reflection as if the grating were a plane mirror.

The cut-on curve is very similar to the intensity distribution for the zero-order spectrum. The cut-on wavelength occurs at about one-half the grating constant. The region of wavelengths from this value to that equalling the grating constant contains light from both the first and zero-order spectra, whereas the region of wavelengths greater than the grating constant contains light from only the zero-order spectrum. This is shown in Figure 9A. Since this cut-on curve has a relatively poor slope, it is necessary to use more than one reflection. Theory implies that the cut-on wavelength should vary approximately with the sine of the angle of incidence. Experi-mental investigation shows that the cut-on slope becomes steeper with
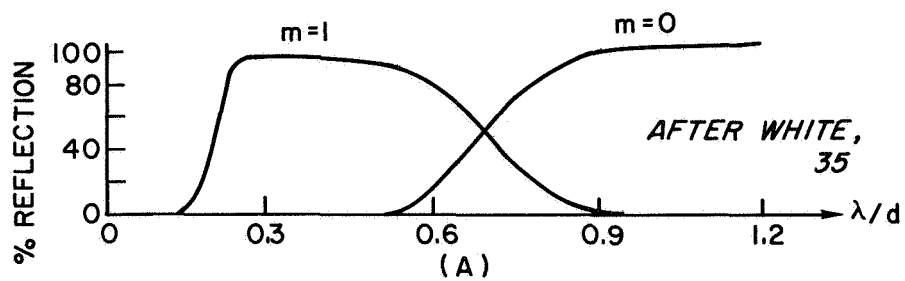
CUT-ON CURVE FOR REFLECTION-FILTER GRATING

FIGURE 9A
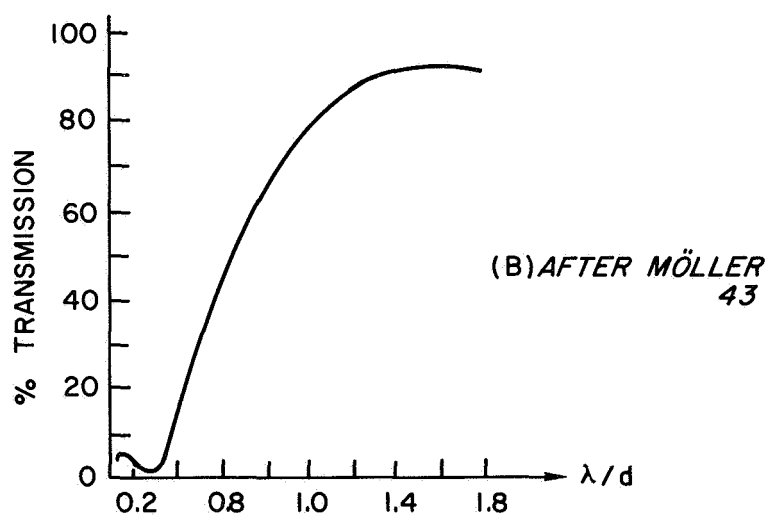
CUT-ON CURVE FOR TRANSMISSION GRATING

FIGURE 9B
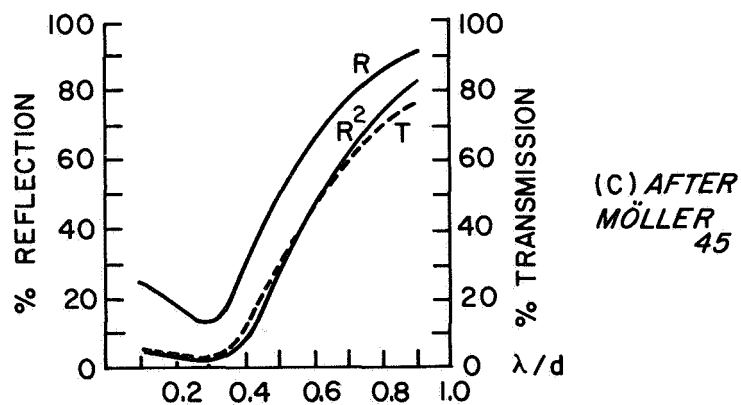
COMPARISON OF CUT-ON CURVES FOR T AND R^2

FIGURE 9C

decreasing angle of incidence. The long-wavelength-region trans-
mission also increases with decreasing incidence angle. Detailed
investigations of the properties of these gratings in the far-infrared
have been made by Hadni, et al.[138-140]

This type of filter no longer enjoys popular usage since the
development of the transmission-grating filter and metal-mesh re-
flection filter.

D. Transmission-Grating Filters

These filters are similar in nature to the reflection-grating
filter in that both types are used to diffract the short-wavelength
energy out of the beam of light illuminating the entrance slit of a
spectrometer. In both types of filters, the cut-on wavelength is
determined arbitrarily by varying the grating constant. The trans-
mission-grating filters are made simply by pressing polyethylene
sheets on heated forms on which grooves have been machined as in
the reflection-gratings. These filters were first proposed by Möller
and McKnight,[43] and have been discussed further by Möller,
et al.[44-47, 97] Both groove shape, and orientation of the grooves
with respect to the direction of incident light and the direction of the
grooves of the main dispersion grating have been studied. These
investigations have revealed that the symmetric groove with a 45
degree angle has the lowest transmission below the cut-on wave-
length. Four different orientations were studied. These were with
the grooves parallel and perpendicular to those of the dispersion
grating, and with the grooves or flat surfaces facing the incident
light. For gratings with symmetrical 45 degree groove shapes, the
orientation was found to have no effect on the cut-on curves.

A typical cut-on curve is illustrated in Figure 9B. It shows
that the cut-on wavelength occurs for $\lambda/d = 0.3$, where d is the

grating spacing. The transmission reaches a value of 50 percent at about $\lambda/d = 0.65$.

In order that the filters are not used at a wavelength such that one-half this wavelength is greater than the cut-on wavelength, these filters cannot be used for wavelengths greater than twice the cut-on wavelength. This condition is required so that the second order of a given wavelength is not transmitted by the filter. The above range of utilization of wavelengths from λ_c to $2\lambda_c$ is called one octave. Hence, the usable range of these filters is from $\lambda_c = 0.3d$ to $2\lambda_c = 0.6d$. Since the filter has zero transmission at λ_c, some other wavelength greater than λ_c must be chosen as the lower limit for the usable range. The value of $\lambda = 0.5d$ has been chosen by this author as being a reasonable choice, considering the tradeoff between minimum transmission and wavelength range for each filter. With this choice, these filters will be used in the 30 to 50 percent transmission region. This condition is a rather large reduction in energy, but these filters are the most efficient available for the region of wavelengths greater than 250 microns.

A comparison of reflection and transmission-grating filters, as shown in Figure 9c, implies that one transmission grating results in an equivalent filtering curve as for two reflection gratings. This result is the main reason for choosing transmission gratings over the reflection type. Another reason for this choice is the ease in which the transmission gratings can be applied; they can simply be placed in the beam, whereas the reflection gratings must be mounted at a point of reflection, usually by replacing a plane mirror. It has been established that combinations of two transmission-grating filters, quartz plate, and black polyethylene can be used to obtain good spectra in the far-infrared.[42] Since two of the transmission

gratings are necessary, Richards[91] has proposed pressing grooves on both sides of a polyethelene sheet with the grooves perpendicular to each other on opposite sides. This procedure also eliminates any polarization effects which may be caused by these filters. The sheets are usually about 0.2 to 0.4 mm thick before pressing.

E. Metal-Mesh Reflection Filters

Excellent reflection filters made of metal meshes of brass wire have been proposed by Renk and Genzel.[40] These filters consist of commercially available metal mesh or wire grid which can be described by the type of metal, the wire diameter a, and the distance d between the centers of adjacent wires. The parameter d has been referred to as the mesh constant. Mitsuishi, et al.,[41] and Vogel and Genzel[42] have carried out measurements of reflection and trans-mission in the far-infrared for meshes of various values of d and a. The former investigators used brass mesh at incidence angles of 15 and 52 degrees, while the latter used nickel at zero and 45 degrees. It has been established that the steepness of the cut-on slope is increased as the incident angle of light is decreased. A comparison of reflections from a 145# mesh at 15 and 52 degrees is given in Figure 10C. The reflectances of several meshes at 15 degrees is shown in Figure 10A for use as filters in the range from 150 to 800 microns.

The cut-on wavelength occurs at about $\lambda/d = 1.3$ to 1.5, with reflectivity exceeding 95 percent at $\lambda/d = 2$. These cut-on curves are much steeper than those for the two previous filter types discussed above. The reflectivity for wavelengths less than the cut-on wavelength is about 5 percent. This can be reduced substantially by using two or three reflections of the same mesh at nearly normal incidence. This last property makes the metal mesh a rather inconvenient filter.
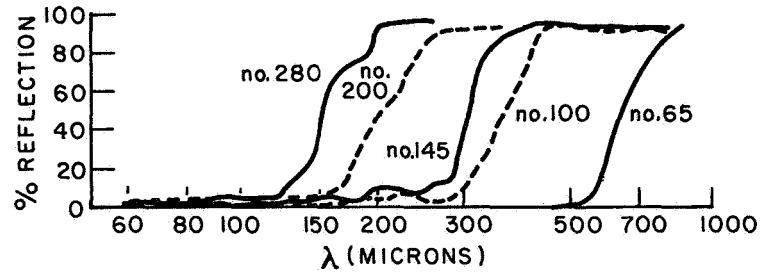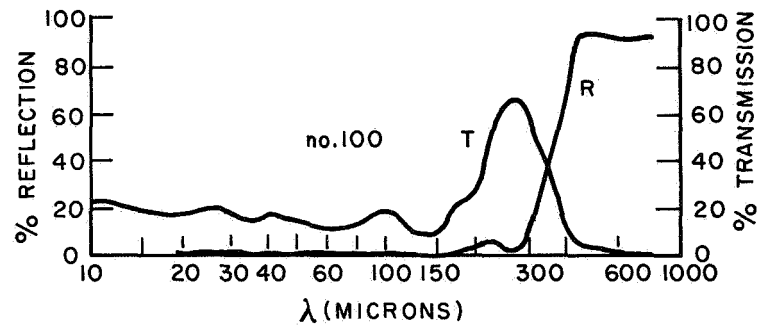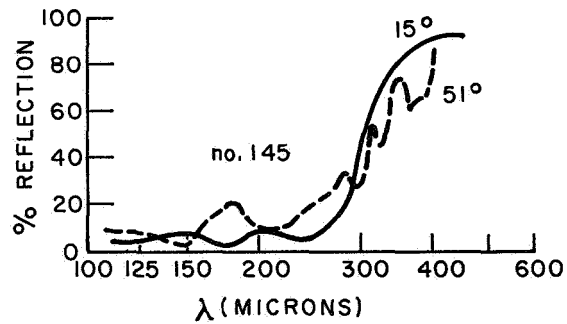
CUT -ON CURVES FOR METAL MESH FILTERS

FIGURE 10

The use of these meshes in a spectrometer has been discussed by Möller, et al.[45] They have established a useful wavelength region for filtering purposes as being from $\lambda/d \approx 1.8$ to $\lambda/d \approx 3.6$. The transmission is over 80 percent in two-thirds of this region. These authors have obtained good spectra in the region from 200 to 1000 microns by using three metal-mesh filters and 0.7 mm of black polyethylene.

Two types of metal mesh are commercially available. Inexpensive wire cloth may be purchased from the Newark Wire Cloth Co.[141] More expensive electroformed mesh is available from Buckbee Mears Co.[142]

It has been pointed out by Vogel and Genzel[42] that the excellent results obtained by Mitsuishi, et al., are in part due to the fact that the mesh used in the latter's measurements were made of wires with round cross-sections. The former investigators used mesh of rectangular shaped wires and obtained less steep cut-on slopes.

F. Selective Chopping

The last filtering mechanism to be discussed is that of selective chopping. This is done by constructing a chopper wheel made of blades of reststrahlen crystals which transmit the short wavelength energy, but absorb all the far-infrared energy. With this type of chopper, only the long wavelengths are amplified by the lock-in amplifier in the detecting circuit. The unmodulated short wavelength energy reaching the detector is constant in magnitude and, therefore, only affects the d.c. level or background radiation level. Figure 11 and Table 3 give the transmission curves and cut-off wavelengths for selected chopper materials. This type of filtering has one very undesirable quality; it cannot be rotated at very high speed due to the strength of the crystals. When working with fast response time
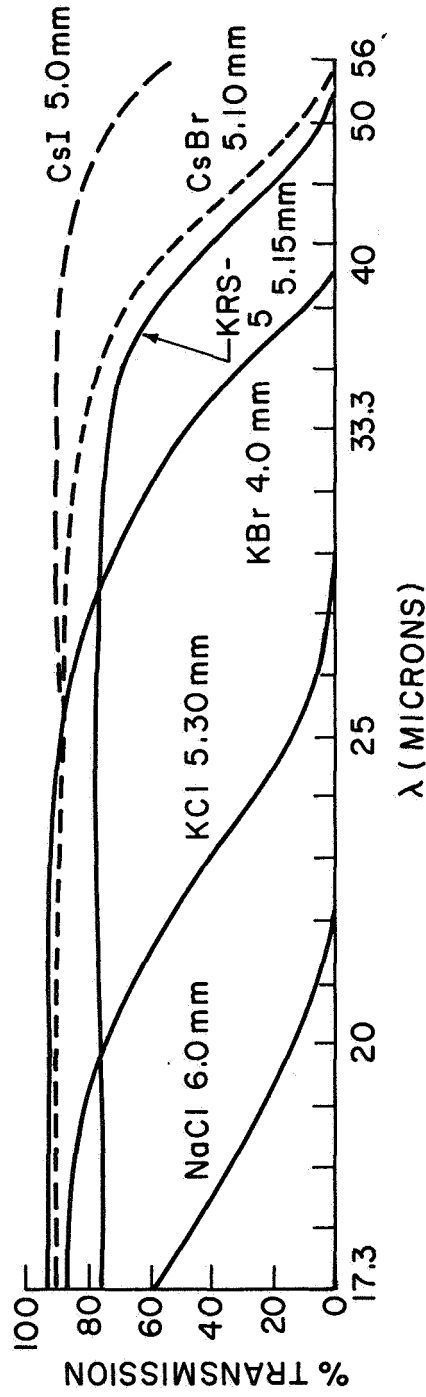
TRANSMISSION CURVES FOR CHOPPER MATERIALS

FIGURE 11

photodetectors, it is very desirable to use modulating frequencies of around 1000 cps. For a chopper with four blades, this corresponds to 30,000 RPM.

TABLE III

Cut-off Wavelengths for Selected Chopper Materials
(After Plyler and Blaine[125])

Material	Thickness (mm)	Wavelength of Null Transmission (microns)
NaCl	6.0	20
K Cl	5.3	30
K Br	4.0	40
KRS-5	5.1	50
CsBr	5.1	55
CsI	5.0	75

Section 6   Detector Optics

As mentioned in Chapter II, Section 2, the detector optics consist of all optical components between the exit slit and the detector. The purpose of these optics is to reduce the image of the exit slit to the size of the sensitive area of the detector. In the far-infrared, this problem is extremely difficult because of the use of very large exit slits which are necessary to obtain enough energy to be able to detect a signal. Typical sizes for the exit slits and detector areas are 2 inches by 1/2 inch, and 2 mm square, respectively. Hence, a reduction of 25 is necessary. The maximum practical reduction which can be accomplished by any of the systems mentioned above is about 5 or 6, except for the light-pipe and condensing-cone systems. The latter system can be designed to accomplish any finite reduction with only small losses due to reflection. In contrast to mirrored image reducing systems, the light-pipe condensing-cone

system is not image forming. In fact, the radiation flux at the end of the system will be nearly uniformly distributed across its diameter. Since this type of detector optics is almost universally used in the far-infrared, it will be the only one discussed in detail.

Ohlmann, et al.,[80] have analyzed the transmission of light pipes based on simple electromagnetic theory. Their result for the total transmission is given by

$$T = \frac{1}{2} e^{-2q} + \left(1 - e^{-q/2F^2}\right) F^2/q \approx \frac{1}{2}\left(1 + e^{-2q}\right) - \frac{8}{8F^2} \quad,$$

where $\quad q = \left(2\epsilon_o \omega \rho\right)^{1/2} L/d = 0.18 \left(\rho/\lambda\right)^{1/2} L/d$,

where ρ is the resistivity of the pipe material in ohm-cm, λ is the wavelength in cm, L is the total length of the pipe in cm, d is the diameter of the pipe in cm, and F is the f/number of the incoming light. This curve is shown in Figure 12A, where it has been compared to the transmission of brass pipe at wavelengths of 70 and 140 microns. Several materials have been studied experimentally by Harris, et al.,[82] and Richards.[97] The transmission curves relative to that for brass are given in Figure 12B. This curve shows that a transmission of better than 50 percent can be achieved for pipes of about 4 feet in length. The material of highest transmission in the far-infrared is brass. Since light pipes very often carry radiation to cooled detectors immersed in liquid helium, it is very desirable to use materials of low thermal conductivity.

In the article by Harris, et al.,[82] it is shown that the transmission of far-infrared energy is very poor for materials of low thermal conductivity. The use of light pipes to carry radiation from the exit slit to the detector is greatly improved by the use of condensing cones at each end of the pipe. The analysis of cone channel condenser optics has been carried out by Williamson,[79] and Witte.[81]
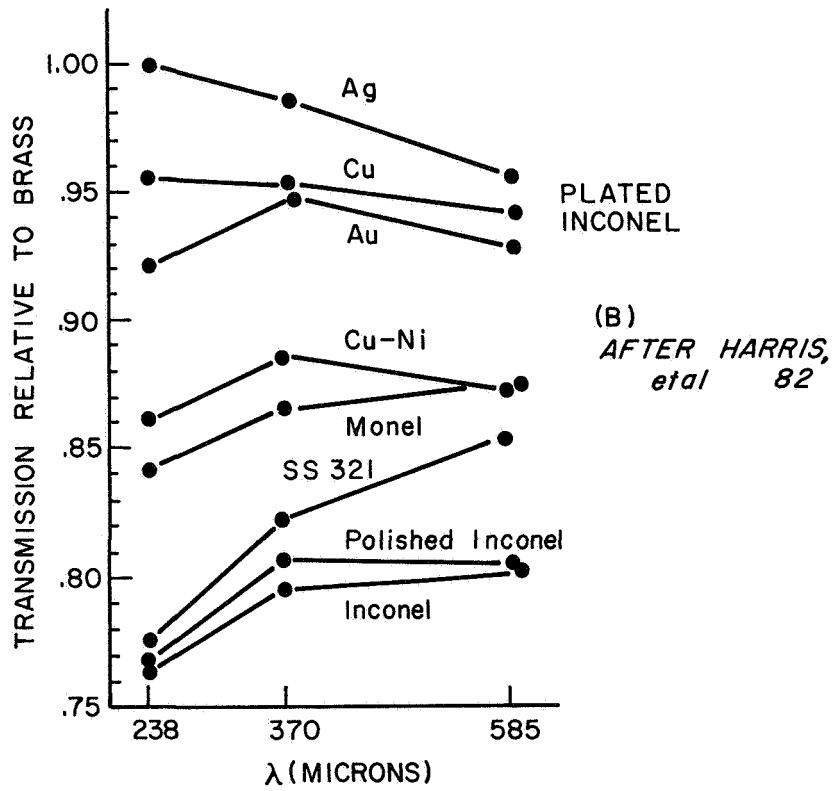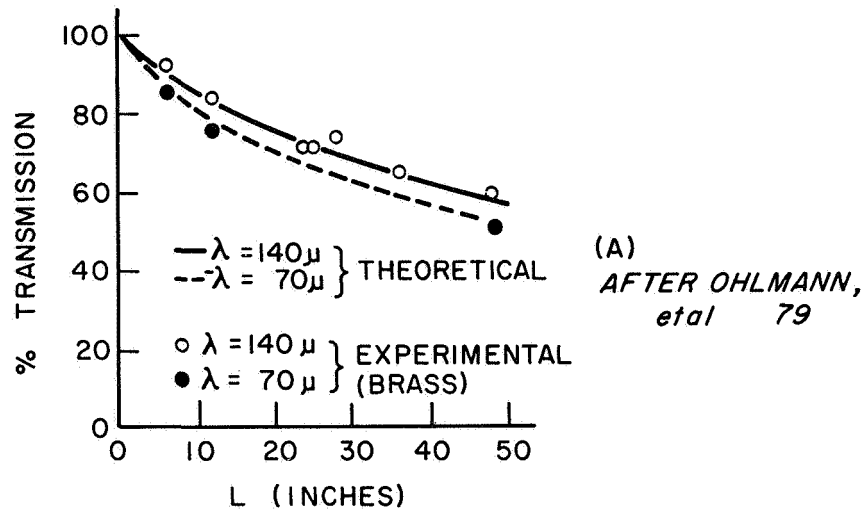
TRANSMISSION CURVES FOR LIGHT PIPE MATERIALS

FIGURE 12

Williamson has provided a solution which gives the cone length in terms of the diameters of the large and small ends, and the angle of the most skew ray of light relative to the cone axis. This relation has been developed based on the condition that no ray of light shall be reflected back toward the large end of the cone. It is given by

$$X = \left(1 - \frac{C}{S}\right) \frac{S \cos V}{\frac{C}{S} - \sin V}$$

where the parameters are defined in Figure 13.

The primary cone is usually placed adjacent to the exit slit, which determines the value of S. The f/number of the telescope mirror illuminating the exit slit determines V. The value of C coincides with the diameter of the adjacent light pipe, which is determined by several factors. The transmission of the light pipe increases directly with the diameter at the pipe. Since it is undesirable to place a large pipe into liquid helium, this factor must be considered in choosing the value of C. Once C has been determined, the length of the primary cone is fixed. Next, the value of C also determines the diameter of the large end of the secondary cone, which is located between the light pipe and detector. The diameter of the small end of this cone is fixed by the particular detector being used. The value of V to be used in conjunction with this cone can be determined graphically by determining the maximum angle of skew rays being reflected down the pipe. Finally, the value of X for the secondary cone is fixed by the above parameters, and the system is designed.

For very short distances between the exit slit and the detector, a single condensing cone may be sufficient. A very elaborate procedure for electroforming long cones has been discussed by Kneubuhl, et.al.[143]
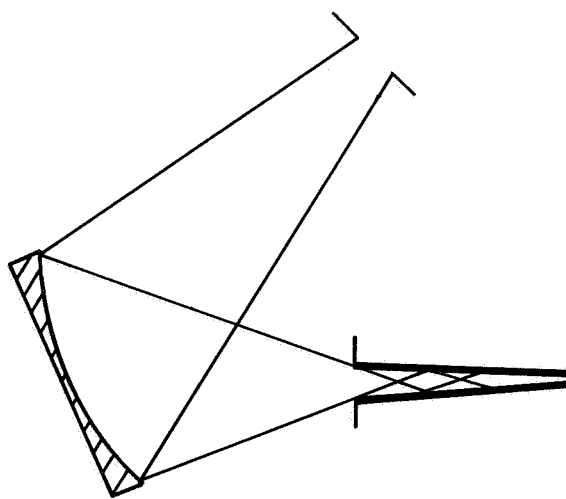
(A)

(A) FOR USE WITH MIRRORS
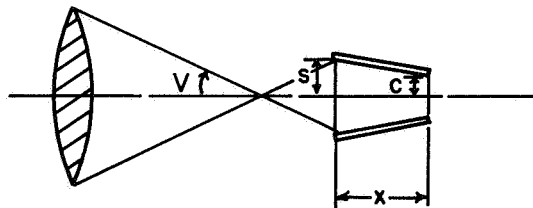
(B)

(B) FOR USE WITH LENSES

CONE CHANNEL CONDENSER OPTICS

FIGURE 13

Richards[97] has made measurements on polished brass cones which transmit approximately 90 percent while reducing the aperture by a factor of ten. Estimates on the attenuation of energy by a system consisting of one meter of polished brass pipe, two 90 degree bends using plane mirrors oriented at 45 degrees with respect to the pipe axes, and a polished brass cone have been given by the above author to be about a factor of 2.5.

Section 7. Detector electronics

It is not possible at this time; nor is it necessary, to probe deeply into the design criteria for the electronic equipment used with infrared detectors. On the other hand, it is convenient to discuss a few factors concerning this aspect of the spectrometer design. A complete discussion of amplifiers for use with infrared detectors is given by Smith, et al.[50]

In most practical cases, the main point for consideration in the design of an amplifier system for use with a particular infrared detector must be to insure that the performance of the detector is determined by its own inherent limitations and not by the design of the amplifier. In order to reach the limiting sensitivity of the particular detector, it is necessary to design the amplifier to give rise to less noise or fluctuations than the detector itself. Also, since it is necessary to modulate the light beam in order to amplify the signal with an alternating current amplifier, then care must be taken to modulate the beam at a frequency which matches the response time of the detector. Finally, the gain of the amplifier must be constant during the time interval of measurement, and its gain must be known as a function of incident energy.

Since several lock-in type A. C. amplifiers are commercially available, the above considerations are not of concern to this investigation. There are, however, several parameters which must be specified upon obtaining one of these amplifiers. First, the amplifier must have a frequency band width covering the range of modulating frequencies of interest to the investigators. Second, the amplifier must be compatible with respect to the impedance of the various detectors. Finally, the gain of the amplifier must be consistent with the power necessary to drive a strip-chart recorder on which the resulting spectra will be presented.

CHAPTER III

DESCRIPTION OF THE SPECTROMETER

Section 1. Optical Arrangement

The different optical arrangements available for use in designing a far-infrared spectrometer have been discussed in Chapter II, Section 2. The spectrometer to be discussed in this chapter utilizes the Czerny-Turner mirror arrangement in both the fore-optics and monochromator sections, as shown in Figure 14. The reasons for this choice is relatively straightforward. First, the necessity for very large optics creates a considerable economic factor in purchasing mirrors of quadric surfaces. The least expensive of these mirrors is the spheroidal mirror. The Czerny-Turner mirror arrangement utilizes two of these spheroidal mirrors in such a way that results in the second mirror partially cancelling the aberrations which were caused by the first mirror being used off axis. In contrast to this arrangement, the Littrow mount requires a very expensive paraboloidal mirror. The Pfund system, even though it utilizes spheroidal mirrors, wastes much of the grating surface area due to the large hole cut in the center of the grating. The Ebert mount is just a special case of the Czerny-Turner mount, but does not have the extra degree of freedom needed to minimize the overall aberrations of the monochromator. It has been shown by Shafer, et al.,[67] that the coma of the image of the entrance slit can be minimized by rotating the second Czerny-Turner mirror while experimentally observing the image until the best condition is realized. This condition is referred to as the asymmetric Czerny-Turner arrangement.

While designing this spectrometer, it was desired to be able to obtain continuous spectra throughout the range of the instrument
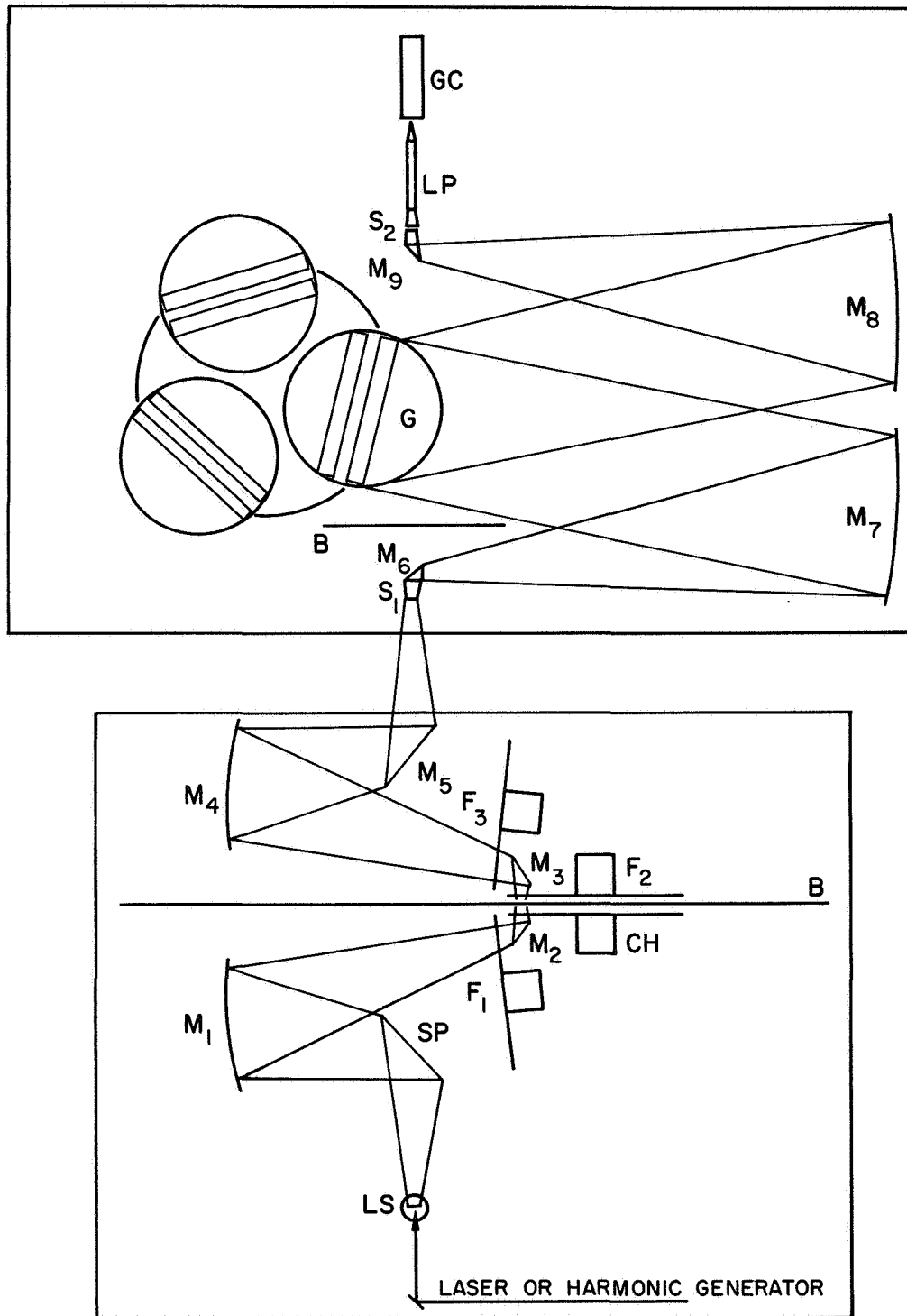
OPTICAL ARRANGEMENT OF THE SPECTROMETER

FIGURE 14

without having to dismantle the instrument in order to change filters or gratings. This requirement implied that all the gratings and filters must be contained within the instrument and be changed by remote operation. The design of a special grating interchange, shown in Figure 15, made it necessary to place the entrance and exit slits physically in front of the gratings. It is not always neces- sary to do this, and many spectrometers have their slits behind the grating.

In designing the Czerny-Turner mount, it is desirable to use the spheroidal mirrors at the smallest off-axis angles as possible so to keep the spherical aberrations to a minimum. This off-axis angle, and the included angle between the incident and diffracted central rays at the grating are both fixed by the diameter of the Czerny-Turner mirrors and the distance between the grating and these mirrors. For compactness of the instrument, it is desirable to keep this distance at a minimum. But, because of the fact that the slits must be in front of the gratings, this distance is determined by the focal length of the Czerny-Turner mirrors.

The size of these mirrors is determined by the size gratings to be illuminated. In turn, the grating size is determined by the wavelength, and desired resolution, i.e., the width of each grating is $W = Nd$, where N is the number of grooves of width d, and N determines the resolution. It was decided to use 6 inch high by 9 inch wide gratings, partially because of the 6 inch groove-length limit imposed by the grating ruling engine being used. In order to properly illuminate gratings of this size, it was necessary to use 12 inch diameter Czerny-Turner mirrors. In order to have a reason- ably compact instrument, the focal length was chosen to be 33 inches, giving optics of $f/2.75$.
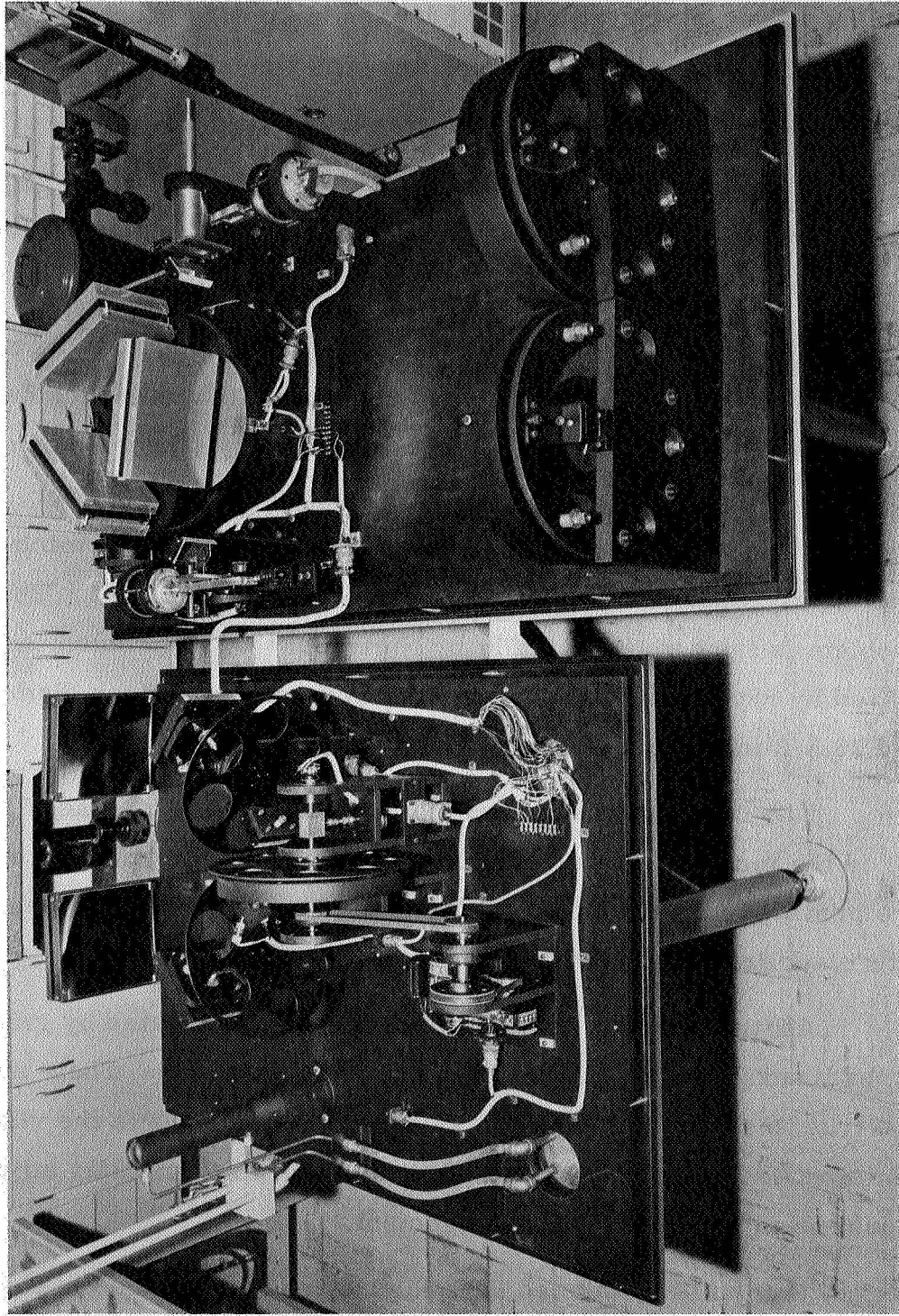
THE SPECTROMETER (PHOTO)

FIGURE 15

The size of the slits was determined by the size of the energy source, and the magnification of the source by the fore-optics. For a source area of approximately 2 inches high by 5/8 inch wide, and fore-optics of unit magnification, the slits were fabricated to be 2 inches high and open to 5/8 inch wide.

Two auxiliary plane mirrors, labeled M_6 and M_9 in Figure 14, were provided for ease of illumination access into and out of the mono-chromator.

The fore-optics, also shown in Figure 14, contain six mirrors of which four are plane and two are spheroidal. The spheroidal mirrors, M_1 and M_4 are arranged in the Czerny-Turner mount for the same reasons as mentioned above for the monochromator. The size and focal length of these identical mirrors was determined so that the entrance slit and grating were totally illuminated. This problem is treated analytically by Nielsen.[144] The problem was solved by ray tracing, and resulted in mirrors of 10 inch diameter and 25 5/8 inch focal length, given f/2.56 optics.

The flat mirrors SP and M_5 play analogous roles as M_6 and M_9 in the monochromator section. Finally, flat mirrors M_2 and M_3 are provided for convenient reflection filter positions if so desired in future applications.

All the mirrors described above were fabricated by grinding pyrex blanks and then aluminizing the front surfaces. Their surfaces are true to spheroidal shape or flatness to within $\lambda/4$ in the visible region. Each mirror is mounted on a three-dimensionally adjustable mount so to facilitate optical alignment.

Two baffles, labeled B in Figure 14, were placed in the spectrometer in order to reduce the possibility of any stray unfil-tered or unchopped light entering the monochromator.

As also shown in Figure 14, an image of the source is provided between mirrors M_2 and M_3. This focus has the smallest aperature area and is, therefore, the best position for the chopper. The small area of the beam in this region is also very desirable for filter positions. As can be seen in the figure, the chopper CH, and three filter wheels F_1, F_2, and F_3 are placed adjacent to mirrors M_2 and M_3.

Finally, the figure shows the light source (LS), and the light pipe (LP) and Golay cell (GC) at the extreme ends of the light path.

Section 2. Energy Sources

As mentioned previously, three types of energy sources have been considered for use with this spectrometer. They are the high pressure mercury arc, gas laser, and microwave harmonic generator. The first source produces incoherent light which can be made to fill the aperature and solid angle of the fore-optics. The latter two sources are of the coherent type, and have much different energy distribution patterns. The laser produces a collimated beam of about a few millimeters diameter, which must be coupled to the spectrometer. This beam area must be spread in order to cover at least several grooves on the grating, so to get an interference pattern. No exact method has been developed to accomplish this task; however, it is assumed that a spheroidal mirror of a few millimeters in diameter, and of very short focal length would cause the beam to diverge enough to solve this problem. The harmonic generator usually terminates in a wave guide, which radiates energy as if it were a microwave horn antenna. This procedure may be used for coupling to the spectrometer, or the use of a horn may be used to improve the coupling.

The large size of far-infrared gas lasers makes it necessary to have the laser outside the spectrometer vacuum chamber. This requirement also involves the problem of aligning the laser beam to the spectrometer. A suggested arrangement for laser coupling is shown in Figure 14. This figure also shows a possible coupling arrangement for the harmonic generator.

Section 3. Filters

The different types of filters used in far-infrared spectroscopy have been discussed above. Since well established filtering programs have not been formulated by far-infrared spectroscopists, it was decided to provide positions in the instrument for all types of available filters. Figure 14 shows all the filtering positions. As shown, filter wheels F_1, F_2, and F_3 are used for transmission filters of the reststrahlen or grating types. But by rotating mounts F_1, and F_3, these wheels can be used to hold reflection filters by replacing mirrors M_2 and M_3. Table IV lists the powder and transmission-grating filters to be tested in the instrument, along with their usable ranges. If it is desirable to use more than one transmission filter of a given type, a separate filter can be placed on either side of the filter wheels. Thus, it is possible to have six transmission filters in the light beam simultaneously. Since the powder filters are more difficult to manufacture, they will be placed on filter wheel F_2 because of its smaller aperature size; whereas wheels F_1 and F_3 will hold transmission-grating filters. Since only six powder filters are necessary to cover the short wavelength region, filter wheel F_2, which has eight positions, is capable of containing all the short wavelength filters, with one free position to be used during long wavelength scans. The eighth position can be used for samples or testing of new filters. Filter wheels F_1 and F_3, which have six positions each, are capable of holding all six of the transmission-grating filters

TABLE IV

TRANSMISSION FILTERS FOR USE IN THE SPECTROMETER

Filter Number	Powder Filters	Grating Filters d(mm)	Cut-on Wave-length (microns)	50% T Wave-length (microns)	Usable Range (microns)
1	LiF	—	30	46	46-60
2	LiF + SrF$_2$	—	40	60	60-80
3	U$_3$O$_8$ + Cu$_2$O	—	50	70	70-100
4	LiF + SrF$_2$ + BaF$_2$	—	60	100	100-120
5	4 + KCl + KBr	—	100	150	120-200*
6	5 + TlI + TlCl	—	150	250	200-300**
7		0.60	180	360	300-400
8		0.78	234	468	390-520
9		1.00	300	600	500-667
10		1.30	390	780	650-868
11		1.70	510	1020	850-1130
12		2.24	672	1344	1120-1500

* 25% T at 120 u

** 30% T at 200 u

needed to cover the long wavelength range, with four positions unoccupied. Two of these unoccupied positions are necessary when working in the short wavelength region, whereas the remaining two positions can be used for samples and filter testing as in F_2.

As previously mentioned, either or both filter wheels F_1 and F_3 can be used to hold reflection filters. This is accomplished by removing mirrors M_2 and M_3, and moving wheels F_1 and/or F_3 to positions such that the reflection filters occupy the same positions as previously held by M_2 and M_3. Hence, wire grid and reflection-grating filters may be used in these positions. It is planned to test the metal mesh filters only. These are listed in Table V. As in the case of multiple transmission filters, more than one reflection filter may be placed in the light beam simultaneously, by having similar filters on both wheels F_1 and F_3. Even though this arrangement provides only two positions, if it is desirable, mirrors M_5, M_6 or M_9 can be replaced by metal mesh filters. Since the undesirable wavelengths are transmitted through these mesh, then a properly placed absorbing material can be used behind these mirrors to prevent any stray light from entering the monochromator.

The extremely short wavelength energy is filtered out by the roughened aluminum scatter plate (SP), which is the first reflecting surface encountered by the light beam after the light source (LS). Further short wavelength attenuation is accomplished by multiple sheets of black polyethylene placed over the aperature in the baffle adjacent to the chopper. This baffle and black polyethylene sheet combination absolutely shields the remainder of the instrument from short wavelength energy.

TABLE V

PARAMETERS OF SELECTIVE
METAL-MESH FILTERS[*]
(After Mitsuishi, et al.[41])

Mesh Number	Mesh Constant d (microns)	Wire Diameter a (microns)	a/d
280	95	39	0.41
200	127	46	0.36
145	171	60	0.35
100	212	82	0.39
65	384	177	0.46

[*] These mesh are made of brass

Section 4. Dispersion Gratings

Since the size of the main dispersion gratings has been determined, then the remaining grating parameters which must be specified are the blaze angle ϕ, the grating spacing d, and the usable range in wavelengths. The latter two are most easily specified. The wavelength limits at which echelette gratings have an efficiency of 50 percent or greater are given by

$$\lambda_L = \frac{3}{4}\,\lambda_\beta, \quad \text{and} \quad \lambda_u = \frac{3}{2}\,\lambda_\beta$$

where λ_β λ_L, and λ_u are the blaze, lower limit, and upper limit wavelengths. These limits have been determined experimentally and analytically.[116] Since $\lambda_u = 2\lambda_L$, it is seen that each grating can be used over one octave.

The grating constant d is determined by the wavelength region for which the grating is to be used. For a given grating of spacing d, the blaze wavelength is determined by the blaze angle and the included angle between the incident and diffracted first order light beams. This relationship is derived easily from the grating equation and the geometry of the monochromator. Referring to Figure 4B, the included angle is given by

$$\theta_{in} = \theta \pm i$$

where i and θ are the incidence and diffraction angles measured with respect to the grating normal. The plus and minus signs refer to the cases when i and θ are on opposite sides or the same sides of the grating normal respectively. Calculations show that for a grating in a position such that λ_L is diffracted into the exit slit, the incident angle is zero. Hence, the condition of i and θ being on opposite sides of the grating normal never occurs in practice. Thus,

the above relation reduces to $\theta_{in} = \theta - i$. The condition for the blaze wavelength to be incident at the exit slit is given by

$$i = \phi - \frac{\theta_{in}}{2} \, , \qquad \theta = \phi + \frac{\theta_{in}}{2} \, ,$$

where ϕ is the blaze angle. It is seen from the above condition that the incident and diffracted light angles are equal with respect to the facet normal. Hence, this condition is that which corresponds to specular reflection by the individual facet surfaces, i.e., each facet or groove behaves like a plane mirror with respect to the blaze wavelength. Combining the above relations with the grating equation results in

$$\lambda_\beta = d \left[\sin\left(\phi + \frac{\theta_{in}}{2}\right) + \sin\left(\phi - \frac{\theta_{in}}{2}\right) \right]$$

$$= 2d \sin\phi \cos\frac{\theta_{in}}{2}$$

for the first order. From this relation, it can be seen that any ratio λ_β/d can be achieved simply by varying ϕ and θ_{in}. But further investigation reveals that there exist other restrictions on these angles.

Calculations show that for a given included angle, as the blaze angle increases, the diffraction angle decreases. By looking at the equation for angular dispersion, it is evident that large diffraction angles are desirable for large dispersion. The included angle is determined partially by the size and speed of the monochromator optics, and the optical arrangement. By imposing limits on the size of the instrument, and requiring maximum dispersion for high resolution, values of $\phi = 15$ degrees and $\theta_{in} = 22$ degrees were accepted as giving the most desirable properties. Substituting these values into the last equation results in

$$\lambda_\beta = 0.5082d$$

This relation, along with those between λ_L, λ_u, and λ_β, determine the wavelength range of each grating. The overall range of the instrument was specified by experimental requirements as extending from 30 to 1600 microns wavelength. Thus the lower limit for the first grating is set at 30 microns. This value determines the blaze wavelength for the first grating as

$$\lambda_{\beta_1} = \frac{4}{3} \lambda_{L_1} = \frac{4}{3} (30u) = 40u .$$

And hence,

$$d_1 = \frac{\lambda_{\beta_1}}{0.5082} = 78.7u ,$$

and

$$\lambda_{u_1} = \frac{3}{2} \lambda_{\beta_1} = 2\lambda_{L1} = 60u ,$$

i.e., the first grating covers the octave of 30 to 60 microns with 50 percent efficiency. The lower limit of the second grating is not chosen to be equal to the upper limit of the first grating because it is desirable to have some overlap for continuity reasons. A minimum overlap of 20 percent was chosen, which resulted in

$$\lambda_{L2} = 0.80 \lambda_{u1} = 54u .$$

The remaining values for λ_{Li}, $\lambda_{\beta i}$, and λ_{ui} follow by applying the same conditions as above. Table VI gives all these values for the gratings to be used in this instrument. Small deviations from the calculated values are a result of the restrictions placed on grating ruling by the ruling engine being used. Gratings could be ruled with grating spacings of fractions of 200ths of a millimeter.

TABLE VI

DISPERSION GRATINGS FOR USE IN THE SPECTROMETER

Grating Number	Blaze Angle ϕ (degrees)	Lines/Inch $1/d$ (inch^{-1})	Grating Spacing d (microns)	Blaze Wavelength λ_β (microns)	Usable Range $\frac{3}{4}$ to $\frac{3}{2}$ λ_β (microns)
1	15	320	79.4	40.3	30 – 60
2	15	180	141	71.6	54 – 107
3	15	100	254	129	97 – 194
4	15	60	424	216	162 – 323
5	15	30	848	431	323 – 647
6	15	17	1492	758	568 – 1138
7	15	17.1	1483	754	565 – 1130
8	7.5	12.7	2000	757	567 – 1137

With the above values of the blaze and included angles, a total rotation of the gratings of 12 degrees is necessary to allow the full range of wavelengths to be focused at the exit slit. These angles correspond to

$$i = 0 \quad , \theta = 22^O \quad \text{for} \quad \lambda = \lambda_L \quad ,$$

$$i = 12^O , \theta = 34^O \quad \text{for} \quad \lambda = \lambda_U \quad ,$$

and

$$i = 4^O \quad , \theta = 26^O \quad \text{for} \quad \lambda = \lambda_\beta \quad .$$

One may notice in Figure 4B that the light is shown illuminating the grating at an angle which is on the side of the grating normal closest to the facet normal. This condition is referred to as right tilt, since the grating is rotated toward the right hand direction with respect to the beam of incident light. This is not the only means of illumination. Calculations show that for the left tilt case, the diffraction angle ranges between 0 and 12 degrees in contrast to that of 22 to 34 degrees for the right tilt case. Hence, the right tilt illumination condition results in larger angular dispersion. If lower dispersion is desirable, the left tilt condition may be used by simply inverting the grating.

In the long wavelength region of the spectrometer range, the intensity of the source becomes very low. By decreasing the blaze angle of the gratings used in this region, it is possible to increase the energy density at the exit slit plane by reducing the angular dispersion. Many spectrometers use this device. At the same time, the grating spacing must be increased to keep the blaze wavelength and usable wavelength range as it was with the higher blaze angle. One grating with a blaze angle of 7.5 degrees and grating spacing of 2 mm has been fabricated for the wavelength range of 560 to 1140

microns. Another grating has been made for this range by ruling on soft solder which has been melted on a brass plate, whereas the previous gratings were ruled on aluminum cast tool and jig plate. The reflectivity in the far-infrared of the solder grating has been said to be three times that of the aluminum gratings. The main disadvantage of the solder gratings is the extreme ease in which they can be destroyed by scratching.

Section 5. Detector Optics

As mentioned in Chapter 2, the most convenient type of detector optics for use with low temperature detectors is the light-pipe condensing-cone system. Since almost all the detectors to be used with this spectrometer operate at liquid helium temperatures, this system is used.

The light-pipe and cones are of cylindrical cross-section, and made of brass. The primary cone located at the exit slit has a 2 1/8 inch diameter aperature at the large end to match the diagonal of the slits when fully opened. This cone condenses the beam to the 5/8 inch diameter of the light-pipe over a 4 inch distance. The size of the light pipe was determined by two criteria. First, Ohlmann, et al.,[80] have shown that the transmission of the pipe increases with increasing diameter, since less reflections are encountered per unit length of pipe. And second, it is desirable to have a reasonably small pipe enter the liquid helium dewar for heat leak considerations. This 5/8 inch inner diameter pipe has an outer diameter of 7/8 inch, and is available commercially. It is very straight and has very uniform circular cross-section, which are ideal for light pipe application. A number of light pipe sections have been made, each of which has one straight unaltered end, and one end fitted with an "o"-ring quick-connecting seal. This arrangement allows

any length of light pipe to be used by simply adding the desired number of sections. This method also makes it very simple to measure the attenuation due to a given length of light pipe.

The terminating end of the system consists of several condensing cones used for different detectors. One cone used for the Golay cell condenses the aperature from 5/8 inch to 1 cm., which is the window size of the cell. This cone is fitted with a clear polyethylene sheet window so that the entire light pipe is evacuated along with the spectrometer. By placing the Golay cell within about 1/2 mm of the cone window, the water vapor absorption in this small distance can be made to be negligible.

The second cone is fitted onto the end of the light pipe which carries the light into a liquid helium dewar to illuminate low temperature detectors. Since most solid state detectors have sensitive areas of about one millimeter diameter, this cone condenses the 5/8 inch light pipe aperature to a one millimeter diameter aperature. A polyethelene window is placed at one of the joints in the light pipe to isolate the two vacuum systems, i.e., that of the spectrometer and that of the helium dewar.

Long sections of light pipe can be sealed off at each end by windows so that gas samples may be analyzed. The gases are placed into the pipe through radial fittings equipped with valves so that high pressures can be obtained.

Section 6. Mechanical Design

A. Vacuum Chambers

There are several requirements which are unique to the mechanical design of far-infrared spectrometers. The most outstanding of these is the necessity of enclosing the instrument within

a vacuum chamber in order to remove the atmospheric water vapor absorption. This requirement is complicated by the large size of the optical system required for these instruments. The size of this instrument is so large that it had to be enclosed by two separate chambers.

The fore-optics are mounted on a 3 foot by 4 foot by 1/2 inch steel optical bench, as compared to the 2 1/2 foot by 5 1/2 foot by 1/2 inch monochromator optical bench. These sections of the instrument are enclosed by chambers of 38 inches wide by 50 inches long by 23 3/4 inches high and 32 inches wide by 68 inches long by 23 3/4 inches high respectively. All plates are made of 1/2 inch thick cold-rolled steel, with both sides and all edges blanchard ground for flatness and squareness. The sides are electric welded together, but remain separate from the bottom and tops so that they can be removed for adjusting the instrument. The fore-optics chamber has two tops, while there are three for the monochromator. These are made of aluminum and have been made small so that they could be removed by hand. The tops and sides can be raised by the use of a one-ton electric hoist, and rolled out of the way of the instrument on a 6 inch I-beam. The vacuum sealing is accomplished by 1/4 inch diameter cross-section neoprene "o"-rings, which were custom fabricated. The light beam passes from the fore-optics to the monochromator through a 6 inch inner diameter stainless steel bellows. This bellows also provides the vacuum connection between the two chambers. Each chamber is supported by three steel pipe legs in a triangular arrangement. This type of support eliminates the redundant fourth leg of conventional tables. The fore-optics support is adjustable in height so to be able to align the chambers with each other. When applying vacuum to these chambers, the sides, tops, and bottoms all buckle, which requires careful

consideration so that this motion is not transferred to the optical system.

Each optical bench is supported by three ball bearings located on the bottom plates above the upper ends of the supporting legs. The buckling of the bottom plates pivots about these points, and hence, these balls remain fixed in place. Each ball is placed into a conically shaped socket in hardened steel pads bolted to the bottom plate. The optical benches have three similar pads attached to their lower sides. One of these three pads contains a socket, one a V-shaped groove, and the last a flat plate. This kinematic support allows the benches freedom of expansion and contraction, but also fixes them rigidly in all three directions. This type of support which is described in Reference 145 was used throughout the instrument where redundant mounting would be detrimental.

Two vacuum pumping systems are available to evacuate the instrument. The large system (380 cfm) can lower both chambers from atmospheric pressure to less than 20 microns in about 15 minutes. The second, and smaller system (16 cfm), is used to maintain the low pressure and to free the large system for liquid helium temperature control.

Three 6.7 inch diameter access ports are provided in each chamber. One port on each chamber is provided for electrical and/or vacuum access. The fore-optics chamber has two more ports provided for access by the laser and harmonic generator energy sources. The last port on the monochromator chamber is provided for the light-pipe. This port is directed toward free laboratory space where the low temperature cryostat is to be located.

All permanent electrical wiring and vacuum or water piping enters the instrument through the bottom of the fore-optics chamber.

In this way, the instrument is fully operable with the chamber sides and tops on or off.

B. Scan Mechanism

The scan mechanism is the most complex subsystem of this spectrometer. It consists of two main sections, the sine-drive, and the grating interchange. The latter rotates the gratings by a compound table to select one of the six gratings on the interchange. The former rotates the grating located in the optical position by the sine of the angle of the incident light, which provides an output which is linear in wavelength.

The grating interchange shown in Figure 16 consists of one 16 inch diameter disk on which are placed three 10 inch diameter disks with their centers located at the vertices of an equilateral triangle. The center of the triangle coincides with that of the large disk. The small disks are attached to the large disk by vertical shafts mounted in pairs of precision ball bearings. These shafts protrude through the large disk and each has a spur gear attached to its lower end. These three gears mesh with one larger gear fixed to the center shaft on which the large disk is mounted by similar bearings. These four gears form a planetary system. As the large disk is rotated, with the large gear fixed, the small disks are forced to rotate in an opposite direction and at a speed proportional to the ratio of the pitches of the planet gears to that of the sun gear. This ratio has been chosen to be three-halves, so that one-third of a revolution of the large disk causes the small disks to rotate one-half a revolution. By placing two dispersion gratings back to back on each of the small tables, it is possible to rotate the system in 120 degree increments and, thereby, place each grating in the optical position by remote operation. It is necessary to lock the grating being used in
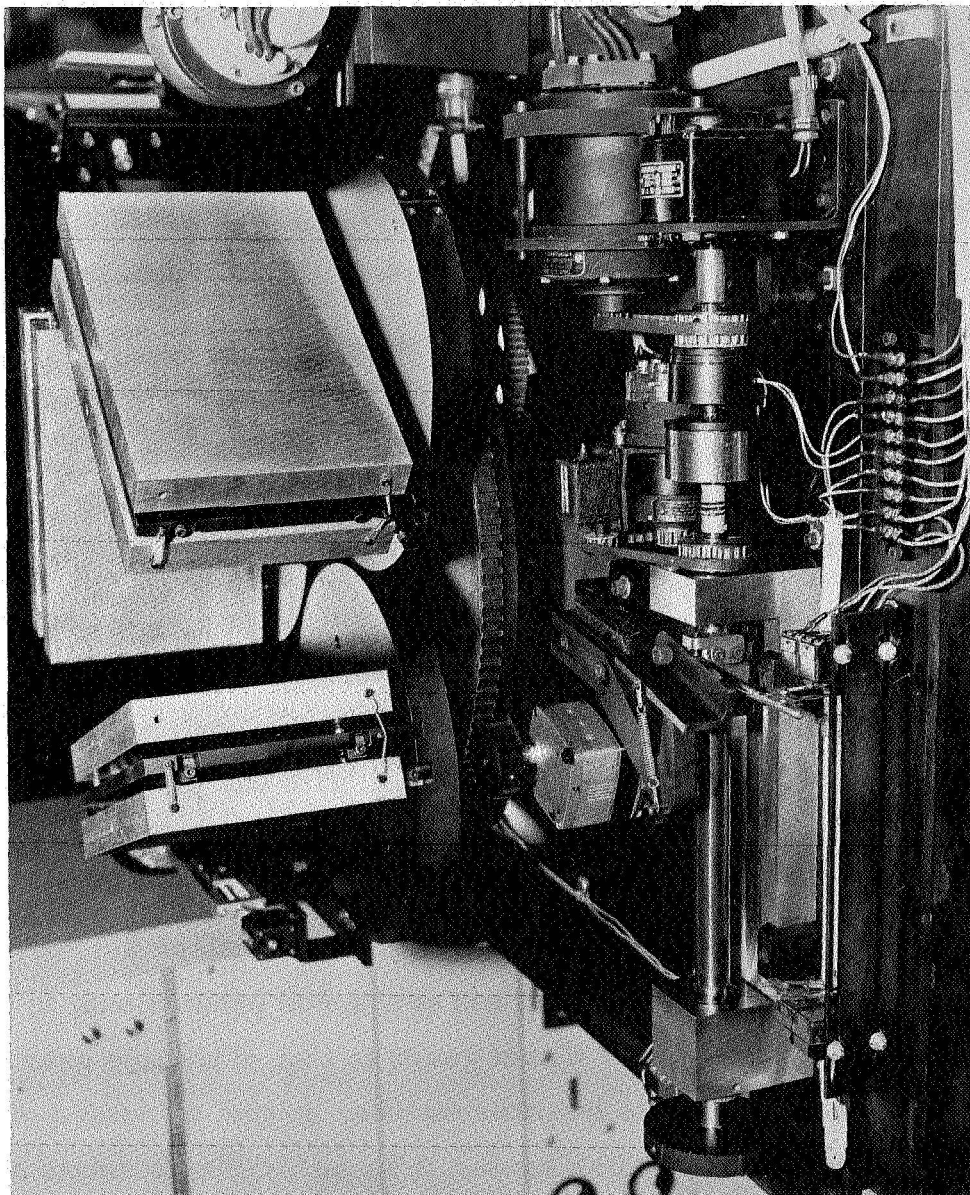
THE SINE -DRIVE (PHOTO)

FIGURE 16

place so that it will be mechanically rigid after interchange. This locking device must be repeatable in order that the calibration of the instrument be repeatable. This locking is accomplished by two indexing pins and nine hardened V-grooves. The pins lock the large disk and the small disk being used in the optical position. Three V-grooves are located on the circumference of the large disk radially outward from the centers of the small disks. The remaining six V-grooves are located on the circumferences of the small tables in front of each of the six gratings. Each pin is actuated by an electromagnetic solenoid. Microswitches and small screws are used to deactivate the solenoids when the disks have rotated to the proper positions. The rotation is accomplished by a single 5.7 RPM, 75 oz-in reversible motor which drives the large disk. It takes about 30 seconds to rotate from one grating to the next.

Each grating is kinematically mounted to a vertical plate attached to the tops of the small disks. Three springs hold each grating against three ball bearings which can be adjusted to rotate the grating in three mutually perpendicular directions.

The supporting shaft of the large table is mounted on a rotating arm, which is an integral part of the sine-drive mechanism. This arm is supported at its pivoting end by two precision ball bearings on a vertical shaft bolted to the optical bench. This shaft is centered below the center of the ruled face of the grating in the optical position. Hence, by rotating this arm, the grating being used is rotated about the center of its ruled face, but not translated. This motion is necessary for the wavelength scanning procedure. As mentioned above, a rotation of 12 degrees is required for each grating. This mechanism is capable of about 16 degrees rotation. The weight of the grating interchange system is supported by two

ball bearings located under the sine-bar directly below the shaft supporting the large disk. These balls roll in a curved V-groove which has a radius of curvature equal to the distance from the pivot point of the arm to the position of the balls on the arm. Thus, the balls roll only and never slide, which causes wear and gradual decay of the bearing plates. The under side of the sine-bar is re-inforced at this point by a flat hardened steel plate. The sine-bar is rotated by a precision lead screw and nut arrangement as shown in Figure 16. How this mechanical arrangement results in a linear wavelength drive is described in the following analysis. The instrument axis is defined as the line passing through the center of the ruled face of the grating and bisecting the distance between the centers of the main mirrors. If α is the angle which the grating normal makes with the instrument axis, then the relations between this angle and the incidence and diffraction angles are given by

$$\alpha = \frac{\theta_{in}}{2} + i = \theta - \frac{\theta_{in}}{2} \; ,$$

where θ_{in}, i, and θ are defined above. Combining these equations with the grating equation gives

$$\lambda = d \left\{ \sin \left(\alpha - \frac{\theta_{in}}{2} \right) + \sin \left(\alpha + \frac{\theta_{in}}{2} \right) \right\}$$

$$= K \sin \theta,$$

where $K = 2d \cos \dfrac{\theta_{in}}{2}$ is a geometrical constant for a given grating.

Since the chart paper on the strip chart recorder is driven by synchronous motors, then it is necessary to have the rate of change of wavelength with respect to time be a constant. This requirement is specified as

$$\frac{d\lambda}{dt} = K \frac{d(\sin \theta)}{dt} = \text{constant} .$$

If x is the distance the nut travels along the lead screw, then the velocity of this nut, when the screw is driven by a synchronous motor, will be given by

$$\frac{dx}{dt} = \text{constant} .$$

From the figure, it is seen that the geometry gives the relation between x and θ as

$$x = A \sin \theta$$

where A is the length of the sine-bar. By taking the time derivative of this equation

$$\frac{dx}{dt} = A \frac{d(\sin \theta)}{dt} = \frac{A}{K} \frac{d\lambda}{dt}$$

and by setting either side equal to a constant, both required conditions are satisfied. The above analysis neglects one factor, that the length A is not constant as the ball slides across the optical flat on the nut. This small error can be compensated for by providing the mechanism with two adjustments. These are the angle of the optical flat with respect to the screw axis, and the length of the sine-bar. By trial and error methods of adjusting these parameters, almost perfect linear wavelength scanning can be accomplished. This design was first proposed by Badger, et al.,[146] and is discussed in detail by Dimock.[147]

Since this scan mechanism must be controlled from outside the vacuum chamber, two motors are used to rotate the lead screw. To provide a number of discrete but repeatable scan speeds, a six-speed synchronous motor is used for normal scanning. This motor is located on the control console. The output of this multi-speed

motor is transmitted to the lead screw by means of a selsyn transmitter and receiver. Hence, the scan speed is selected externally to the instrument. The six speeds and corresponding wavelength scan rates for each grating are listed in Table VII. For example, the fastest and slowest times for a 12 degree rotation of a grating by this motor are 30 minutes and 19 1/2 hours respectively. A second high speed motor is also used to drive the screw for fast scans and to return the nut to either end of the screw rapidly. This is accomplished in 6 minutes.

The equation relating the RPM of the lead screw to the wavelength scan rate is

$$\frac{d\lambda}{dt} = \left(2d \cos \frac{\theta_{in}}{2}\right) \frac{1}{A} \frac{RPM}{m} \, ,$$

where

$$\frac{dx}{dt} = \frac{RPM}{m} \, ,$$

and m is the thread pitch of the screw. For θ_{in} = 22 degrees, A = 16 inches, m = 50 threads per inch, and at λ = 100 u, with d = 250 u, then

$$\frac{d\lambda}{dt} = 0.612 \ RPM$$

The fastest and slowest rates corresponding to 6 and 6/32 RPM are 3.67 and 0.115 microns per minute.

The angle of the sine-bar relative to the instrument axis is transmitted to the control console by the following apparatus. Two rotation counters are used. One directly attached to the lead screw, and the second mounted on the console panel. The second counter is driven by a set of selsyn motors, the transmitter being driven by the lead screw. Hence, both counters indicate the number of

TABLE VII

SCAN RATES FOR THE VARIOUS GRATINGS

Motor Speed (RPM)	Gear Ratio	Lead* Screw Speed (RPM)	Lead** Screw Traverse Time (hours)	Scan Rate for Grating Number i, $\frac{d\lambda}{dt}$ (microns/minute)							
				i = 1	2	3	4	5	6	7	8
3600	1:1	36	0.10	7.00	12.45	22.20	37.40	74.8	132.0	132.0	176.2
600	1:1	6	0.60	1.17	2.07	3.73	6.22	12.4	22.0	22.0	29.4
600	2:1	3	1.20	0.58	1.04	1.87	3.11	6.22	11.0	11.0	14.7
600	4:1	1.5	2.40	0.29	0.57	0.93	1.56	3.11	5.50	5.50	7.34
600	8:1	0.75	4.80	0.15	0.29	0.47	0.78	1.56	2.74	2.74	3.67
600	16:1	0.375	9.60	0.08	0.15	0.24	0.39	0.78	1.37	1.37	1.84
600	32:1	0.1875	19.20	0.04	0.08	0.12	0.20	0.39	0.68	0.68	0.92

* There is a 100:1 gear reducer between the drive motors and the lead screw.

**For 4.5 inches traverse, or 12 degrees grating rotation.

revolutions of the screw, or the position of the nut along the screw, or the angle of the sine-bar. The range of the counters are from 0 to 9,999, where one revolution of the screw corresponds to 10 counts. A calibration curve will be made for each grating relating the counter number to wavelength. The position of the sine-bar is recorded on the chart paper by using an event marker. This event marker is a solenoid-driven pen which is activated by a reed switch and five magnets mounted on a wheel on one end of the lead screw. Hence, five equally spaced marks are made on the chart for each screw revolution. Since the wavelength output on the chart is linear, then it is possible to linearly interpolate between these marks. Each mark will correspond to a number on the counter and, hence, some wavelength. By manually recording this number on the chart paper every few feet, any wavelength between two numbers can be determined by counting marks from one of these recorded numbers. The grating being used optically must also be recorded on the chart paper so that the correct calibration curve will be used.

C. Mirror, Chopper, and Mercury Arc Mounts

The mechanical apparatus composing the scan mechanism resulted in the center of the height of the gratings being 10 inches above the optical bench. Thus, all other optical components had to be mounted with their centers at this height. The ten mirror mounts are of the same basic design, but differ slightly due to mirror size and weight. Each mirror is mounted on a backing plate by the use of nylon screws so not to create any local stress regions. Then each backing plate is held against three round end adjusting screws by a spring. These screws set into cones drilled in the backing plates. With this type of mount, the mirror positions are adjustable in two mutually perpendicular rotations, and also translation

perpendicular to the mirror face. The height of each mirror is adjusted by the use of shims, if necessary.

The chopper wheel consists of a 10 1/2 inch diameter, 1/8 inch thick aluminum disk with six partial sectors removed. The area of each open or metal sector is slightly larger than that of the beam at the point of location of the chopper. Thus, the beam is modulated six cycles per chopper revolution. The wheel is mounted on a 3/8 inch diameter shaft which is held by two precision ball bearings. Two synchronous motors are used to rotate the chopper at two different speeds. A two-hundred RPM motor drives the wheel through a 2:1 ratio timing belt drive giving a chopping frequency of 10 cps. This is used with the Golay cell. A second motor drives the chopper at 3600 RPM for a chopping frequency of 360 cps for use with photodetectors. Many other speeds can be developed by simply changing the gear ratios. Timing belt drives have been employed here so that heat from the motors is not transferred to the chopper blade, and hence, cause radiation into the light beam. Since the chopper is rotated at relatively high speeds, it has been dynamically balanced. Also, a mechanical one-way clutch is provided in the 2:1 gear train of the slow motor so that the high speed motor does not have to drive the slow motor backwards.

The mercury arc source being used in the instrument is a General Electric Uviarc UA-2 lamp. This lamp has been designed for large factory or exterior illumination, and must be either forced air or water cooled. In the spectrometer vacuum chamber, only water cooling is available, and hence, this type of cooling is used. This is accomplished by flowing water through a cooling water jacket formed by two concentric brass tubes with the lamp

located along the cylindrical axis. A window the size of the lamp is cut out of both tubes to provide a light path for illuminating the fore-optics. Thus, the lamp is cooled strictly by radiation to the inside wall of the water jacket. By blackening this surface, the absorption of radiation, and therefore, the cooling efficiency is increased. The electrical terminals of the lamp are supported by teflon spacers located in the ends of the water jacket. Thus, the lamp is electrically isolated from the jacket. It has been mentioned by Richards[97] that it is necessary to dimple the quartz envelope of the lamp to remove any interference resonance effects. This will be investigated experimentally by comparing two lamps with and without dimples.

Section 7. Electric Control Circuits

A. The Scan System

A switching logic circuit containing an eight switch programming timer, one rotary switch, two push button switches, five toggle switches, eight microswitches, and three motors is used to obtain semi-automatic scanning with this spectrometer. The circuit is shown in Figure 17. With the programming timer in the initial condition, the timer switches are set by adjustable cams such that the lead screw is being driven by the six speed scan motor. Assuming that the lead screw nut is at the extreme short wavelength end of the screw, then the rotary switch is turned to the "increase wavelength" position. Under these conditions, the grating in the optical position will be rotated through 12 degrees, at the speed selected by the investigator, until a microswitch is activated (by the nut) at the other end of the screw. This microswitch starts the programming timer, which in turn, goes through the following cycle. First, one timer switch starts the high speed

scan motor to return the nut to the other end of the lead screw in 6 minutes. The direction that this motor rotates is also selected by "wavelength direction" rotary switch. Second, another timer switch starts the grating change motor, which advances the next grating to the optical position via the grating interchange. The next grating is stopped and locked in place automatically by micro-switches located on the grating interchange. Also, three micro-switches and three pilot lights are used logically to indicate which of the six gratings is in the optical position. At about this time, the "program timer maintain switch" is opened automatically and the first part of the cycle has been completed. When the nut is returned to the first end of the screw, a microswitch is activated, which in turn starts the second part of the program cycle. This part of the cycle is simply the resetting of the program timer to the initial conditions so that the scan motor will start scanning the next grating.

There are several alternatives built into this scan cycle. First, the rotary switch can be placed in the "decrease wavelength" position, which just reverses the directions of all the motors, and hence, the direction of scan, return, and grating change. Second, if it is desirable to have the cycle stop at the end of scanning over one grating, just flip the "scan cycle" switch from "automatic" to "manual." On the other hand, to have the cycle repeat over the same grating indefinitely, throw the "grating change" switch from "on" to "off." As may be seen in the circuit diagram, there are four microswitches on the lead screw. One of these on each end is for starting the program timer cycle in either scan direction, and the other two are for stopping the high speed return motor from overrunning the microswitches in either direction.
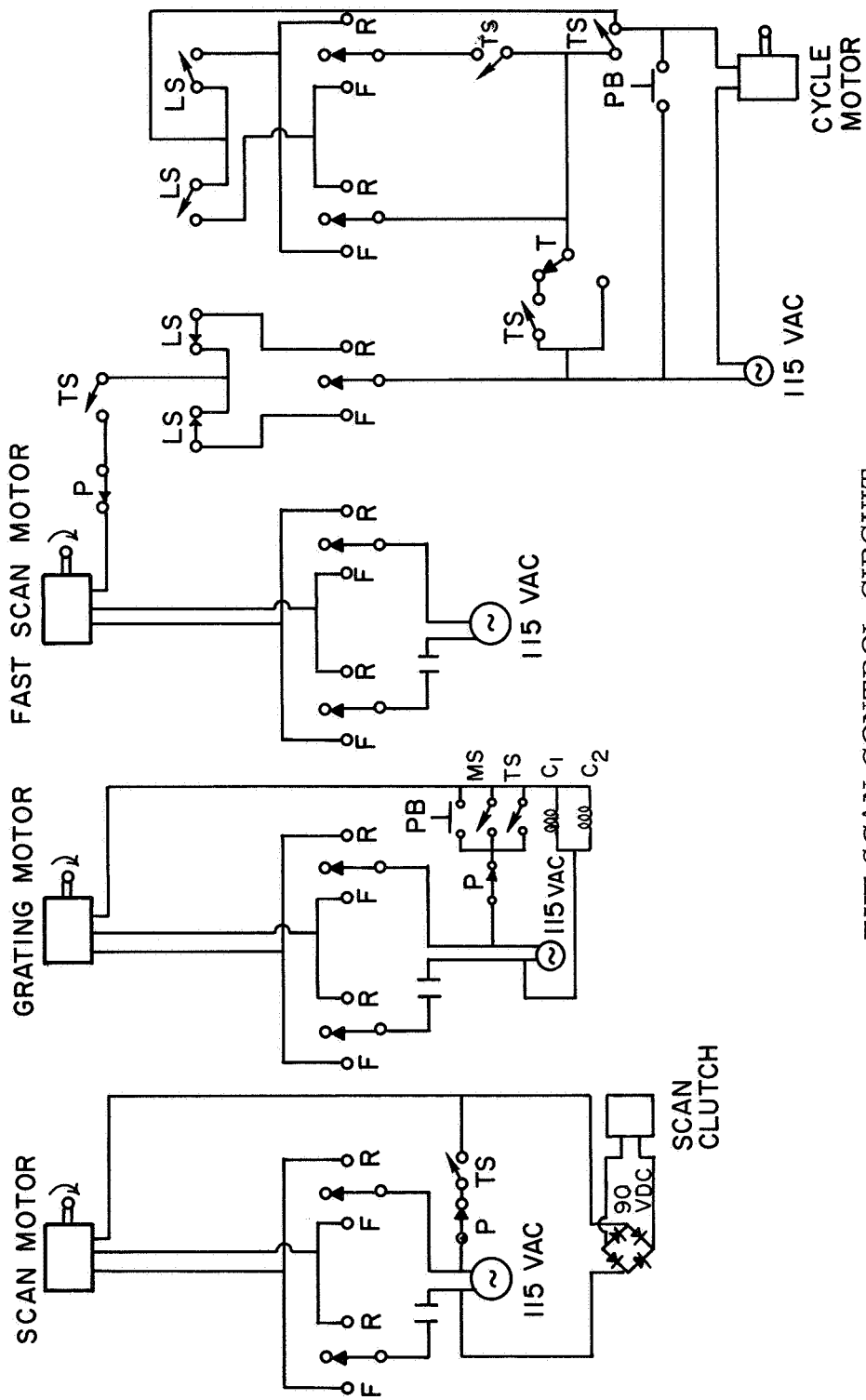
THE SCAN CONTROL CIRCUIT

FIGURE 17

There are several other switches related to this scan system. One of the timer switches is used to stop the strip chart recorder chart-drive during grating changes so that spectra will not be recorded during these periods. The event marker is also inactivated by this switch. But, in case the high speed scan motor is used for fast scans which are to be recorded, there is a defeat switch located on the rear panel of the main console.

Finally, two push button switches are provided for the following uses. One of these switches is used for changing gratings at any time without returning the program cycle to the initial conditions, i.e., in the middle of a scan. The other push button switch is used to return the cycle to the initial conditions, at any time, for incomplete scans.

By using combinations of the above switches, this scan system is an versatile as any commercial non-remote control system. Scanning with this system is semi-automatic in the respect that filter changing and slit width adjustment are not controlled automatically. These two controls are separate and are discussed next.

B. Filter Changing

The filter changing circuit shown in Figure 18A is used for filter wheels F_1, F_2 and F_3. The circuit is very simple, using only two identical rotary switches, a relay and a motor. The motor drives the filter wheel and one of the rotary switches, while the relay and second switch are located in the control console. Any position on the filter wheel is placed in the optical path by dialing the corresponding number on the panel switch. The relay and motor are activated as soon as the two switches are not at corresponding positions, and will remain activated until the motor has driven the wheel and switch to the corresponding position on the panel switch.
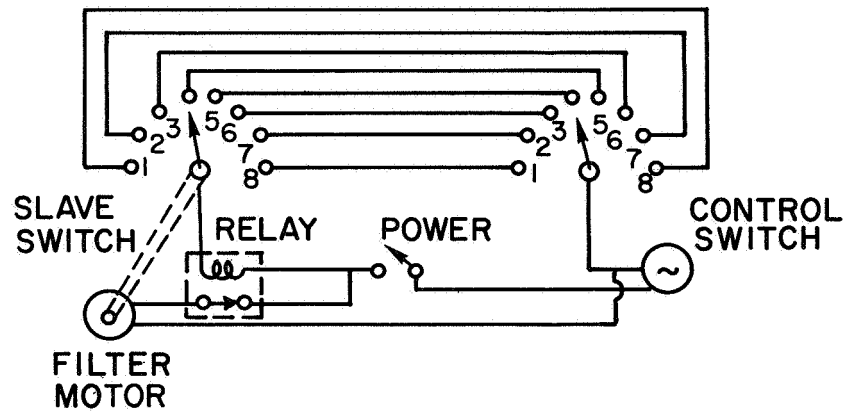
(A)

THE FILTER CHANGING CIRCUIT

FIGURE 18A
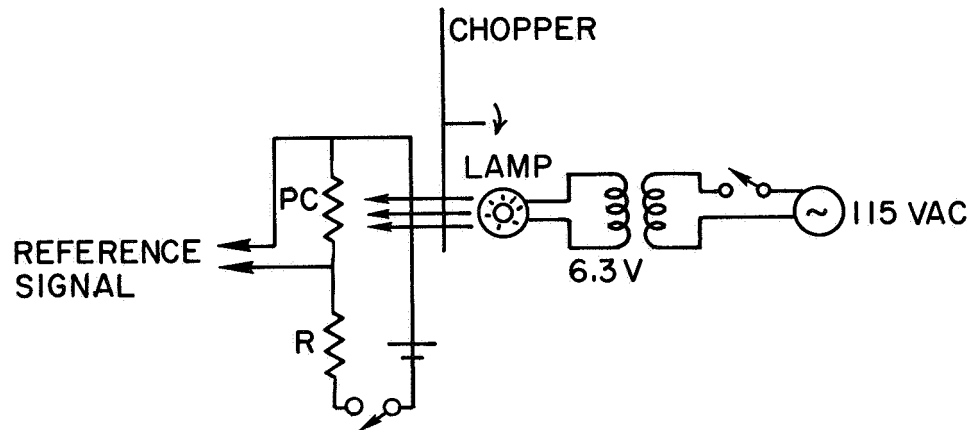
(B)

THE REFERENCE SIGNAL CIRCUIT

FIGURE 18B

Since the wheels are driven by small clock motors, which are unidirectional, a filter wheel must go through all positions even if the panel switch is rotated by one position in the opposite direction. The wheels make one revolution in one minute, and hence, an adjacent filter change is accomplished in less than 10 seconds. Pilot lights are provided to indicate when the wheels have stopped.

Also, since the indexing mechanism of the rotary switch is used to index the filter wheels, precision switches must be used. For transmission filters, this requirement is somewhat relaxed, but it is very important for reflection filters.

C. Slit Width Control

The mechanical width of the slits is controlled by using selsyn motors. One hand driven transmitter located on the control panel is wired in parallel to two receivers, one driving each pair of slits. The slits are mounted on dove-tail slides driven by a right and left hand 40 threads per inch precision screw. Thus, by rotating the screw, the slit jaws are moved away or toward each other. Three revolution counters are used to indicate the positions of the two slit pairs. One of these counters is on the control panel, and the others are on the slit shafts. A change in one number on the counters corresponds to 0.005 inch slit width change. This is about the smallest controllable change.

D. Safety Switch Circuits

Two safety switch devices have been included in the design of this spectrometer. The first is the mercury lamp cooling water safety circuit. This circuit contains a water flow switch on the lamp cooling water pipeline which shuts off the lamp power when insufficient water flow conditions exist. This circuit is given in Figure 19A, which also shows the power supply for the UA-2 lamp.

The second safety circuit is provided for severe pressure increase, due to either water pipe failure or vacuum leaks. This circuit is activated by a pressure sensitive switch which is set at approximately one millimeter of mercury absolute pressure. This switch activates a power relay in the control console which disconnects all power to the spectrometer and the auxiliary vacuum pumping system. The pumps are shut off in case the pressure increase is due to water contamination, which could damage the pumps. This circuit is shown in Figure 19B.

E.   Chopper Frequency Reference Signal

As mentioned previously a lock-in amplifier is used to amplify only that part of the signal received by the detector which has been modulated by a predetermined frequency. This frequency is determined by the type of detector used and is generated by the chopper wheel. There are two ways to simultaneously generate a reference signal from the chopper with the exact frequency as that imposed on the optical beam. These methods are the mechanical rectifier, and the photocell-lamp systems. The former method consists of a mechanical rotating device attached to the chopper drive shaft. By the use of brushes and commutators, it generates a train of pulses of the same frequency as that of the chopper. This method is liable to malfunction due to dirt in the brushes, etc. The second method is more reliable. This spectrometer uses a very fast response photocell which is illuminated by light eminating from the photocell exciter lamp. The cell and lamp are located on the same side of the chopper blade, and in such a way that the light is reflected into the cell by the metal sectors of the chopper. Hence, a square wave signal is generated by the photocell with the exact frequency of the chopper. The side of the chopper facing the cell and
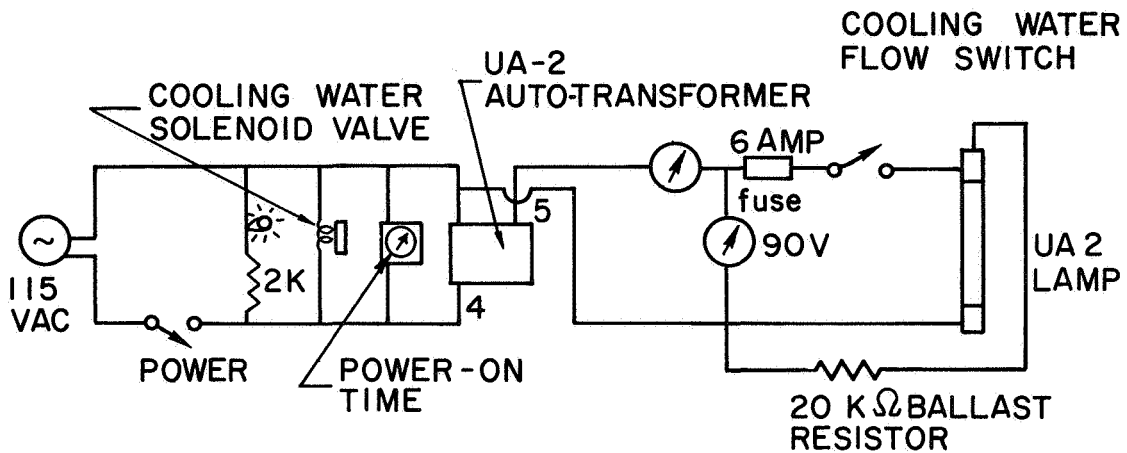
(A)

THE MERCURY LAMP COOLING
WATER SAFETY CIRCUIT

FIGURE 19A
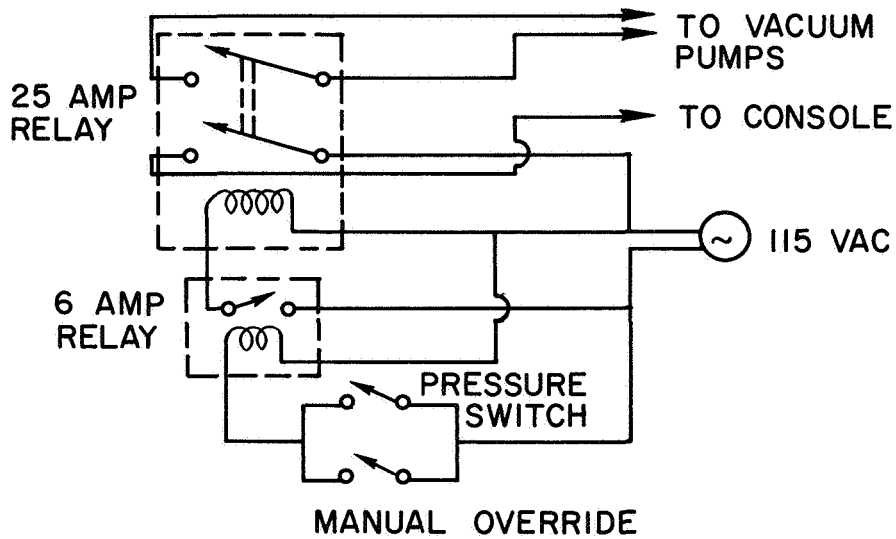
(B)

THE HIGH PRESSURE SAFETY SWITCH CIRCUIT

FIGURE 19B

lamp has been polished for high reflectivity. This circuit is illustrated in Figure 18B. The photocell is a model TPC-4L made by Farmer Electric Products Co., Inc.

CHAPTER IV

OPERATION, CALIBRATION, AND PERFORMANCE
OF THE SPECTROMETER

Section 1. Selection, Preparation, and Performance of the Filters.

The different types of filters available for use in far infra-
red spectroscopy have been described in Chapter II, Section 5. The
criteria for selection of filter types has been the ease of fabrication
and operation of the filters. On this basis, powder filters have been
used from 30 to 320 microns, and transmission-grating filters from
300 to 1100 microns.

The preparation of powder filters was made in the following
manner, First, many filters, each consisting of a single reststrahlen
crystal powder were fabricated by mixing the proper proportion of
each powder to a fixed amount of polyethylene powder. Each crystal
powder was obtained from various chemical manufactures in the
purest state available, usually reagent quality. Then each powder
was ground by hand using a mortar and pestle, until the fine powder
could pass through a 400 mesh sieve (approximately 37 micron hole
size). The powder was made to pass through the sieve by the use of
a homemade sieve shaker. The proper amount of each powder (as
determined by References 39, and 135) was weighed and then mixed
with the proper amount of polyethylene powder. The polyethylene
powder used was "Microthene 620"; a high-density polyethylene of
approximately 100 micron particle size as received from the manu-
facturer, U. S. Industrial Chemicals.

The mixing of the powders was carried out in a homemade
shaker with stainless steel vials about three inches long by one and one-
half inches diameter. After mixing for at least one hour, the mix
was placed in a stainless steel die heated to about 300°F. The die

97

was three inches in diameter, and made to produce a thin wedged filter of about 0.030 inch on the thick side and 0.001 inch on the thin side. The center portion of the disk, which is to be placed in the optical beam, is about 0.015 inch (380 microns). The wedged shape of the filters eliminates any interference effects, which modify spectrum recordings. After allowing the mix to melt on the lower surface of the die, the heated top of the die was put in place, and pressed down with the heated platen of a hydraulic press until the surface of the upper platen had reached the top of the outer cylinder of the die. At this point the remaining filter had the same dimensions as mentioned above. All excess molten mix is allowed to escape through small holes in the die. After cooling the entire assembly with water, the filter is removed from the die and inspected for uniformity. If any light or dark spots are seen, the filter is rejected. These spots refer to clumps of polyethylene or crystal powder which did not break up during the mixing process. This overall procedure produced about two good filters out of every three attempted. After producing a complete set of these single component filters, the next step was to test them in the spectrometer.

By using crystal quartz, a 240 grit scatter plate and two sheets of 0.1 mm black polyethylene, all radiation of wavelengths below 40 microns were attenuated to the point where a signal to noise ratio of about one was recorded from 30 to 40 microns on the first grating. The spectral purity in this region was checked by placing a 5 mm thick plate of KBr in front of the detector. The KBr will pass all radiation below 40 microns with little attenuation, but blocks all radiation longer than 42 microns. Thus, any signal measured must come from the region below 40 microns. If no signal is recorded, then the attenuation produced by the filters below 40 microns is sufficient. The quartz used was from a natural crystal cut along the

Ý-axis to give maximum transmission. The plate was wedged two degrees, and was 1.5 mm thick on the thick side. No interference fringes were detected with this crystal, in contrast to another crystal used, which was 1 mm thick and had parallel surfaces. Since the cut on wavelength of the quartz was 40 microns, it is used as a filter from about 50 to 80 microns. Below 50 microns, the transmission is too low.

Since the quartz, scatterplate, and black polyethylene filters produced monochromatic radiation in the 40 to 80 micron region, the transmission of the above powder filters could be checked in this region. This was done for several filters, and it was found that the cut on wavelengths compared very well to those published by Yoshinaga.[39] It was found that by adding a filter with BaF_2 only, no radiation was detected below its cut on wavelength of 57 microns. Hence, the region of monochromatic radiation was extended to 114 microns. In this manner, all the single component powder filters were tested, and by selecting overlapping sets of these filters, a complete set of composite filters was obtained by simply mixing all the components together in a single filter. Finally, the region from 30 to 320 microns can be covered with the use of eight transmission filters. These filters are listed in Table VIII.

As mentioned above, the region from 300 to 1100 microns is covered using transmission-grating filters. The selection of the ranges of these filters is carried out as follows. The cut on wavelength has been shown to be $\lambda c = 0.3d$, and from the experimentally derived transmission curves, the wavelengths at which these filters transmit 30 and 50 percent are given by $\lambda(30\%) \approx 0.50$ d and $\lambda(50\%) \approx 0.65$ d. The lower limit of 30% transmission was chosen by energy requirements, and the upper limit of 50% transmission is the point

TABLE VIII

TRANSMISSION FILTERS*

FILTER NUMBER	POWDER FILTERS	GRATING FILTERS d(mm)	CUT-ON WAVELENGTH (microns)	USABLE RANGE (microns)
1	BeO + ZnO**	---	23	30-45
2	BeO + LiF**	---	30	40-60
3	Quartz***	---	40	50-80
4	3 + BaF$_2$†	---	57	80-114
5	3 + BaF$_2$ + KCl	---	74	100-150
6	3 + BaF$_2$ + KBr	---	93	110-185
7	6 + CsBr	---	140	170-270
8	6 + CsBr + CsI	---	160	220-320
9	---	0.60	180	300-400
10	---	0.78	234	390-520
11	---	1.00	300	500-667
12	---	1.30	390	650-868
13	---	1.65	495	825-1100

*one 240 grit Al scatter plate and 0.2 mm Black Polyethylene permanently installed.

**used with diamond Golay cell or cooled detector.

***1.5 mm, Y-cut, 2 degree-wedge crystal.

†Filters 4 through 16 used with Quartz Golay cell or cooled detector.

when second order wavelengths begin to pass through the filter. The first filter was chosen to have $\lambda_1(30\%) = 300$ microns. This choice fixes d_1, and $\lambda_1(50\%)$. The remaining filters were chosen in a similar manner, each overlapping the previous filter by about 20 microns. The calculation of the values for the various grating spacings, d_i, was always controlled by the limitations of the ruling machines used to make the gratings. The shorter wavelength gratings, which were ruled at the U. C. Berkeley, Physics Department Machine Shop could be ruled only by spacings of 1/200 ths. of a mm. The shaper used at UCLA to rule the longer wavelength gratings could rule gratings in multiples of 0.005 inch. Once a compatible set of grating spacings was developed, the gratings were ruled on four-inch square aluminum plates, one-half inch thick. These plates were heated to about 300°F, and pressed onto sheets of white, high-density polyethylene. The fabrication of these filters was carried out as follows. One grating and one unruled plate were heated on the lower platen of a hydraulic press to 300°F. Upon reaching this temperature, a precut four-inch square sheet of polyethylene was placed on the unruled plate until it had softened. At this time, the ruled plate was inverted, placed on the polyethylene and then pressed until the grooves in the grating were filled with molten polyethylene. The three pieces were kept in alignment by a square frame with a wooden handle, which could be used to remove the hot assembly and place it into a bucket of water. In about one minute, the plates could be removed by hand, revealing a perfect replica grating. If the replica was warped due to stress, it could be flattened out by placing a heated plate on top of the unruled surface, and pressing on it until the stresses were removed. A set of seven filters was obtained to cover the region from 300 to 1100 microns. These are included in Table VIII.

The spectral purity, or the monochromaticity of the radiation at the exit slit was tested by two different methods. The first method has been described above, and consists of using an ionic crystal to block the first order and pass the second and higher order wavelengths incident on a grating. This technique is limited by the availability of crystals which pass long wavelength radiation. Common crystals used for this purpose have been listed in Table III. Beyond the region where this technique can be used, a second method is used. This method consists of using a grating of spacing $d_2 = \frac{1}{2} d_1$ to scan over the second and higher orders of the grating with spacing d_1. When using this method, all the filters normally used with grating number one must be placed into the optical path. Each filter and grating combination was tested by one or both of these methods, and the filters were improved until a signal to noise ratio of one was achieved in the region below the cut-on wavelength. Further improvement beyond this point is immeasurable, and therefore futile.

The performance of the filters can be demonstrated by the quality of the spectra which can be obtained using them. The most convenient and popular gas to use for this demonstration is atmospheric water vapor. Figures 20 through 24 show medium resolution spectra obtained with the filters in Table VIII in conjunction with a Golay Detector. The spectrometer settings are given in the figures. These spectra compare very well to those obtained by other far-infrared instruments.

Section 2. Calibration, Linearity, and Repeatability

Calibration of far-infrared spectrometers is usually accomplished by recording spectra of well known gases, such as water vapor, CO, HCN, N_2O, etc. The most convenient gases are water vapor and CO. The water vapor spectrum runs out to about 540 microns,
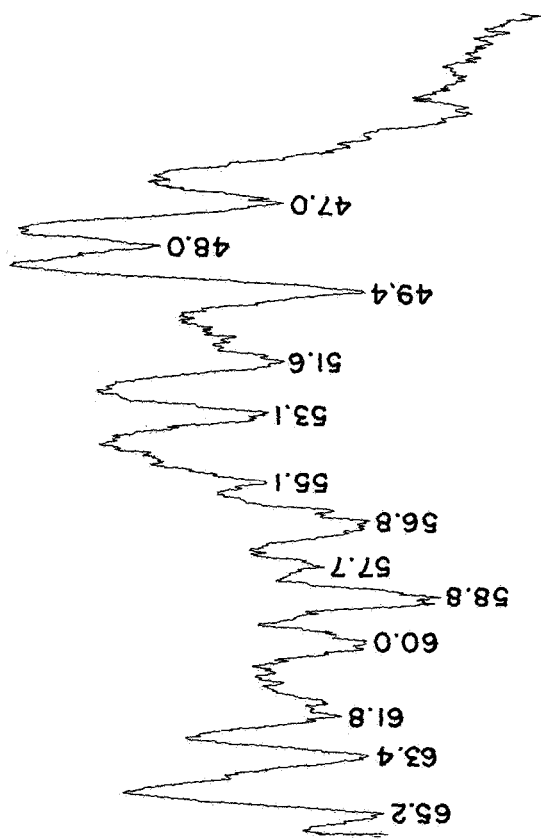
Legend: **Grating #1**
Slit Width ~ 5.1 mm
Time Constant ~ 35 sec
Scan Speed ~ 3.6 cm^{-1}/min
Pressure ~ 2.5 psia

WATER VAPOR SPECTRUM FROM 40 TO 65 MICRONS

FIGURE 20
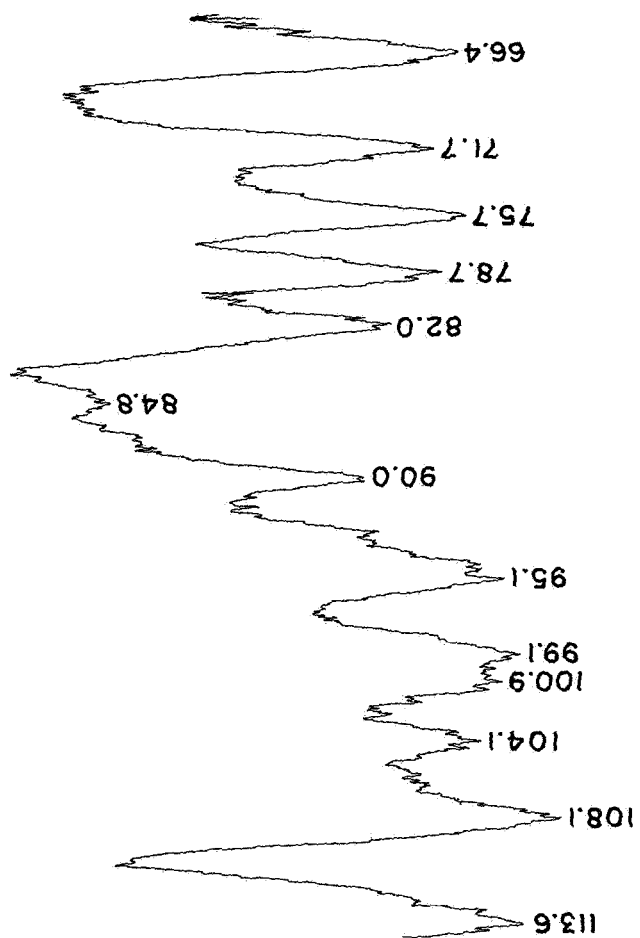
Legend: Grating #2
Slit Width ~ 6.4 mm
Time Constant ~ 35 sec
Scan Speed ~ 2.0 cm^{-1}/min
Pressure ~ 2.5 psia

WATER VAPOR SPECTRUM FROM 65 TO 114 MICRONS

FIGURE 21

99.1
100.9
104.1
108.1
113.6
116.8
121.8
126.0
132.4
135.8
138.5
144.5
146.8
156.2
160.5
166.8
169.9
174.5
180.0
187.1

Legend: Grating #3
Slit Width ~ 3.8 mm
Time Constant ~ 35 sec
Scan Speed ~ 1.1 cm^{-1}/min
Pressure ~ 2.5 psia

WATER VAPOR SPECTRUM FROM 100 TO 190 MICRONS

FIGURE 22
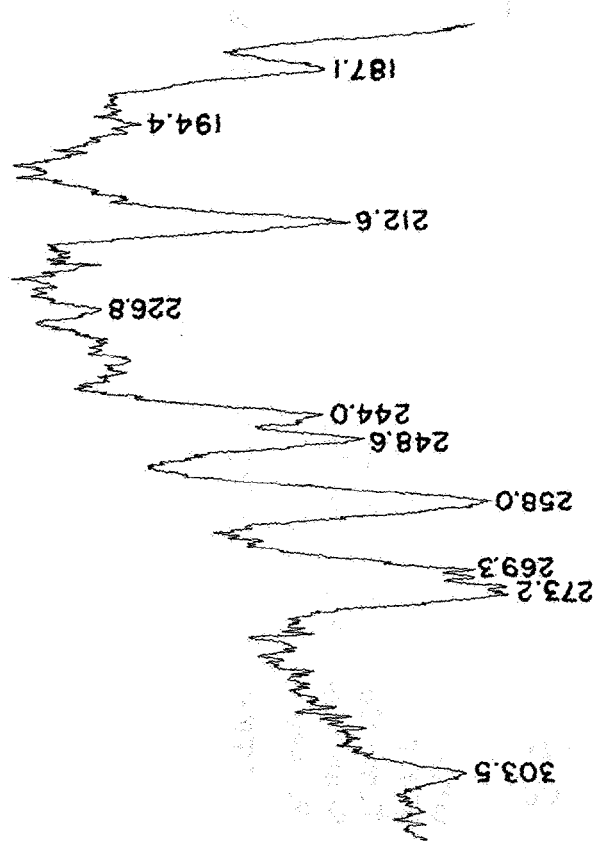
Legend: Grating #4
Slit Width ~ 5.1 mm
Time Constant ~ 35 sec
Scan Speed ~ 0.67 cm^{-1}/min
Pressure ~ 2.5 psia

WATER VAPOR SPECTRUM FROM 185 TO 320 MICRONS
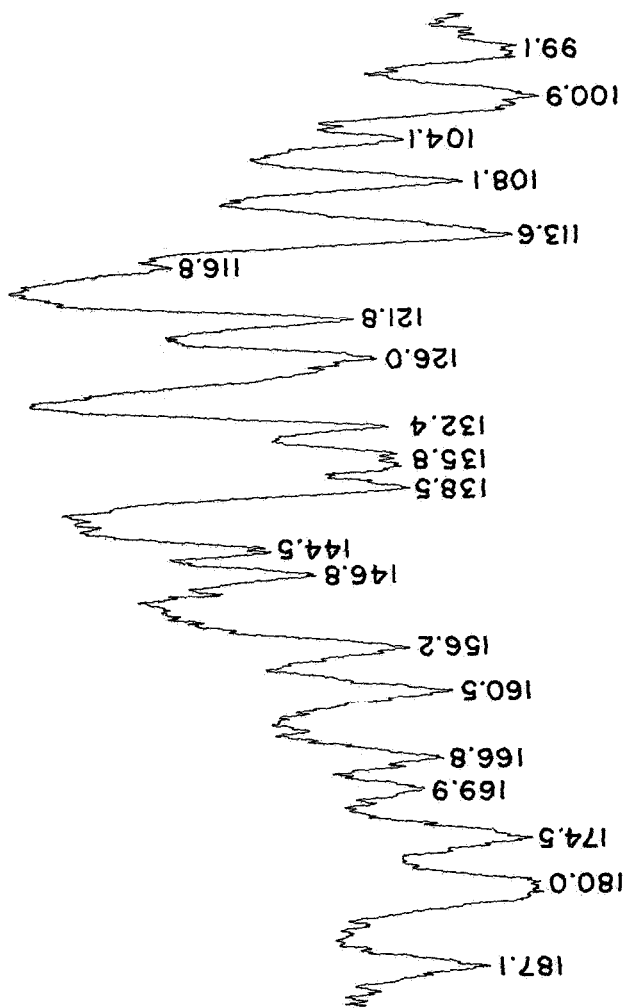
FIGURE 23
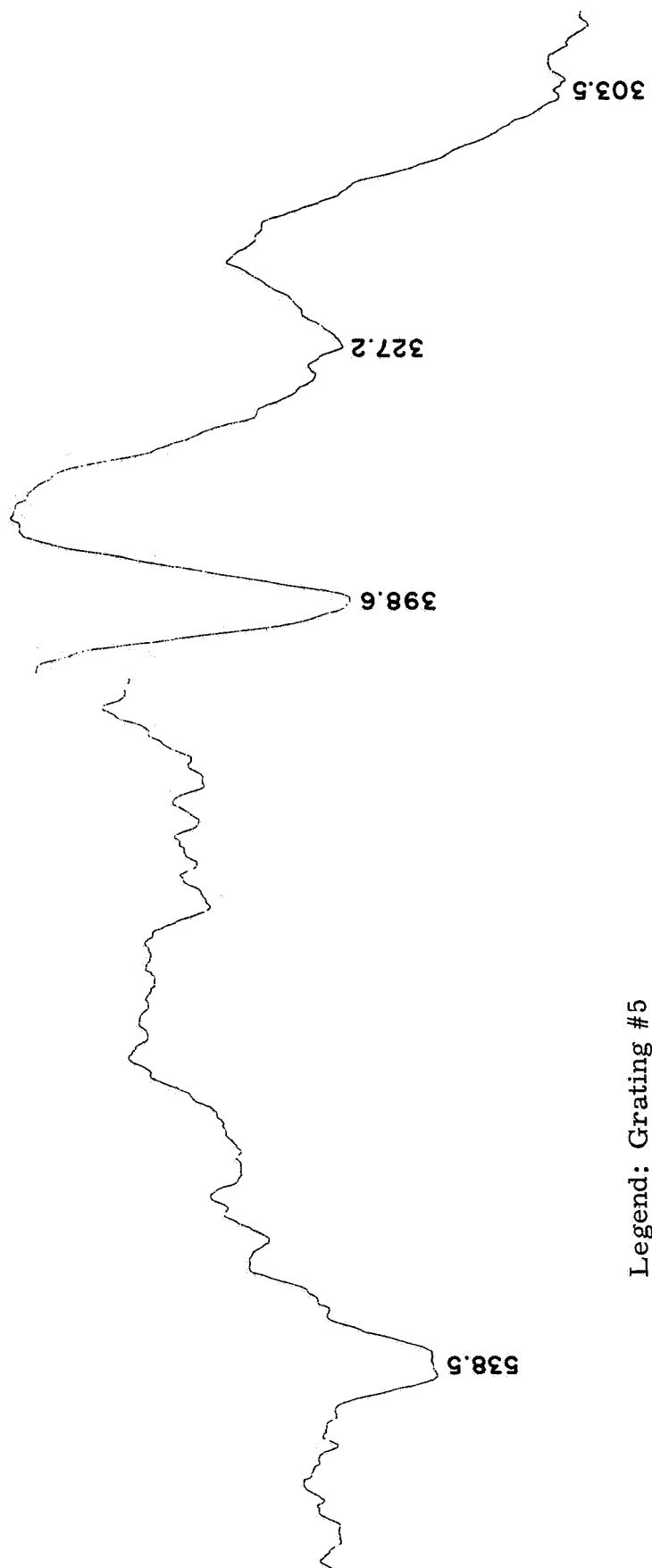
Legend: Grating #5
Slit Width ~ 10.2 mm
Time Constant ~ 350 sec
Scan Speed ~ 0.17 cm^{-1}/min
Pressure ~ 2.5 psia

WATER VAPOR SPECTRUM FROM 300 TO 580 MICRONS

FIGURE 24

and that of CO to a few centimeters. Hence, CO has been used for calibration beyond 500 microns. Since adjacent absorption lines for CO are separated by 3.84 cm^{-1}, high resolution is not required.

Since each line of CO absorption is identical to the next, it is difficult to locate which line is which for calibration. This location can be accomplished by allowing second order water vapor lines to be recorded and then comparing the results to the first order CO spectra.

Since the spectrometer is equipped with a sine-drive mechanism, calibration procedures are greatly simplified. After a spectrum has been recorded using a single grating, and some familiar water vapor lines are recognized by comparison to other published spectra, the wavelengths of these lines are plotted against the event marker numbers on the recording. These curves will be straight lines as a result of the sine-drive system. Hence, all lines between those recognized can be located by use of the straight line. This curve is the calibration curve, giving wavelength versus event marker number for each grating. These curves actually do become straight lines after adjustment of the sine-drive is carried out. Thus the linearity of the recorded spectra has been established. A typical calibration curve is shown in Figure 25.

The wavelength repeatability can be tested by recording the same water vapor spectra several times separated by some time interval. This has been done on several of the gratings, and the repeatability is about 0.1 cm^{-1} near 50 microns.

Section 3. Selection of Operating Parameters.

An important part of spectroscopy is being able to use a spectrometer easily and to its best ability. Thus, optimizing such
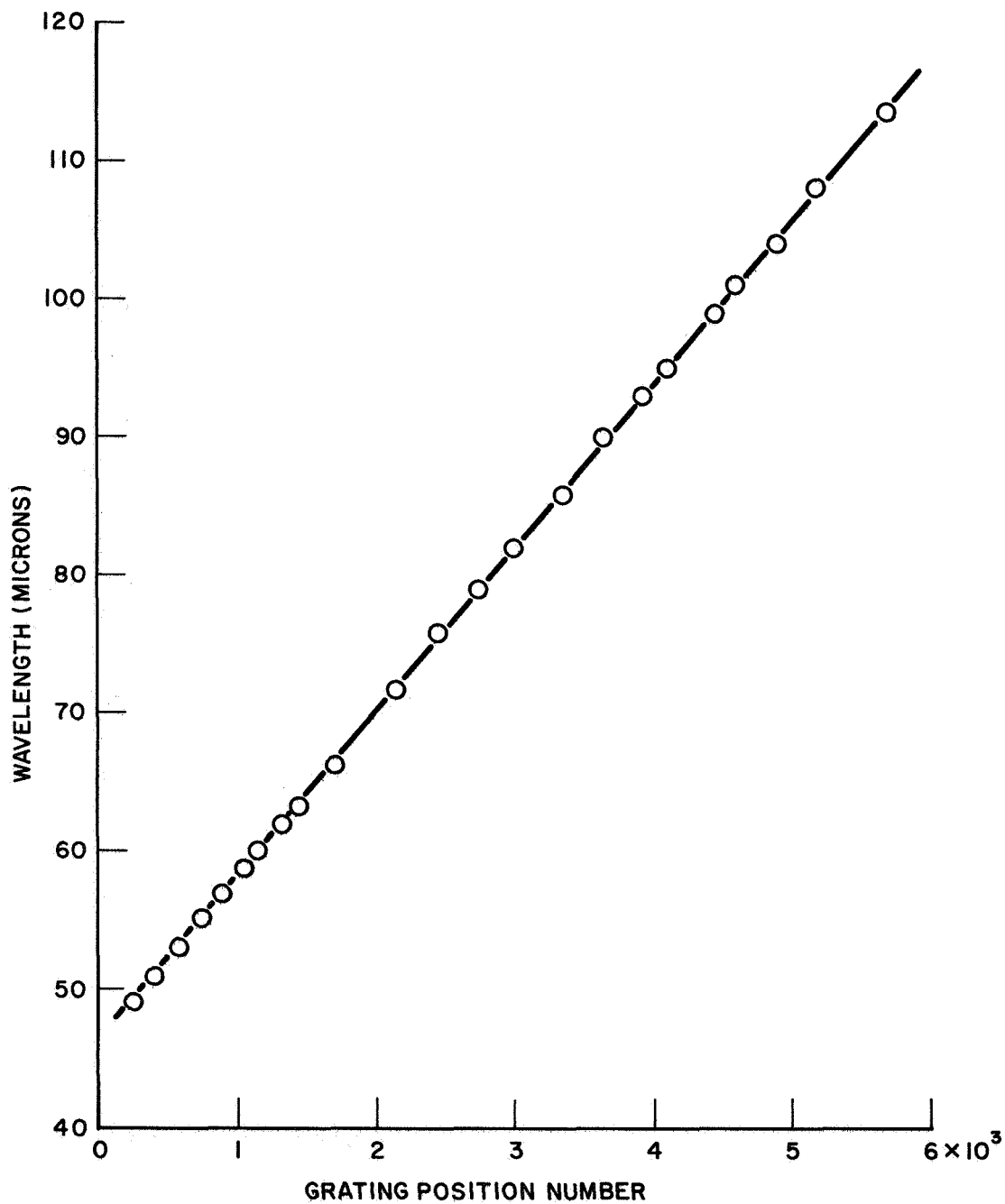
CALIBRATION CURVE FOR GRATING #2

FIGURE 25

parameters as scan speed, slit width, electronic sensitivity, electronic time constant, chart speed, etc. are important to obtain clear useful recordings of spectra. A few simple techniques and calculations can simplify this task.

The first parameter which is usually considered in obtaining spectra is the required spectral slit width. This number may be difficult to determine in some cases, but most often it is available from other spectra. That is, when one is recording water vapor spectra for calibration purposes a resolution of 2 to 3 cm^{-1} is usually sufficient. The relation between the mechanical slit width and the spectral slit width can be derived as follows:

$$\lambda = 2d \sin \theta, \quad d\lambda = 2d \cos \theta \, d\theta = 2d \left(1 - \sin^2\theta\right)^{\frac{1}{2}} d\theta$$

$$\frac{d\lambda}{\lambda} = \frac{2d(1-\sin^2\theta)^{\frac{1}{2}} d\theta}{\lambda} = \frac{(4d^2 - 4d^2 \sin^2\theta)^{\frac{1}{2}} d\theta}{\lambda}$$

$$= \frac{(4d^2 - \lambda^2)^{\frac{1}{2}} d\theta}{\lambda} = \frac{\left[1 - \left(\frac{\lambda}{2d}\right)^2\right]^{\frac{1}{2}}}{\left(\frac{\lambda}{2d}\right)} \frac{dx}{f}$$

where $dx = f \, d\theta$ is the physical slit width, and f is the focal length of the telescope mirror. For $f = 840$ mm, and at the blaze wavelength, $dk = dx/22\lambda$, where dk is in cm^{-1}, λ and dx are in mm, and $d\lambda/\lambda = dk/k$.

Table IX gives the mechanical slit width versus spectral slit width for each grating at its blaze wavelength. For a fixed mechanical slit width, the spectral slit width becomes smaller as the wavelength increases; thus the resolution improves as a grating is scanned toward longer wavelengths.

The next parameter to consider is the electronic sensitivity required to give a full scale chart reading at the wavelength

RESOLUTION VS. SLIT WIDTH AT BLAZE

GRATING	ν(cm^{-1})	λ(microns)	SLIT SETTING	PHYSICAL SLIT WIDTH dx(mm)	SPECTRAL SLIT WIDTH dν(cm^{-1})
1	250	40	10	1.27	1.44
			15	1.91	2.17
			20	2.54	2.89
			30	3.80	4.32
			40	5.08	5.77
			50	6.35	7.22
			60	7.62	8.65
			70	8.89	10.0
			80	10.17	11.5
2	143	70	20	2.54	1.65
			30	3.80	2.47
			40	5.08	3.30
			50	6.35	4.12
			60	7.62	4.94
			70	8.89	5.77
			80	10.17	6.60
			90	11.42	7.42
			100	12.70	8.25
3	77	130	30	3.80	1.33
			40	5.08	1.78
			50	6.35	2.22
			60	7.62	2.66
			70	8.89	3.10
			80	10.17	3.55
			90	11.42	4.00
			100	12.70	4.44
			110	13.40	4.69

GRATING	ν(cm^{-1})	λ(microns)	SLIT SETTING	PHYSICAL SLIT WIDTH dx(mm)	SPECTRAL SLIT WIDTH dν(cm^{-1})
4	46	216	40	5.08	1.07
			50	6.35	1.34
			60	7.62	1.61
			70	8.89	1.88
			80	10.17	2.14
			90	11.42	2.41
			100	12.70	2.68
			110	13.40	2.82
			120	15.23	3.21
5	23	430	40	5.08	0.54
			50	6.35	0.67
			60	7.62	0.80
			70	8.89	0.94
			80	10.17	1.07
			90	11.42	1.20
			100	12.70	1.34
			110	13.40	1.41
			120	15.23	1.60
6, 7, 8	13	760	70	8.89	0.53
			80	10.17	0.60
			90	11.42	0.68
			100	12.70	0.75
			110	13.40	0.79
			120	15.23	0.90
9	7.45	1345	100	12.70	0.43
			110	13.40	0.45
			120	15.23	0.46

of maximum transmission for a given sample – filter – grating combination. This is determined by rapidly scanning the interesting region to find the wavelength of maximum transmission, and then selecting the proper sensitivity to give an on-scale chart reading.

Once the electronic sensitivity has been established, the electronic time constant must be increased until a satisfactory signal to noise ratio is obtained. It must be remembered that the longer this time constant, the longer the time required to scan the given region. This brings in the next parameter, which is the scan speed. The electronic resolution is defined as the product of the scan speed times the electronic time constant. In order to obtain spectra which reflect the true wave form of the absorption lines, the electronic resolution should be from 0.1 to 0.5 times the spectral resolution. Thus, for a fixed spectral resolution, a longer time constant requires a slower scan speed, and hence, longer scan time for a given spectral region. Table IX gives the electronic resolution for each grating at the blaze wavelength for each scan speed and each time constant available in the spectrometer. Table IX is based on the scan speeds tabulated in Table X.

The last parameter to select is the chart speed. This is chosen to give spectral recordings of convenient length for storage and interpretation. This selection is controlled by the scan speed selected above.

TABLE X

WAVELENGTH SCAN RATES IN
CM^{-1}/MIN AT BLAZE

SCAN SPEED SETTING	GRATING							
	1	2	3	4	5	6	7	8
1/1	7.35	4.06	2.25	1.33	0.67	0.38	0.38	0.51
2/1	3.67	2.03	1.13	0.67	0.33	0.19	0.19	0.26
4/1	1.84	1.02	0.56	0.33	0.17	0.10	0.10	0.13
8/1	0.92	0.51	0.28	0.17	0.08	0.05	0.05	0.06
16/1	0.46	0.25	0.14	0.08	0.04	0.02	0.02	0.03
32/1	0.23	0.13	0.07	0.04	0.02	0.01	0.01	0.02
Blaze Wave-Length (microns)	40	70	130	216	430	758	754	757

BIBLIOGRAPHY

1. Eppley, M. and A. R. Karoli. "Use of Wave numbers in Radiation Formulas." J. Opt. Soc. Amer. 43, 957-959 (Nov. 1953).

2. Rubens, H. and R. W. Wood. "Focal Isolation of Long Heat Waves." Phil. Mag. 21, 249-261 (Feb. 1911).

3. Lord, R. C. and T. K. McCubbin. "Infrared Spectroscopy from 5 to 200 Microns with a Small Grating Spectrometer." J. Opt. Soc. Amer. 47, 689-697 (Aug. 1957).

4. Kruse, P. W., and others. Elements of Infrared Technology: Generation, Transmission, and Detection. Wiley, New York, 1963.

5. Rubens, H. and O. V. Baeyer. "On Extremely Long Waves Emitted by the Quartz Mercury Lamp." Phil. Mag. 21, 689-695 (May 1911).

6. McCubbin, T. K., Jr. Far Infrared Spectroscopy from 100 to 700 Microns, Ph. D. dissertation, Johns Hopkins University, Baltimore, Maryland, 1951.

7. McCubbin, T. K., Jr. and W. M. Sinton. "A Twelve-Inch Far-Infrared Grating Spectrometer." J. Opt. Soc. Amer. 42, 113-115 (Feb. 1952).

8. Plyler, E. K., and others. "Radiant Energy from Sources in the Far-Infrared." J. Opt. Soc. Amer. 52, 859-861 (Aug. 1962).

9. Elenbaas, W. The high pressure mercury vapour dischange. North Holland, Amsterdam, 1951.

10. Lebedew, P. "Electrische Wellen imder Ultrarot." Wied. Ann. 50, 1-3 (1895).

11. Liebreich, E. "Bercht über neuere Fortschritte in der Untersuchung des lang welligen ultra roten Spektrums." Jahrbuch der Rad. and Electr. 12, 205-230 (1915).

12. Mobius, W. "Über diedispersion von Wasser und Äthylalkohol Zwiscken 7 und 35 mm Wellen länge und Vorversuche zur Verwendung noch kurzerer electrischer Wellen." Ann. der Physik 62, 293-322 (June 1920).

13. Nichols, E. F. and J. D. Tear. "Joining the infrared and electric-wave spectra." Astrophys. J. 61, 17-21 (1925).

14. Lewitsky, M.A. "Electrische Wellen im Gebiete des äusseren Ultrarot." Phys. Z. 27, 177-182 (March 1926).

15. Glagolewa-Arkadiewa, A. "Short electromagnetic waves of wavelength up to 82 microns." Nature 113, 640 incl. (May 1924).

16. Rubens, H. and O.V. Baeyer. "Über eine äusserst Lang-Wellige Strahlung des Quecksilberdampfs." Berl. Ber., p. 339, (1911).

17. Rubens, H. "Gitter massungen in lang welligen spektrum." Berl. Ber., p. 8, (1921).

18. Czerny, M. "Messungen in Rotationsspektrum des Hel im langwelligen Ultrarot." Z. Physik 34, 227-244 (Sept. 1925).

19. Czerny, M. "Die Rotationsspektrum der Halogenwasser stoffe." Z. Physik 44, 235-255 (Aug. 1927).

20. Barnes, R.B. "Measurement in the Long wavelength infrared from 20 to 135 microns." Phys. Rev. 39, 562-575 (Feb. 1932).

21. Cartwright, C.H. and M. Czerny. "Dispersionsmessungen am NaCl im langwellen Ultrarot." Z. Physik. 85, 269-277 (Sept. 1933).

22. Badger, R.M. and C.H. Cartwright. "The pure rotation spectrum of ammonia." Phys. Rev. 33, 692-700 (May 1929).

23. Kuhne, J. "Messungen im Rotationsspektrum des Wassen dampfes." Z. Physik. 84, 722-731 (Aug. 1933).

24. Cartwright, C.H. and M. Czerny. "Dispersionsmessungen am NaCl und KCl im langwelligen Ultrarot." Z. Physik 90, 457-467 (Sept. 1934).

25. Cartwright, C.H. "Durchläss ig keitsmessungen im Spektralbereich von 50 bis 240 u." Z. Physik, 90, 480-488 (Sept. 1934).

26. Koch, B. "Messungen im langwelligen Ultrarotspektrum der Quarz quecksilber lampe." Ann. der Physik. 33, 335-358 (Oct. 1938).

27. Marr, O. "Spektralmessungen bei 0.2-0.5 mm Wellenlange an einigen Hochfrequenzisolier stoffen und Oxyden." Z. Physik. 113, 415-430 (Aug. 1939).

28. Dahlke, W. "Die spektrale Energie verteilung der langwelligen UR-Emission (300u) von verschieden Hochdruckentladungen." Z. Physik. 114, 672-681 (Dec. 1939).

29. Hopf, H. "Wasser dampf absorptions linien im spekralgebiet von 0.15 bis 0.5 mm Wellenlange." Z. Physik. 116, 310-316 (Sept. 1940).

30. Randall, H.M. "Infrared spectrometer of large aperature." Rev. Sci. Instr. 3, 190-200 (April 1932).

31. Randall, H.M. "The Spectroscopy of the far infrared." Rev. Mod. Phys. 10, 72-85 (Jan. 1938).

32. Randal, H.M. and others. "The far infrared spectrum of water vapor." Phys. Rev. 52, 160-174 (Aug. 1937).

33. Mitsuishi, A. and others. "Reflection measurements on reststrahlen crystals in the far-infrared region." J. Opt. Soc. Amer. 52, 14-16 (Jan. 1962).

34. Turner, A.F. and others. "Enhanced reflectance of rest-strahlen reflection filters." Appl. Opts. 4, 927-933 (Aug. 1965).

35. White, J.U. "Gratings as broad band filters for the infrared." J. Opt. Soc. Amer. 37, 713-717 (Sept. 1947).

36. Oetjen, R.A. and others. "An infrared spectrograph for use in the 40-150-micron spectral region." J. Opt. Soc. Amer. 42, 557-566 (Aug. 1952).

37. Yoshinaga, H. and others. "Far infrared spectrograph for use from the prism spectral region to about 1-mm wave-length." J. Opt. Soc. Amer. 48, 315-323 (May 1958).

38. Czerny, M. and A.F. Turner. "Uber der astigmatismus bei spiegel spektrometern." Z. Physik. 61, 792-797 (March 1930).

39. Yamada, Y., A. Mitsuishi and H. Yoshinaga. "Transmission filters in the far-infrared region." J. Opt. Soc. Amer. 52, 17-19 (Jan. 1962).

40. Rank, K.F. and L. Genzel. "Interference filters and fabry-perot interferometers for the far infrared." Appl. Opts. 1, 643-648 (Sept. 1962).

41. Mitsuishi, A. and others. "Metal mesh filters in the far infrared region." Japan J. Appl. Phys. 2, 574-577 (Sept. 1963).

42. Vogel, P. and L. Genzel. "Transmission and reflection of metallic mesh in the far infrared." Infrared Phys. 4, 257-262 (1964).

43. Möller, K. D. and R. V. McKnight. "Far-infrared-transmission filter gratings." J. Opt. Soc. Amer. 53, 760-761 (June 1963).

44. Möller, K. D. and R. V. McKnight. "Measurements on transmission-filter gratings in the far infrared." J. Opt. Soc. Amer. 55, 1075-1078 (Sept. 1965).

45. Möller, K. D. and others. "Far-infrared vacuum grating spectrometer." J. Opt. Soc. Amer. 55, 1233-1238 (Oct. 1965).

46. Möller, K. D. and others. "Far infrared transmission filters for the 300-18 cm^{-1} spectral region." Appl. Opts. 5, 403-406 (March 1966).

47. Russell, J. W. and H. L. Strauss. "Czerny-Turner far infrared spectrometer for the 300-10 cm^{-1} region." Appl. Opts. 4, 1131-1136 (Sept. 1965).

48. Palik, E. D. "A far infrared bibliography." J. Opt. Soc. Amer. 50, 1329-1336 (Dec. 1960).

49. Palik, E. D. "A far infrared bibliography." USNRL Bibliography No. 21 (April 1963), (AD-40704).

50. Smith, R. A., F. E. Jones and R. P. Chasmar. The detection and measurement of infrared radiation. Clarendon Press, Oxford, 1957.

51. Ebert, H. "Uber die Spektrum im der Ultrarot." Wied. Ann. 38, 489-491 (1889).

52. Fastie, W. G. "Image forming properties of the Ebert monochromator." J. Opt. Soc. Amer. 42, 647-651 (Sept. 1952).

53. Littrow, O. "A new spectroscope." Am. J. Sci. 35, 413 incl. (May 1862).

54. Pfund, A. H. "An infrared spectrometer of large aperature." J. Opt. Soc. Amer. 14, 337-338 (April 1927).

55. Barnes, R. B. "The infrared absorption of some organic liquids under high resolution." Phys. Rev. 36, 296-304 (July 1930).

56. Hardy, J. D. "High resolution in the infrared." Phys. Rev. 38, 2162-2167 (Dec. 1931).

57. Welford, W. T. "Stigmatic Ebert-type plane grating mounting." J. Opt. Soc. Amer. 53, 766 (1963).

58. Filler, A. S. "Stigmatic Ebert-type plane grating mounting." J. Opt. Soc. Amer. 54, 424 (Dec. 1964).

59. Mielenz, K. D. "Theory of mirror spectrographs III. Focal surfaces and slit curvature of Ebert and Ebert-Fastie spectrographs." J. Res. NBS 68C, 205-213 (Oct. -Dec. 1964).

60. Welford, W. T. "Aberration theory of gratings and grating mountings." Progr. in Optics 4, North-Holland, Amsterdam, 1965.

61. Kudo, K. "Optical properties of plane grating monochromator." J. Opt. Soc. Amer. 55, 150-161 (Feb. 1965).

62. Kudo, K. "Plane grating monochromator of Littrow type." Sci. of Light 9, 65-74 (Oct. 1960).

63. Kudo, K. "Plane grating monochromators of Ebert, Pfund, and Czerny-Turner types." Sci. of Light 9, 1-30 (June 1960).

64. Kudo, K. "On the aberration of optical system used in infrared spectrometer." Sci. of Light 4, 105-112 (Nov. 1955).

65. Mielenz, K. D. "Theory of mirror spectrographs II. General theory of focal surfaces and slit curvatures." J. Res. NBS 68C, 201-204 (Oct. -Dec. 1964).

66. Yoshinaga, H. and others. "Geometrical optical image formation in infrared spectrometers." J. Opt. Soc. Amer. 50, 437-445 (May 1960).

67. Shafer, A. B. and others. "Optimization of the Czerny-Turner spectrometer." J. Opt. Soc. Amer. 54, 879-887 (July 1964).

68. Dalton, M. L. Jr. "Astigmatism compensation in the Czerny-Turner spectrometer." Appl. Opts. 5, 1121-1123 (July 1966).

69. Rosendahl, G. R. "Contributions to the optics of mirror systems and gratings with oblique incidence II. A discussion of aberrations." J. Opt. Soc. Amer. 52, 408-411 (April 1962).

70. Rosendahl, G. R. "Contributions to the optics of mirror systems and gratings with oblique incidence III. Some applications." J. Opt. Soc. Amer. 52, 412-415 (April 1962).

71. Walsh, A. "Multiple monochromators. I. Design of multiple monochromators." J. Opt. Soc. Amer. 42, 94-95 (Feb. 1952).

72. Walsh, A. "Multiple monochromators. II. Application of a double monochromator to infrared spectroscopy." J. Opt. Soc. Amer. 42, 96-100 (Feb. 1952).

73. Fastie, W. G. and W. M. Sinton. "Multiple diffraction in grating spectroscopy." J. Opt. Soc. Amer. 44, 103-108 (Feb. 1954).

74. Kudo, K. "A double beam, double and multiple pass infrared spectrophotometer." Sci. of Light 5, 1-3 (March 1956).

75. Kudo, K. "Double beam infrared spectrophotometer using double pass, triple pass, double monochromator and double pass double monochromator." Sci. of Light 5, 89-109 (Dec. 1956).

76. Christensen, R. L. and R. J. Potter. "Double monochromator systems." Appl. Opts. 2, 1049-1054 (Oct. 1963).

77. Roberts, V. "Double monochromator optical system based upon ideas of Czerny and Turner." J. Sci. Inst. 29, 134-135 (April 1952).

78. Nielsen, J. R. "Aberrations in ellipsoidal mirrors used in infrared spectrometers." J. Opt. Soc. Amer. 39, 59-63 (Jan. 1949).

79. Williamson, D. E. "Cone channel condenser optics." J. Opt. Soc. Amer. 42, 712-715 (Oct. 1952).

80. Ohlmann, R. C. and others. "Far infrared transmission through metal light pipes." J. Opt. Soc. Amer. 48, 531-533 (Aug. 1958).

81. Witte, W. "Cone channel optics." Infrared Phys. 5, 179-185 (Dec. 1965).

82. Harris, R. E. and others. "Far infrared transmission through metal light pipes with low thermal conductance." Appl. Opts. 5, 1083-1084 (June 1966).

83. Daich, A. R. and others. "Passage of light through light guides." Opt. and Spectry. 8, 375-378 (May 1960).

84. Pargamanik, L. E. and others. "Passage of light through diffuse light pipes." Opt. and Spectry. 17, 418-422 (Nov. 1964).

85. Benesch, W. and J. Strong. "The optical image transformer." J. Opt. Soc. Amer. 41, 252-254 (April 1951).

86. Strong, John. Concepts of Classical Optics. W. H. Freeman, San Francisco, 1958.

87. Harrison, G. R. "The production of Diffraction Gratings: II. The Design of Echelle and Grating Spectrographs." J. Opt. Soc. Amer. 39, 522-528 (July 1949).

88. Harrison, G. R., and G. W. Stroke. "Attainment of High Resolution with Diffraction Gratings and Echelles." J. Opt. Soc. Amer. 50, 1153-1158 (Dec. 1960).

89. Wood, R. W. "The Echellette Grating for the Infra-Red." Phil. Mag. 20, 770-778 (1910).

90. Hatcher, R. D. and J. H. Rohrbaugh. "Theory of the Echelette Grating. I." J. Opt. Soc. Amer. 46, 104-110 (Feb. 1956).

91. Rohrbaugh, J. H. and R. D. Hatcher. "Theory of the Echelette Grating. II." J. Opt. Soc. Amer. 48, 204-709 (Oct. 1958).

92. Rohrbaugh, J. H. and others. "Theory of the Echelette Grating III." J. Opt. Soc. Amer. 48, 710-711 (Oct. 1958).

93. Williams, W. E. "The Echelon Diffraction Grating." Proc. Phys. Soc. (London) 45, 699-702 (Oct. 1933).

94. Strong, John. "Interferometry in the Far Infrared." J. Opt. Soc. Amer. 47, 354-357 (May 1957).

95. Strong, John and G. A. Vanasse. "Interferometric Spectroscopy in the Far Infrared." J. Opt. Soc. Amer. 49, 844-850 (Sept. 1959).

96. Strong, John and G. A. Vanasse. "Lamellar Grating Far-Infrared Interferometer." J. Opt. Soc. Amer. 50, 113-118 (Feb. 1960).

97. Richards, P. L. "High-Resolution Fourier Transform Spectroscopy in the Far-Infrared." J. Opt. Soc. Amer. 54, 1474-1484 (Dec. 1964).

98. Hall, R. T. and others. "A High-Resolution, Far Infrared Double-Beam Lamellar Grating Interferometer." Appl. Opts. 5, 1147-1158 (July 1966).

99. Jenkins, F. A. and H. E. White. Fundamentals of Optics. McGraw-Hill, New York, 1957.

100. Sassa, N. "Resolving Power of Infrared Grating Monochromator." Sci. of Light 11, 41-62 (Jan. 1962).

101. Mielenz, K. D. "Theory of Mirror Spectrographs. I. Astigmatic Illumination of Plane Gratings and Prisms." J. Res. NBS. 68C, 195-200 (Oct. -Dec. 1964).

102. Murty, M. V. R. K. "Use of Convergent and Divergent Illumination with Plane Gratings." J. Opt. Soc. Amer. 52, 768-773 (July 1962).

103. Palmer, C. H. "Parallel Diffraction Grating Anomalies." J. Opt. Soc. Amer. 42, 269-276 (April 1952).

104. Stewart, J. E. and W. S. Gallaway. "Diffraction Anomalies in Grating Spectrophotometers." Appl. Opts. 1, 421-429 (July 1962).

105. Palmer, C. H. and others. "Diffraction Anomalies for Gratings of Rectangular Profile." Appl. Opts. 4, 1271-1274 (Oct. 1965).

106. Hessel, A. and A. A. Olmer. "A New Theory of Wood's Anomalies on Optical Gratings." Appl. Opts. 4, 1275-1297 (Oct. 1965).

107. Harrison, G. R. "The Production of Diffraction Gratings. I. Development of the Ruling Art." J. Opt. Soc. Amer. 39, 413-426 (June 1949).

108. Harrison, G. R. and J. E. Archer. "Interferometric Calibration of Precision Screws and Control of Ruling Engines." J. Opt. Soc. Amer. 41, 495-503 (Aug. 1951).

109. Harrison, G. R. and G. W. Stroke. "Interferometric Control of Grating Ruling with Continuous Carriage Advance." J. Opt. Soc. Amer. 45, 112-121 (Feb. 1955).

110. Harrison, G. R. and others. "Ruling of Large Diffraction Gratings with Interferometric Control." J. Opt. Soc. Amer. 47, 15-22 (Jan. 1957).

111. Harrison, G. R. and others. "Interferometrically Controlled Ruling of Ten-Inch Diffraction Gratings." J. Opt. Soc. Amer. 49, 205-211 (March 1959).

112. Jarrell, R. F. and G. W. Stroke. "Some New Advances in Grating Ruling Replication, and Testing." Appl. Opts. 3, 1251-1262 (Nov. 1964).

113. Stroke, G. W. "Attainment of High-Resolution Gratings by Ruling under Interferometric Control." J. Opt. Soc. Amer. 51, 1321-1339 (Dec. 1961).

114. Stroke, C. W. "Ruling, Testing and use of optical Gratings for High-Resolution Spectroscopy." Progr. in Optics 3, North-Holland, Amsterdam, 1963.

115. Babcock, H. D. "Bright Diffraction Gratings." J. Opt. Soc. Amer. 34, 1-5 (Jan. 1944).

116. Babcock, H. W. "Control of a Ruling Engine by a Modulated Interferometer." Appl. Opts. 1, 415-420 (July 1962).

117. Stamm, R. F. and J. J. Whalen. "Energy Distribution of Diffraction Gratings as a Function of Groove Form." J. Opt. Soc. Amer. 36, 2-12 (Jan. 1946).

118. Meecham, W. C. "Variational Method for the Calculation of the Distribution of Energy Reflected from a Periodic Surface. I." J. Appl. Phys. 27, 361-367 (April 1956).

119. Meecham, W. C. and C. W. Peters. "Reflection of Plane-Polarized, Electromagnetic Radiation from an Echelette Diffraction Grating." J. Appl. Phys. 28, 216-217 (Feb. 1957).

120. Madden, R. P. and John Strong. "Diffraction Gratings." Concepts of Classical Optics, Appendix P, W. H. Freeman, San Francisco, 1958.

121. Sakayanagi, Y. "Intensity Distribution of Ideal Echelette Gratings." Sci. of Light 11, 99-115 (Oct. 1962).

122. Strong, John. "Resolving Power Limitations of Grating and Prism Spectrometers." J. Opt. Soc. Amer. 39, 320-323 (April 1949).

123. Barrekette, E. S. and R. L. Christensen. "On Plane Blazed Gratings." I.B.M.J. Res. Dev. 9, 108-117 (March 1965).

124. Jacquinot, P. "The Luminosity of Spectrometers with Prisms, Gratings, or Fabry-Perot Etalons." J. Opt. Soc. Amer. 44, 761-765 (Oct. 1954).

125. Plyler, E. K. and L. R. Blaine. "Transmittance of Materials in the Far Infrared." J. Ros. N. B. S. 64C, 55-56 (Jan-March 1960).

126. Blaine, L. R. "A Far-Infrared Vacuum Grating Spectrometer." J. Ros. N. B. S. 67C, 207-215 (July-Sept. 1963).

127. McKnight, R. V. and K. D. Moller. "Far-Infrared Spectrum of Polypropylene, High-Density Polyethylene, and Quartz-Crystal Plates." J. Opt. Soc. Amer. 54, 132-133 (Jan. 1964).

128. Strong, John. "Investigations in the Far-Infrared." Phys. Rev. 38, 1818-1926 (Nov. 1931).

129. Kittel, C. Introduction to Solid State Physics, Wiley, New York, 1953.

130. Sinton, W. M. and W. C. Davis. "Far Infrared Reflectances T1Cl, T1Br, T1I, PbS, PbCl$_2$, ZnS, and CsBr." J. Opt. Soc. Amer. 44, 503-504 (June 1954).

131. Yoshinaga, H. "Reflectivity of Several Crystals in the Far Infrared Region between 20 and 200 Microns." Phys. Rev. 100, 753-754 (Dec. 1955).

132. Plyler, E. K. and N. Acquista. "Transmittance and Reflectance of Cesium Iodide in the Far Infrared Region." J. Opt. Soc. Amer. 48, 668-669 (Sept. 1958).

133. Mitsuishi, A. and others. "The Far Infrared Reflectivity of NaCl, KCl and KBr Crystals, J. Phys. Soc. Japan 14, 110 (Jan. 1959).

134. McCarthy, D. W. "The Reflection and Transmission of Infrared Materials, Part I: Spectra, 2 through 50 Microns." Appl. Opts. 2, 591-595 (June 1963); "Part II: Bibliography." Ibid., 596-603; "Part III: Spectra from 2 to 50 Microns." Ibid. 4, 317-320 (March 1965); "Part IV: Bibliography." Ibid, 507-511 (April 1965).

135. Manley, T. R. and D. A. Williams. "Scattering Filters in the Far Infrared." Spectrochimica Acta 21, 737-745 (Feb. 1965).

136. Clewell, D. H. "Scattering of Light by Pigment Particles." J. Opt. Soc. Amer. 31, 521-527 (Aug. 1941).

137. Henry, R. L. "The Transmission of Powder Films in the Infrared." J. Opt. Soc. Amer. 38, 775-789 (Sept. 1948).

138. Hadni, A. and others. "Contribution to the Study of Reflection of the Far-Infrared by Echelette Gratings." J. Phys. Radium 20, 705-711 (July 1959).

139. Hadni, A. and others. "Spectrometry in the Far Infrared." Rev. d'Optique 38, 463-474 (Aug. 1959).

140. Hadni, A. and others. "Experimental Study of the Polarization of Light by Echelette Gratings between 1 and 600 Microns." Compt. Rendu 250, 2007-2009 (March 1960).

141. The Newark Wire Cloth Company, 351 Verona Avenue, Newark, New Jersey.

142. The Buckbee Mears Company, 245 Sixth Street, St. Paul 1. Minnesota.

143. Kneubuhl, F. K. and others. "High-Resolution Grating Spectrometer for the Far-Infrared." J. Opt. Soc. Amer. 56, 760-764 (June 1960).

144. Nielsen, J. R. "The Filling of a Spectrograph with light considered as a geometrical radiation Problem." J. Opt. Soc. Amer. 20, 701-718 (Dec. 1930).

145. Elliott, A. and J. H. Dickenson, Laborlatory Instruments, Chapman and Hall, London, 1959.

146. Badger, R. M. and others. "A Vacuum Spectrograph for the Infrared." Rev. Sci. Instrs. 19, 861-865 (Dec. 1948).

147. Dimock, D. L. "Temperature Compensation of Sine-Drive Monochromators." J. Opt. Soc. Amer. 50, 819-820 (Aug. 1960).